REPORT DOCUMENTATION PAGE

Form Approved
OMB No. 0704-0188

1. AGENCY USE ONLY (Leave blank)	2. REPORT DATE	3. REPORT TYPE AND DATES COVERED
	12/6/96	Final 3/1/94 - 8/31/96

4. TITLE AND SUBTITLE
Structure-Property Behavior of Organic-Inorganic Hybrid Materials Based on Sol Gel Chemistry

5. FUNDING NUMBERS
G F49620-94-1-0149
2303/CS

6. AUTHOR(S)
Garth L. Wilkes

AFOSR-TR-97
0051

7. PERFORMING ORGANIZATION NAME(S) AND ADDRESS(ES)
Garth L. Wilkes
Department of Chemical Engineering
Virginia Polytechnic Institute & State Universit
Blacksburg, VA 24061-0211

9. SPONSORING / MONITORING AGENCY NAME(S) AND ADDRESS(ES)
AFOSR/~~PKA~~ NL
110 Duncan Avenue Suite B115
Bolling AFB, DC 20332-0001

10. SPONSORING / MONITORING AGENCY REPORT NUMBER

11. SUPPLEMENTARY NOTES

19970117 069

12a. DISTRIBUTION / AVAILABILITY STATEMENT
unlimited

12b. DISTRIBUTION CODE

13. ABSTRACT *(Maximum 200 words)*

This work was directed at the synthesis and structure-property behavior of hybrid organic-inorganic network materials prepared by a sol gel reaction. Specific focus concerned the development of optically abrasion resistant coatings that could be utilized for both polymeric and metallic substrates. In the case of the latter, the purpose of the coating was to not only to supply abrasion resistance but, if possible, provide corrosion resistance as well. Considerable success was achieved in that several hybrid coatings were synthesized by reacting one or more metal alkoxides with functionalized organic moieties such as triethoxysilanated diethylene triamine (DETA) and related diamines or di or triol species. These functionalized organics, in conjunction with the alkoxide, were spin or dip coated on appropriate substrates and thermally cured. In some cases a primer molecule was also utilized to promote higher adhesion with the substrate - the principal example being amino propyltrimethoxysilane. It has been demonstrated that the coatings display very good abrasion resistance for polymeric substrates, aluminum and copper but do not perform as well on steel or a phosphate coated steel. The final portion of the work concerned the development of porous inorganics made by the calcination of hybrid organic-inorganic network materials but where these networks were prepared by the use of functionalized polytetramethylene oxide oligomers of varied molecular weight that had been reacted with tetraethylorthosilicate (TEOS). It was demonstrated that calcination of these materials could lead to porous silicate powders possessing a specific surfaces near 1000 meters^2/gram. Furthermore, pore size characteristics of these powders were analyzed. It was concluded that such hybrid materials could serve as the base for developing highly porous powder materials for chromatography, catalyst supports, etc.

14. SUBJECT TERMS	15. NUMBER OF PAGES
sol gel, abrasion resistance, networks, hybrid materials, TEOS, polytetramethylene oxide, calcination, porosity	16. PRICE CODE

17. SECURITY CLASSIFICATION OF REPORT	18. SECURITY CLASSIFICATION OF THIS PAGE	19. SECURITY CLASSIFICATION OF ABSTRACT	20. LIMITATION OF ABSTRACT
unclassified	unclassified	unclassified	UL

GENERAL INSTRUCTIONS FOR COMPLETING SF 298

The Report Documentation Page (RDP) is used in announcing and cataloging reports. It is important that this information be consistent with the rest of the report, particularly the cover and title page. Instructions for filling in each block of the form follow. It is important to ***stay within the lines*** to meet ***optical scanning requirements***.

Block 1. Agency Use Only *(Leave blank)*.

Block 2. Report Date. Full publication date including day, month, and year, if available (e.g. 1 Jan 88). Must cite at least the year.

Block 3. Type of Report and Dates Covered. State whether report is interim, final, etc. If applicable, enter inclusive report dates (e.g. 10 Jun 87 - 30 Jun 88).

Block 4. Title and Subtitle. A title is taken from the part of the report that provides the most meaningful and complete information. When a report is prepared in more than one volume, repeat the primary title, add volume number, and include subtitle for the specific volume. On classified documents enter the title classification in parentheses.

Block 5. Funding Numbers. To include contract and grant numbers; may include program element number(s), project number(s), task number(s), and work unit number(s). Use the following labels:

C	- Contract	**PR**	- Project
G	- Grant	**TA**	- Task
PE	- Program Element	**WU**	- Work Unit Accession No.

Block 6. Author(s). Name(s) of person(s) responsible for writing the report, performing the research, or credited with the content of the report. If editor or compiler, this should follow the name(s).

Block 7. Performing Organization Name(s) and Address(es). Self-explanatory.

Block 8. Performing Organization Report Number. Enter the unique alphanumeric report number(s) assigned by the organization performing the report.

Block 9. Sponsoring/Monitoring Agency Name(s) and Address(es). Self-explanatory.

Block 10. Sponsoring/Monitoring Agency Report Number. *(If known)*

Block 11. Supplementary Notes. Enter information not included elsewhere such as: Prepared in cooperation with ...; Trans. of...; To be published in.... When a report is revised, include a statement whether the new report supersedes or supplements the older report.

Block 12a. Distribution/Availability Statement. Denotes public availability or limitations. Cite any availability to the public. Enter additional limitations or special markings in all capitals (e.g. NOFORN, REL, ITAR).

DOD	- See DoDD 5230.24, "Distribution Statements on Technical Documents."
DOE	- See authorities.
NASA	- See Handbook NHB 2200.2.
NTIS	- Leave blank.

Block 12b. Distribution Code.

DOD	- Leave blank.
DOE	- Enter DOE distribution categories from the Standard Distribution for Unclassified Scientific and Technical Reports.
NASA	- Leave blank.
NTIS	- Leave blank.

Block 13. Abstract. Include a brief *(Maximum 200 words)* factual summary of the most significant information contained in the report.

Block 14. Subject Terms. Keywords or phrases identifying major subjects in the report.

Block 15. Number of Pages. Enter the total number of pages.

Block 16. Price Code. Enter appropriate price code *(NTIS only)*.

Blocks 17. - 19. Security Classifications. Self-explanatory. Enter U.S. Security Classification in accordance with U.S. Security Regulations (i.e., UNCLASSIFIED). If form contains classified information, stamp classification on the top and bottom of the page.

Block 20. Limitation of Abstract. This block must be completed to assign a limitation to the abstract. Enter either UL (unlimited) or SAR (same as report). An entry in this block is necessary if the abstract is to be limited. If blank, the abstract is assumed to be unlimited.

Introduction

It is well recognized that as new technological advances occur, there is generally also an associated need for new materials in order to allow such technologies to be promoted. As a pertinent example, as new polymeric materials are developed, some of these systems display optical transparency and are therefore often selected as potential candidates for structural applications but where transparency can be maintained. However, due to the lower density characteristics of organics in conjunction with weaker secondary bonding, such materials typically suffer greatly from the problem of abrasion resistance thereby often limiting them for the applications where optical transparency is required. Hence, there has been a desire to develop appropriate coatings for such substrates for purposes of maintaining abrasion resistance along with optical transparency. In addition, while metallics do not display optical transparency, some of the softer metals such as aluminum or copper easily undergo abrasion and therefore it is desirable to promote appropriate abrasion resistant coatings for these substrates as well. It is also desirable that these latter coatings may assist in preventing corrosion of various metallic substrates and thereby organics or related materials have been utilized as corrosion coatings for such substrates.

In brief, the research that will be summarized was focused on developing hybrid coatings for polymeric and softer metallic substrates for purposes of providing optically clear abrasion resistant coatings so that either the underlying substrate remains transparent in the case of polymeric systems, or the metallic sheen can be maintained as in the case of polished aluminum or copper. In brief, the project was aimed at the synthesis and structure property response of such coatings as prepared by a sol-gel reaction of functionalized organics that can co-react with various metal alkoxides. Since all of the work that was a part of the contract has been placed into manuscript form, the report will principally address the overall results and then, through use of the attached manuscripts in the appendices, the reader can obtain additional details concerning the specifics of each focused part of this work. In addition, a review regarding the synthesis, structure and property behavior of hybrid organic-inorganic materials is also included within this report since it was also developed through the financial support of this contract.

In addition to the hybrid coatings addressed above, a portion of this project considered the development of porous inorganic powders prepared by calcination of specific hybrid organic-inorganic networks based on polytetramethylene oxide, PTMO, and tetraethylorthosilicate, TEOS. The variable of PTMO oligomer molecular weight was a principle variable in this study. It was demonstrated that PTMO molecular weight did have some effect on pore size distribution. It was also demonstrated that specific surfaces of nearly 1000 m^2/g could be obtained by calcination of such hybrid networks. In view of these significantly high specific surfaces, the use of such a chemical route to porous inorganics seems warranted and deserving of further investigation. Such powders may have applicability in catalytic, chromatographic or related areas of technology. Since

this work has also been prepared in manuscript form, an appendix of this report contains this manuscript and provides the reader with greater detail of the specifics of that portion of the work.

What now follows is a listing of the specific manuscripts that are attached as appendices to this final report. To assist the reader in capturing the significance and general content of each manuscript, either the abstract of the publication or a brief summary is provided.

Results (the title and abstract extends from publications supported by this contract)

(A) Abrasion Resistant Inorganic/Organic Coating Materials Prepared by the Sol-Gel Method - *Journal of Sol-Gel Science and Technology,* **5**, 115-126 (1995).

The following paragraph provides the abstract of the above listed manuscript. The full manuscript is found in Appendix 1.

Novel abrasion resistant coating materials prepared by the sol-gel method have been developed and applied on the polymeric substrates bisphenol-A polycarbonate and diallyl diglycol carbonate resin (CR-39). These coatings are inorganic/organic hybrid network materials synthesized from 3-isocyanatopropyltriethoxysilane functionalized organics and metal alkoxide. The organic components are 3,3'-iminobispropylamine (IMPA), resorcinol (RSOL), diethylenetriamine (DETA), poly(ethyleneimine (PEI), glycerol and a series of diols. The metal alkoxides are tetraethoxysilane (TEOS) and tetramethoxysilane (TMOS). These materials are spin coated onto bisphenol-A polycarbonate and CR-39 sheets and thermally cured to obtain a transparent coating of a few microns in thickness. Following the curing, the abrasion resistance is measured and compared with an uncoated control. It was found that the abrasion resistance of inorganic/organic hybrid coatings in the neat form or containing metal alkoxide can be very effective to improve the abrasion resistance of polymeric substrates. The adhesion tests show that the adhesion between coating and substrate can be greatly improved by treating the polymeric substrate surface with a primer solution of isopropanol containing 3-aminopropyltriethoxysilane (3-APS). The interaction between 3-APS and the polycarbonate surface was investigated by a molecular dynamics simulation. The results strongly suggest that the hydrogen bonding between the amino group of the 3-APS and ester group in the polycarbonate backbone are sufficiently strong to influence the orientation of the primer molecules. The abrasion resistance of these new coating systems is discussed in light of the structure of the organic components. All of these results show that these coating materials have excellent abrasion resistance and have potential applications as coating materials for lenses and other polymeric products.

(B) Synthesis and Characterization of Abrasion Resistant Coating Materials Prepared by the Sol-Gel Approach: I. Coatings Based on Functionalized Aliphatic Diols and Diethylenetriamine - *Journal of Inorganic and Organometallic Polymers,* **5**, No. 4, 343-375 (1995).

The following paragraph provides the abstract of the above listed manuscript. The full manuscript is found in Appendix 2.

The synthesis of inorganic/organic hybrid materials has been undertaken and used as abrasion resistant coatings for polymeric substrates by the sol-gel method. The organic components are diethylenetriamine (DETA), glycerol, and a series of aliphatic diols which are functionalized by 3-isocyanatopropyl-triethoxysilane. The inorganic components are tetramethoxysilane (TMOS), aluminum tri-*sec*-butoxide, titanium *sec*-butoxide and zirconium *n*-propoxide. Solutions of these materials are spin coated onto bisphenol-A polycarbonate sheet and thermally cured to obtain a transparent coating of a few microns in thickness. Following the curing, the abrasion resistance is measured and compared with a control having no coating. It was found that the abrasion resistance of inorganic/organic hybrid coatings in the neat form or containing additional silicon, titanium, zirconium, and aluminum alkoxides can be very effective to improve abrasion resistance. The adhesion tests show that the adhesion between coating and substrate can be greatly improved by treating the polymeric substrate surface with an oxygen plasma or a primer solution of isopropanol containing 3-aminopropyltriethoxysilane. Other experiments, such as the abrasion resistance tests following conditioning in a "hot-wet" condition (boiling water treatment), microhardness tests, UV absorption behavior, and the observation of abraded surfaces, were also undertaken in order to evaluate these coating materials.

(C) Hybrid Organic/Inorganic Coatings for Abrasion Resistance on Plastic and Metal Substrates - *Mat. Res. Soc. Symp. Proc.*, **435**, 207-213 (1996).

The following paragraph provides the abstract of the above listed manuscript. The full manuscript is found in Appendix 3.

Novel abrasion resistant coatings have been successfully prepared by the sol-gel method. These materials are spin coated onto bisphenol-A polycarbonate, diallyl diglycol carbonate resin (CR-39) sheet, aluminum, and steel substrates and are thermally cured to obtain a transparent coating of a few microns in thickness. Following the curing, the abrasion resistance is measured and compared with an uncoated control. It was found that these hybrid organic/inorganic networks partially afford excellent abrasion resistance to the polycarbonate substrates investigated. In addition to having excellent abrasion resistance comparable to current commercial coatings, some newly developed systems are also UV resistant. Similar coating formulations applied to metals can greatly improve the abrasion resistance despite the fact that the coatings are lower in density than their substrates.

(D) Preparation of Highly Porous Silica Gel From Poly(Tetramethylene Oxide) (PTMO)/Silica Hybrids - submitted, *Chemistry of Materials*, (1996).

The following paragraph provides the abstract of the above listed manuscript. The full manuscript is found in Appendix 4.

Porous silica gels with high surface area were prepared by calcination of silica/poly(tetramethylene oxide) (PTMO) hybrid network materials. The variation of surface area of these silica gels with PTMO/silica composition and molecular weight of PTMO was investigated. BET surface area analysis showed that for all oligomeric molecular weights of PTMO, high values in the range of 700-900 m^2g^{-1} could be obtained. The optimum PTMO/TEOS weight ratio was 30-50. Pore size analysis indicated that samples with high surface areas were mesoporous, while samples with low or medium surface areas were nonporous. The hysteresis in the adsorption-desorption isotherms indicated that the pores were cylindrical in shape.

(E) Organic/Inorganic Hybrid Network Materials by the Sol-Gel Approach - *Chem. Mater.*, **8**, No. 8, 1667-1681 (1996).

The following paragraph provides the abstract of the above listed manuscript which is a review of the investigator's work on hybrid organic-inorganic network materials. The full manuscript is found in Appendix 5.

Organic/inorganic hybrid materials prepared by the sol-gel approach have rapidly become a fascinating new field of research in materials science. The explosion of activity in this area in the past decade has made tremendous progress in both the fundamental understanding of the sol-gel process and the development and applications of new organic/inorganic hybrid materials. In this review, a brief summary of the research activities in the field of organic/inorganic nanocomposite materials and a general background of the sol-gel chemistry are first given. The emphasis of this report, however, is placed on the synthesis, structure-property response, and potential applications of the organic/inorganic hybrid networks that possess chemical bonding between the organic and inorganic phases, particularly those systems that were developed in our laboratory since 1985.

Summary

A number of hybrid organic/inorganic network coatings were synthesized utilizing metal alkoxides co-reacted with functionalized organics. Metallic and polymeric substrates were dip coated or spin coated with these materials and thermally cured. Abrasion resistance of the coatings were tested utilizing a Tabor abrader. Very positive results were achieved with a number of these coatings particularly those based on triamines such as diethylenetriamine and also with diols such as butane diol that had been functionalized with triethoxysilane groups. These coatings did not perform well with respect to abrasion resistance when placed on steel substrates but were extremely functional on aluminum and copper as well as the polymeric substrates of bisphenol-A polycarbonate and crosslinked diallyl diglycol carbonate (CR-39).

It is recommended that the hybrid coatings developed be further investigated for their applicability for protecting other polymeric and metallic substrate materials.In addition to the abrasion resistant coating synthesis and testing thereof, specific surface porous silicates were prepared by calcination of hybrid network materials based on polytetramethylene oxide and tetraethylorthosilicate. With appropriate calcination procedures, specific surfaces reaching 1000 m^2/g were obtained. The polytetramethylene oxide oligomer molecular weight for a constant weight percentage of the oligomer to TEOS was of some importance in influencing pore size distribution and specific surface content.

Appendix 1

Journal of Sol-Gel Science and Technology, 5, 115–126 (1995)

Abrasion Resistant Inorganic/Organic Coating Materials Prepared by the Sol-Gel Method

J. WEN
Department of Chemical Engineering, Virginia Polytechnic Institute and State University, Blacksburg, VA 24061

V.J. VASUDEVAN
NSF Science and Technology Center for High Performance Polymeric Adhesives and Composites, Virginia Polytechnic Institute and State University, Blacksburg, VA 24061

G.L. WILKES
Department of Chemical Engineering, Virginia Polytechnic Institute and State University, Blacksburg, VA 24061

Received March 24, 1995; Accepted July 20, 1995

Abstract. Novel abrasion resistant coating materials prepared by the sol-gel method have been developed and applied on the polymeric substrates bisphenol-A polycarbonate and diallyl diglycol carbonate resin (CR-39). These coatings are inorganic/organic hybrid network materials synthesized from 3-isocyanatopropyltriethoxysilane functionalized organics and metal alkoxide. The organic components are 3,3′-iminobispropylamine (IMPA), resorcinol (RSOL), diethylenetriamine (DETA), poly(ethyleneimine) (PEI), glycerol and a series of diols. The metal alkoxides are tetraethoxysilane (TEOS) and tetramethoxysilane (TMOS). These materials are spin coated onto bisphenol-A polycarbonate and CR-39 sheets and thermally cured to obtain a transparent coating of a few microns in thickness. Following the curing, the abrasion resistance is measured and compared with an uncoated control. It was found that the abrasion resistance of inorganic/organic hybrid coatings in the neat form or containing metal alkoxide can be very effective to improve the abrasion resistance of polymeric substrates. The adhesion tests show that the adhesion between coating and substrate can be greatly improved by treating the polymeric substrate surface with a primer solution of isopropanol containing 3-aminopropyltriethoxysilane (3-APS). The interaction between 3-APS and the polycarbonate surface was investigated by a molecular dynamics simulation. The results strongly suggest that the hydrogen bonding between the amino group of the 3-APS and ester group in the polycarbonate backbone are sufficiently strong to influence the orientation of the primer molecules. The abrasion resistance of these new coating systems is discussed in light of the structure of the organic components. All of these results show that these coating materials have excellent abrasion resistance and have potential applications as coating materials for lenses and other polymeric products.

Keywords: polycarbonate, abrasion resistance, sol-gel hybrid coatings, metal alkoxide, inorganic-organic polymers

Introduction

It is well known that many polymeric materials with excellent optical clarity and mechanical properties show poor abrasion resistance which greatly limit their applications. This has promoted the need for developing abrasion resistant hard coatings for organic polymeric substrates. Many of these coatings have been developed and are based on the use of metal alkoxides or organosiloxanes and generated by the sol-gel process [1–3].

Over the last decade, inorganic/organic hybrid network materials known as "ceramers" or "ormosils," [3–18] prepared by a sol-gel approach, have been developed and studied. In general, silicon, aluminum, titanium or zirconium metal alkoxides have been used as the starting inorganic materials. Various oligomers, such as silanol-terminated poly(dimethylsiloxane) (PDMS) and triethoxysilane capped poly(tetramethylene oxide) (PTMO) with low T_g, and polymers with high T_g, such as polyimides and poly(ether ketone) (PEK), [19, 20] have been used as

organic components. They have been processed by the sol-gel method to form transparent hybrid network materials in film form. Depending on the chemical structure and molecular weight of oligomers, the ratio of oligomer to inorganic content and reaction conditions, the resulting composite can vary from soft and flexible to brittle and hard materials. Many of these materials exhibit high optical clarity. In light of the success of making inorganic/organic composites, hybrid materials based on low molecular weight organics have been developed recently in our laboratory and successfully used as optical abrasion resistant coating materials for bisphenol-A polycarbonate substrates [21–24, 26]. These materials, which were prepared through a similar chemical approach but replacing the oligomer with a low molecular weight organic, showed optical clarity and much improved abrasion resistance. The Si—O—Si inorganic backbone structure along with the level of crosslinking has contributed to the high abrasion resistance, and the organics can contribute some other advantages of the resulting coating materials, such as improved adhesion between coating and polymer substrate, reduced shrinkage of the sol-gel material, and appropriate toughness relative to a pure brittle sol-gel coating.

In the preceding paper [26], a series of inorganic/organic coating materials were synthesized and tested. These materials were based on 3-isocyanatopropyltriethoxysilane functionalized diethylene triamine (DETA), glycerol, and diols as organic component and tetramethoxysilane (TMOS), aluminum tri-*sec*-butoxide, titanium sec-butoxide, and zirconium *n*-propoxide as inorganic components. They were spin coated onto bisphenol-A polycarbonate to obtain a transparent coating and thermally cured. It was found that compared to the already improved abrasion resistance of the coatings based on silane-functionalized organics (neat form), the incorporation of TMOS with the silane-functionalized organics can further improve the abrasion resistance. The level of adhesion determined by the direct "pull-off method" showed that the adhesion between coating and substrate can be greatly improved by treating the polycarbonate substrate with an oxygen plasma or a primer solution of isopropanol containing 3-aminopropyltriethoxysilane. Coating durability in a "hot-wet" condition, microhardness tests, UV absorption behavior, and the observation of abraded surfaces by Scanning Electron Microscopy (SEM) were also undertaken to evaluate these coatings.

The research reported in this paper is an extension of the above study. The abrasion resistance of new coatings systems in the neat form or containing metal alkoxide is investigated. New organic components include aromatic diol, resorcinol, 3,3′-iminobispropylamine (IMPA) and oligomeric species poly(ethylene imine) (PEI). An attempt was made to correlate the difference in chemical structure of the organic components to the observed differences in abrasion resistance. The influence of coating thickness to abrasion resistance was also investigated. Some of the coating materials reported in this paper have also been applied on sheets of diallyl diglycol carbonate resin (CR-39) and their abrasion resistance is determined and compared with the results from the bisphenol-A polycarbonate substrates. The effect of the primer 3-APS on the adhesion was studied by a molecular dynamics simulation method. While tetraethoxysilane (TEOS) is also used in the preparation of coating materials, the study will be focused on the coating systems containing TMOS since TMOS can provide better abrasion resistance.

Experimental

Materials

Diethylenetriamine (DETA), 3,3′-iminobispropyl amine (IMPA), glycerol, ethylene glycol, 1,4-butanediol, 1,6-hexanediol, resorcinol and tetraethoxysilane (TEOS) were obtained from the Aldrich Chemical Company and used without further treatment. 3-isocyanatopropyltriethoxysilane and tetramethoxysilane (TMOS) were purchased from Huls America Company. HPLC grade *N*, *N*-dimethylformamide (DMF), tetrahydrofuran (THF), 3-aminopropyltriethoxysilane (3-APS) and isopropanol (IPA) were obtained from the Aldrich Chemical Company. Bisphenol-A polycarbonate (1/16 inch Lexan®) sheets were obtained from General Electric Company and CR-39 sheets (diallyl diglycol carbonate resin) were purchased from Atlantic plastics company. These two sheet stock materials were used as the polymeric substrates. Poly(ethyleneimine) (PEI, Mn = 2000 g/mol) was obtained from Polysciences, Inc. The chemical formula of the metal alkoxides and organics are listed in Table 1.

Sample Preparation Procedure

Substrate Surface Treatment. In order to improve the adhesion between coating and substrate, the polycarbonate substrate was treated with a primer solution,

Table 1. The name and formula of metal alkoxide and organics utilized.

Name	Formula
Tetramethylsilane (TMOS)	$Si(OCH_3)_4$
Tetraethoxysilane (TEOS)	$Si(OC_2H_5)_4$
Titanium butoxide (Ti)	$Ti(OC_4H_9)_4$
Zirconium *n*-propoxide (Zr)	$Zr(OC_3H_7)_4$
Aluminum tri-*sec*-butoxide (Al)	$Al(OC_4H_9)_3$
Glycerol (GLYL)	$OH—CH_2—CH(OH)—CH_2—OH$
Ethylene glycol (ETYL)	$OH—CH_2—CH_2—OH$
Butanediol (BUOL)	$OH—CH_2—CH_2—CH_2—CH_2—OH$
Hexanediol (HXOL)	$OH—CH_2—CH_2—CH_2—CH_2—CH_2—CH_2—OH$
Resorcinol (RSOL)	$C_6H_4—1,3—(OH)_2$
Iminobispropylamine (IMPA)	$HN[(CH_2)_3NH_2]_2$
Diethylenetriamine (DETA)	$NH[(CH_2)_2NH_2]_2$
Poly(ethyleneimine) (PEI)	$(—NHCH_2CH_2—)_n$

0.5 wt.% 3-APS in IPA, in order to achieve good adhesion between coating and substrate. The substrates were cleaned with the primer solution and dried at room temperature for a few minutes before applying the coating. In the case of CR-39, an isopropanol solution containing 5 wt.% primer 3-APS was used in order to promote sufficient adhesion between coating and substrate.

Preparation of Triethoxysilane Functionalized DETA and IMPA. 50 mmol of DETA (or IMPA) and IPA were first mixed together in a 100 ml flask after which the solution was kept in an ice bath. Then, the desired amount of 3-isocyanatopropyltriethoxysilane (one mole of isocyanate to one mole of amine) was slowly added to the above solution and stirred for six hours. The amount of IPA was chosen such that it made up 30 weight percent in the final mixture. Infrared spectroscopy was used to monitor the functionalization reaction. The loss of isocyanate functionality (2273 cm^{-1}) as functionalization takes place was confirmed by FTIR. The reaction was complete when the characteristic absorption band due to the isocyanate group at 2270 cm^{-1} disappeared. This solution was stored under nitrogen before use.

Preparation of Triethoxysilane Functionalized Glycerol and Diols. In the preparation of functionalized glycerol and diols, 50 mmol of glycerol (or diols) and DMF were first mixed together in a 100 ml flask after which the solution was kept in a 80°C oil bath. Then the desired amount of 3-isocyanatopropyltriethoxysilane (one mole of isocyanate to one mole of alcohol) was slowly added to the above solution and stirred for two to four days. The amount of DMF was chosen such that it made up 30 weight percent in the final mixture. Again infrared spectroscopy was used to monitor the endcapping reaction. The loss of isocyanate functionality (2273 cm^{-1}) as endcapping takes place through the formation of urea linkages (1700 cm^{-1}) was confirmed by FTIR. This solution was then stored under nitrogen before use. These reactions can also be carried out at room temperature in the presence of a catalyst (i.e. dibutyltin dilaurate).

Preparation of Triethoxysilane Functionalized PEI. Because of the uncertainty in the number of accessible amine groups due to branching, a different approach was taken with respect to endcapping. The theoretical amount of the silane reagent required to functionalize the amine groups was first calculated based on the molecular weight of PEI. Then 70% of the calculated silane was added in a single dose. Thereafter the silane was added incrementally and the intensity of the —NCO peak was monitored after each addition. The addition was stopped when the isocyanate peak showed no discernible change in intensity after thirty minutes. Only about 80% of all imine groups are accessible to the reaction. This may be due to steric hindrance which reduce accessibility of imine groups to the bulky silane reagents.

Preparation of Coatings. A typical coating recipe consisted of adding aqueous HCl solution (0.5 N or 1 N) and IPA to a solution of functionalized IMPA (or glycerol, diols) and metal alkoxide (if desired) under brisk stirring. The mixture was allowed to stir for 1–2 minutes before being spin coated onto a polycarbonate substrate. The substrate used was a Lexan®grade 3.5″ × 3.5″ square polycarbonate sheet with a thickness

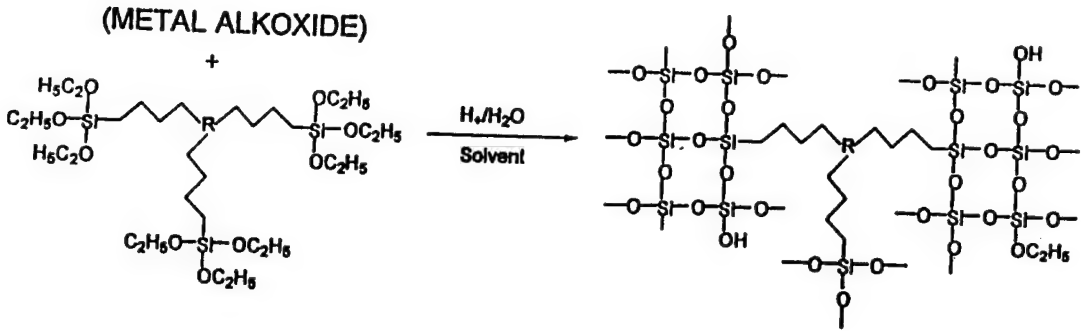

Fig. 1. Generalized reaction scheme for the conversion of functionalized organics into a cured hybrid network coating.

of 1/16″. The polycarbonate was cleaned with primer solution before being spin coated at a speed of 3600 rpm. The spin coated polycarbonate was then placed in a 60°C oven where the coating was allowed to dry until it became non tacky. The coating was then allowed to cure at 60°C for 1 hour and 130°C for 10 hours. The hydrolysis and condensation reactions of functionalized organics and metal alkoxides (if desired) took place when aqueous HCl solution was added. During this procedure, siloxane bonds were formed by the condensation of hydroxyl as well as methoxy groups which led to the formation of an inorganic backbone incorporated with organics as shown in Fig. 1. In related studies on similar coatings, the extent of reaction under similar conditions was estimated by using the weight loss data and ^{29}Si NMR measurements and found to be around 75% [26, 27]. In the case of the PEI coating systems, about 20% of imine groups remained unreacted during the endcapping reaction due to the steric hindrance. The remaining imine groups (unreacted groups in the endcapping reaction) will react with the catalyst (HCl) during the curing process. As a result, a higher HCl concentration (6 to 8 N instead of 0.5 to 1N) was needed. The coating thickness was found to be between 2–4 μm from SEM (scanning electron microscopy) measurements. Thicker coatings (10–12 μm by SEM) can be obtained by using a slower spin speed and/or a double coating technique. In the case of the CR-39 substrate, the curing temperature was 120°C instead of 130°C.

For the results presented in this paper, the sample designation will be denoted as MX-NY where M represents oligomer systems such as IMPA, GLYL (for glycerol), ETGL (for ethylene glycol), BUOL (for 1,4-butanediol), HXOL (for 1,6-hexanediol), RSOL (resorcinol), and PEI (for poly(ethyleneimine)), and N represents metal alkoxides (TMOS or TEOS). X indicates the weight percent of the functionalized organics relative to the weight of precursor metal alkoxide and Y the weight percent of precursor metal alkoxide relative to the weight of the functionalized organics. For example, IMPA60-TMOS40 means that the ratio of IMPA to TMOS is 60 to 40 (in weight) in the starting solution.

Characterization

Optical Abrasion Testing. The coated substrate was subjected to a Taber abrasion test in which standard CS-10 abrader wheels were utilized as reported in our previous studies [21–24, 26]. The loading on each wheel was increased to 500 g in contrast to 250 g that was utilized in our earlier work. The pure and coated substrates were allowed to be abraded cumulatively to 500 cycles. A flowing air stream was used to remove the abraded particles from the coating surface during the entire period of the test. A wear track is created by the rotating wheels. The conventional method of measuring wear by recording weight loss of the coating as a function of Taber cycles cannot be utilized here because the weight loss is too low for thin coatings. Instead, a Shimadzu CS-9000 UV-VIS spectrometer was used for a light transmittance test to measure the percent transmittance change in the wear track area relative to the unabraded materials. At intervals of 50, 100, 150, 200, 250, 350, 500 cycles (up to 1000 in some cases), light absorbance through the wear track was measured at a wavelength of 420 nm using a beam size of 10×0.4 mm.

The measurements were carried out in three-four different points within the wear track and the light absorbance values were averaged. The transmittance can be calculated as described elsewhere [21–24]. The results were plotted as the percent of transmission versus number of wear cycles. For comparison, an uncoated substrate served as the control. While it is realized that this method does not provide all features of abrasion wear rate or level of adhesion of the coating, it does provide a practical and sensitive quantitative index of optical clarity as influenced by uneven disruption of the coating layer (or control substrate).

Other Measurements

SEM (Scanning Electron Microscopy) was performed on a Cambridge Stereoscan 200 apparatus at 30 kV. Samples were coated with gold before performing SEM.

Microhardness tests were performed on a Fischerscope H-100 microhardness tester with a Vicker indenter.

Adhesion Measurement by Direct Pull Method. The so-called "direct pull method" was used to provide a quantitative index of adhesion of the thermally cured coating on the substrate [28]. This technique is based on first forming an adhesive bond with the coating and then applying a force normal to the coating-substrate interface to determine a value for practical adhesion. If the force required to pull the film off the substrate is F, the stress of adhesion, σ, per unit area is defined by

$$\sigma = F/A \tag{1}$$

where A (0.5 cm^2 in this study) is the cross-sectional area of the bar. It is assumed by applying Eq. (1) that the pulling force is normal to and uniformly distributed across the area A (i.e. no shear stress) and fracture occurs at the film-substrate interface. To meet this criteria, samples must be prepared carefully to maintain a flat surface. Also, good alignment of the stress-strain crosshead elements must be maintained.

The coated polycarbonate or CR-39 substrates were cemented to aluminum rods using an epoxy resin adhesive (special F epoxy, Devcon corp.) for the adhesion between rod and coated surface and a methacrylate ester adhesive (plastic welder, Devcon Corp.) for the adhesion between rod and uncoated surface. After the adhesives were cured at room temperature for 16 hours (instructions of adhesive manufacturer), the samples were tested in a Instron (Model 1122).

Molecular Dynamics Simulation

In order to understand the physical interactions and geometric orientations of the primer with respect to the polycarbonate surface, the polymer-primer system was simulated using the molecular dynamics (MD) method. The molecular simulations were carried out on a Stardent-750 workstation using a commercial software, Polygraf (version 3.2.1 from MSI Inc.). An extended chain of a polycarbonate (10-mer) molecule was packed in a unit cell with dimensions of $25 \times 25 \times 250$ Å. The longest side corresponded to the z-axis and the xy-plane reflected a small surface of the polycarbonate film. When periodic boundary conditions were applied the central simulation cell was treated as part of a two dimensional macroscopic system [29].

Results and Discussion

Abrasion Resistance

The Effect of Coating Thickness. In order to compare the abrasion resistance between different coating systems without considering the effect of coating thickness, an important condition has to be satisfied: all the damage caused by the abrader wheels must be confined within the coating layer at the end of test. That means the coating layer has to be thick enough and the adhesion between coating layer and substrate should be sufficient. In our previous study [26], it was shown that the adhesion of these sol-gel coatings can be greatly improved by treating the polymeric substrate with an oxygen plasma or a primer solution of isopropanol containing 3-APS, and the different surface treatments have little influence on the abrasive resistance. In the present study, since more severe test conditions are utilized, e.g. a heavier loading on each abrader wheel (500 g instead of 250 g), the influence of coating thickness had to be considered. Therefore, the polymeric substrates coated with the same coating but different thickness were made and their abrasion resistance are compared in Fig. 2. The results shows that the coating thickness has little to no influence on abrasion resistance up to at least 500 cycles. High abrasion resistance was maintained even at 1000 cycles. This demonstrates that under our test conditions, the coating thickness range we have investigated has no significant influence on abrasion resistance and all the damage is still confined within the coating layer.

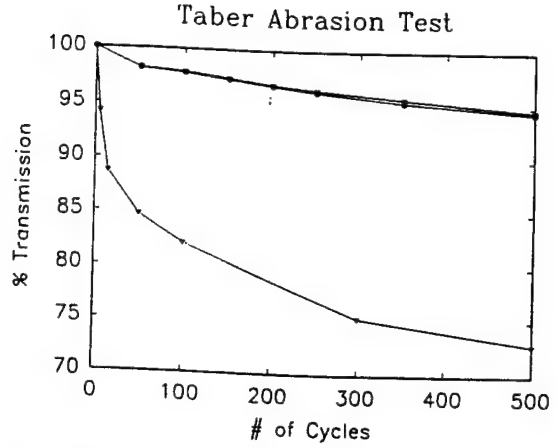

Fig. 2. Light transmittance as a function of number of wear cycles for polycarbonate samples coated with same coating but different thickness: (●) single coated, ca. 4 μm; (▽) double coated, ca. 11 μm; (▼) PC control (no coating). The coating temperature was 130°C and all the coatings were on a ASP primer treated substrate.

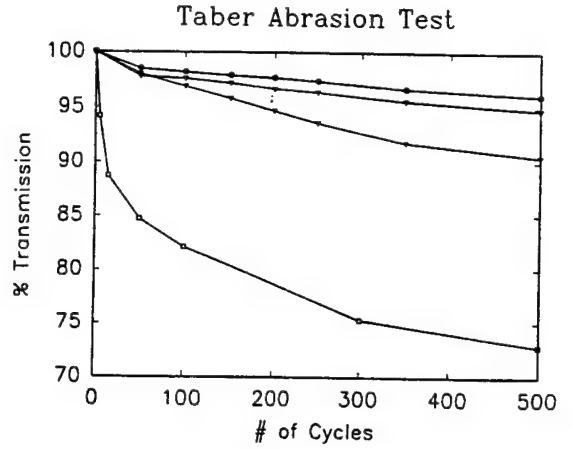

Fig. 3. Light transmittance as a function of number of wear cycles for uncoated and coated polycarbonate samples: (□) PC control (no coating), (▼) PEI60-TMOS40, (▽) RSOL60-TMOS40, (●) IMPA60-TMOS40. The coating temperature was 130°C and all the coatings were on a 3-APS primer treated substrate.

Coating Systems Containing TMOS. In our previous studies it was shown that the coating systems containing TMOS clearly possess a much higher abrasion resistance than the corresponding "neat" coatings without TMOS [26]. That is, the incorporation of TMOS with triethoxysilane endcapped DETA, glycerol, and diols can significantly improve the abrasion resistance. The high abrasive resistance is attributed to the increase of Si—O—Si inorganic backbone structure introduced by TMOS. In order to further study the influence of the organic structure on the abrasion resistance, new organics IMPA, RSOL, and oligomer poly(ethylene imine) were used with TMOS to prepare coatings. The abrasion resistance of three new coating systems were measured and the results are shown in Fig. 3 as a plot of percent transmission as a function of the number of Taber abrader cycles. The typical error bar behavior was marked on a selected curve in Fig. 5. In the present study, recall that the loading of each abrader wheel was increased to 500 g in order to better separate coating performance. It was found that all the coating systems discussed here had much better abrasive resistance than uncoated polycarbonate. Figure 4 compares the abrasion resistance of three new functionalized organic coating systems in the neat form and with the addition of 40 wt.% TMOS (relative to total amount of TMOS and functionalized organics). Again, the incorporation of TMOS significantly improves the abrasion resistance relative to the neat form without added TMOS.

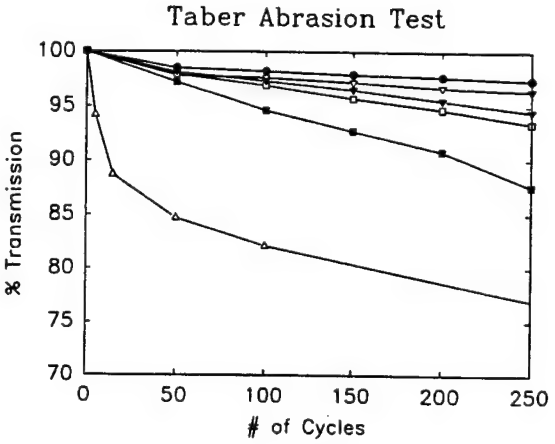

Fig. 4. Light transmittance as a function of number of wear cycles for coated polycarbonate samples. The curing temperature was 130°C: (△) PC control, (■) RSOL100, (□) IMPA100, (▼) DETA100, (▽) RSOL60-TMOS40, (●) IMPA60-TMOS40. All the coatings were on a 3-APS primer treated substrate.

Figure 5 compares the abrasion resistance of IMPA coating systems containing different amounts of TMOS. It was found again that TMOS can greatly improve the abrasion resistance and the abrasion resistance increased as the amount of TMOS is increased. At least 30 wt.% of TMOS in the starting solution is necessary to obtain enhanced abrasive resistance. However, the increase of TMOS amount also increases the coating shrinkage during the drying and curing processes. As a result, a crack-free coating is unable to

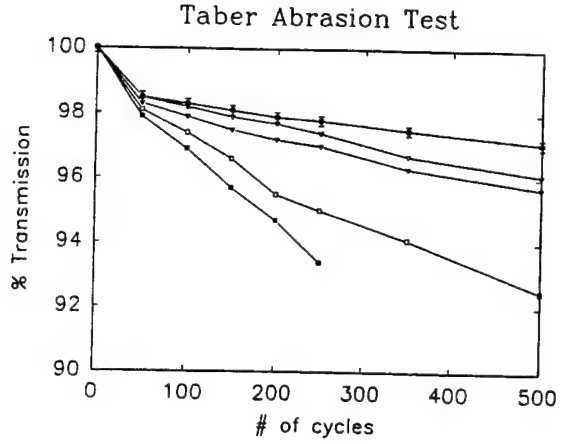

Fig. 5. Light transmittance as a function of number of wear cycles for coated polycarbonate samples. The curing temperature was 130°C: (■) IMPA100, (□) IMPA80-TMOS20, (▼) IMPA70-TMOS30, (▽) IMPA60-TMOS40, (●) IMPA40-TMOS60. The error bar behavior of all samples is marked in the curve for IMPA40-TMOS60. All the coatings were on a 3-APS primer treated substrate.

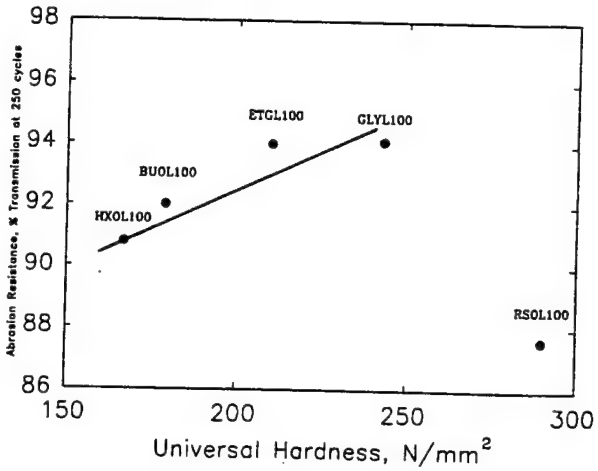

Fig. 6. The relationship between the abrasion resistance of glycerol and diol coatings and indentation hardness.

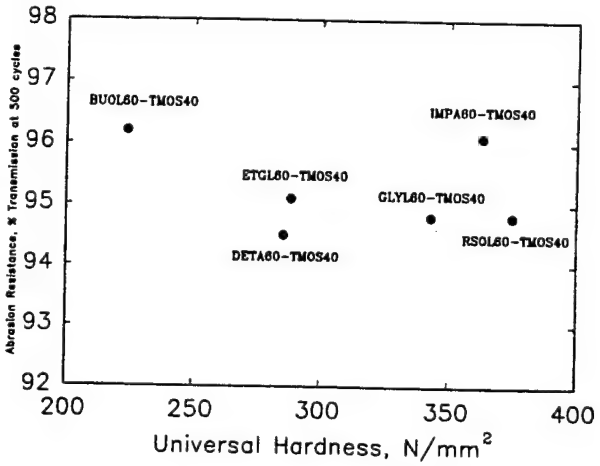

Fig. 7. The relationship between the abrasion resistance of TMOS-containing coatings and indentation hardness.

be obtained when the TMOS content is higher than 60 wt.%. Similar results have also been observed for RSOL-TMOS and PEI-TMOS coatings. It should be pointed out here that for PEI, the remaining amine groups will react with the catalysts HCl which the complicates the curing process.

Discussion on the Influence of the Structure of Organics to Abrasion Resistance. So far seven different silane-functionalized organics have been discussed that were utilized to make coatings either in the neat form or in the presence of metal alkoxide such as TMOS. By comparing their difference in abrasion resistance, useful information about how the structure of organics influence the abrasion resistance may be obtained which will be helpful in guiding the selection of organics for future research.

Figure 6 correlates the observed abrasion resistance at 250 cycles with their indentation hardness. It was found that for glycerol and the aliphatic diols, the abrasion resistance systematically increased as the indentation hardness increased. In these cases, the abrasion resistance is inversely proportional to the flexibility of the low molecular weight moiety. The aromatic diol, resorcinol, is an exception which displayed poor abrasion resistance but high indentation hardness. However, no clear correlation was found between abrasion resistance and indentation hardness when TMOS was added into the coating systems, as shown in Fig. 7. While it appears that increasing the TMOS content always increases abrasion resistance, the change of organic components at a given TMOS composition (40 wt.% in this study) has a relatively small effect on the abrasion resistance compared to the cases of non-TMOS coating systems, as shown in Fig. 8. For example, the coating from BUOL60-TMOS40 and IMPA60-TMOS40 both had excellent abrasion resistance but totally different indentation hardness. Clearly the content of organics decreased in the final coating materials as TMOS was added which helps explain the smaller difference in abrasion resistance between different organics. It should also be no surprise that sometimes abrasion resistance can not be correlated to indentation hardness. The relationship between

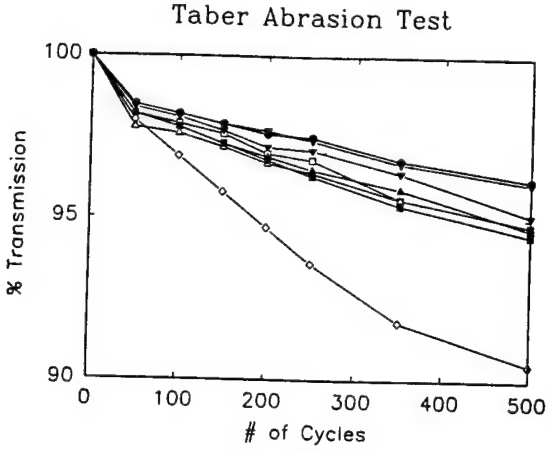

Fig. 8. Light transmittance as a function of number of wear cycles for coated polycarbonate samples. The curing temperature was 130°C: (◊) PEI60-TMOS40, (■) DETA60-TMOS40, (▲) RSOL60-TMOS40, (△) HXOL60-TMOS40, (□) GLYL60-TMOS40, (▼) ETGL60-TMOS40, (▽) IMPA60-TMOS40, (●) BUOL60-TMOS40. All the coatings were on a 3-APS primer treated substrate.

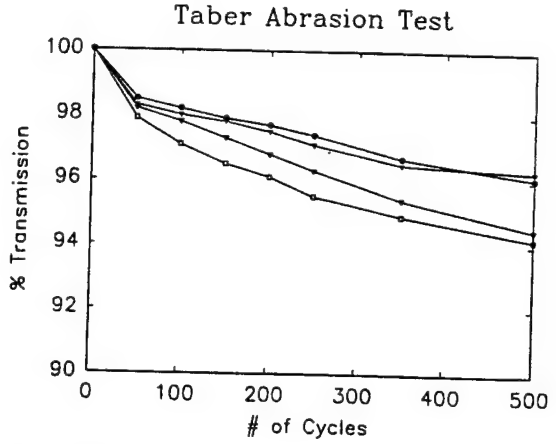

Fig. 9. Light transmittance as a function of number of wear cycles for coated polycarbonate samples. The curing temperature was 130°C: (□) DETA55-TEOS45, (▽) DETA60-TMOS40, (▼) IMPA55-TEOS45, (●) IMPA60-TMOS40. All the coatings were on a 3-APS primer treated substrate.

abrasion and other physical properties of many coating materials, including those based on polymers and ceramics, can be better explained by Selwood's theory [30]. He found that the abrasion resistance could be expressed in terms of two parameters: indentation hardness and extensibility. A highly rigid backbone is not necessarily the most desirable. A certain degree of flexibility can enhance wear resistance. For our coating systems, the hardness of the coating materials is mainly determined by the TMOS content. The high abrasion resistance at high TMOS content is attributed to the increase of Si—O—Si inorganic backbone structure and higher level of crosslinking introduced by TMOS. The major effects of varying the structure of organics at a given TMOS content are to affect the extensibility and level of crosslinking of the final materials. Other roles of the organics are to improve adhesion between coating and polymer substrate, reduce shrinkage of the sol-gel coating, and offer appropriate extensibility relative to a pure brittle sol-gel coating.

TEOS-Containing Coating Systems. Since the incorporation of TMOS in functionalized organics coating systems can significantly increase the abrasion resistance, it is natural to also consider TEOS as an alternative inorganic alkoxide component in view of the more favorable economics. The disadvantage of using TEOS is that there is more shrinkage during the drying process due to the loss of the larger ethoxy group. The preliminary results for two TEOS and TMOS-containing coating systems are shown in Fig. 9. A higher HCl concentration (2 M instead of 0.5 M) was used considering the slower hydrolysis and condensation rates of TEOS. Figure 9 compares the abrasion resistance between the coatings from TEOS and functionalized organics and that from TMOS and functionalized organics. In order to compare the coatings with *similar inorganic content in the final coating materials*, a higher TEOS content was used in the starting solution. The results in Fig. 9 shows that by using *suitable reaction conditions*, nearly the same improvement in abrasion resistance can also be achieved by TEOS.

Coating Application to CR-39 Substrates. Compared to many of the other optically transparent polymers, CR-39, diallyl diglycol carbonate resin, is a more highly scratch-resistant crosslinked polymer. It is polymerizable with sufficient optical quality and of high chemical and mechanical stability. As a result, it has been widely used as the materials for eyeglass lenses. However, its surface hardness is still far well below that of inorganic glasses. The abrasion resistance of CR-39 can be further improved by using our abrasion resistant coating materials if enough adhesion between coating and CR-39 substrate can be achieved. Application of specific coating systems were investigated as shown in Fig. 10 where the abrasion resistance of coated CR-

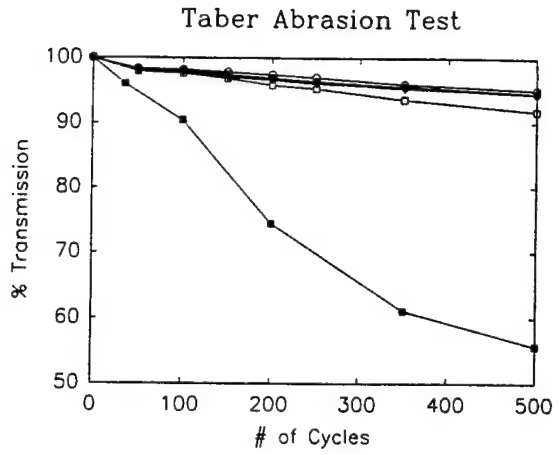

Fig. 10. Light transmittance as a function of number of wear cycles for coated CR-39 samples. The curing temperature was 120°C: (■) CR-39 control, (□) PEI60-TMOS40, (▼) RSOL60-TMOS40, (▽) DETA60-TMOS40, (●) IMPA60-TMOS40, (○) BUOL60-TMOS40. All the coatings were on a 3-APS primer treated substrate.

39 materials are compared with the uncoated CR-39 substrate. It was found again that these coating systems provided a much better abrasive resistance than uncoated CR-39. The adhesion between coating and CR-39 can also be greatly improved by pre-treating the CR-39 substrate with a isopropanol solution of primer 3-APS. As the data in Table 2 display, a 5 wt.% primer solution provides a distinctly greater improvement in the adhesion behavior than does a 0.5 wt.% primer solution. It is noteworthy that the adhesion was sufficient when a 5 wt.% primer solution was used and all the damage caused by the abrader wheels remained within the coating layer up to at least 500 cycles. It is still not clear at this time why a higher concentration primer solution was needed in the case of CR- 39. This may be related to the crosslinked structure of CR-39 or to its different chemical structure compared to bisphenol-A polycarbonate.

Table 2. Results of direct pull-off test for coated CR-39 substrate materials.

Sample	Strength $\sigma = F/A$ (kg/cm^2)								
	1	2	3	4	5	6	7	Ave.	Max.
DETA-TMOS									
0.5 wt.% primer	62	43	91	107	41	109	39	70	109
5 wt.% primer								all > 200	
BUOL-TMOS									
0.5 wt.% primer	139	127	52	77	58	97		106	139
5 wt.% primer								all > 200	

Primer-Polymeric-Substrate Interaction Study by Molecular Dynamics Simulation

Even though 3-APS is mainly used as the adhesion promoter for glass or mineral substrates, it is also effective in bonding coatings to some polymeric surfaces [31–32]. The data in this paper and previous studies clearly show that it can greatly improve the bonding between our coatings and polycarbonate substrates. In order to better understand the physical interactions and geometric orientations of the primer with respect to the polycarbonate surface, the polymer-primer system was simulated using the molecular dynamics (MD) method. The molecular dynamics simulation involved integrating Newton's laws of motion for all the atoms in the unit cell. The temperature, volume and the number of atoms in the simulation cell were kept constant. The total potential energy of the system E, was described by

$$E = E_{\text{stretch}} + E_{\text{bend}} + E_{\text{tors}} + E_{\text{inv}} + E_{\text{vdw}} + E_{\text{hyd}} \quad (2)$$

where the terms on the right-hand side represent the contribution from bond stretching, bond angle bending, torsional, out-of-plane inversions, van der Waals and hydrogen-bonding interactions. All the default settings in the Dreiding (2.21) force field [33] was used. The hydrogen bonding interactions between a suitable acceptor element and a hydrogen atom bonded to a donor element (N, O) were modeled as a 12-10 Lennard-Jones potential weighted by the cosine of hydrogen bonding angle between the donor-H-acceptor atoms.

The molecular dynamics simulation used a time step of 0.001 picosecond (10^{-12} sec, ps) and was run at 300°K. Structural and thermodynamic data from the simulation were recorded at intervals of 0.5 ps. The extended chain began to contract rapidly and because of the periodic conditions, interacted with its images in the x and y directions to form a film. A similar collapse process was reported in the simulation of polybutadiene film [19]. The simulation was carried out for a total of 200 ps to reach thermodynamic equilibrium of the system. The polymer coil dimensions were also found to have reached a constant value.

After the completion of film formation, three primer molecules (3-APS) were introduced into the unit cell with an arbitrary configuration and the MD simulation was performed for a total of 150 ps. Figure 11A shows a "schematic" representation of one primer molecule and the polycarbonate backbone. During the simulation, hydrogen bonding interactions between the amine

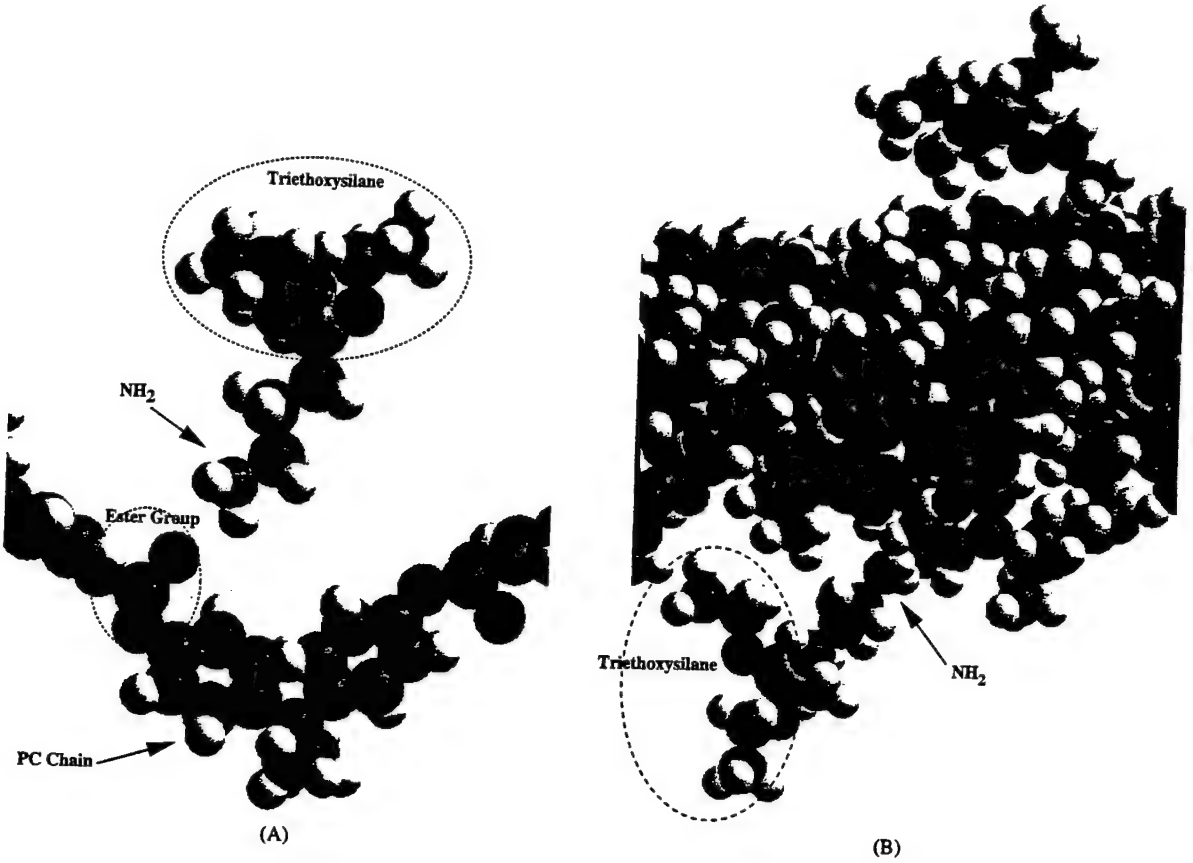

Fig. 11. (A). An arbitrary initial configuration of one primer molecule and the polycarbonate backbone. (B). A side view of two 3-APS molecules hydrogen bonded with polycarbonate—one such interaction is indicated by the arrow pointing to the amine-carbonate ester interaction.

group of the primer and oxygen atoms on the polycarbonate were noted. Figure 11B is a "snapshot" of the configuration at 150 ps and the arrows point to two of the three 3-APS molecules hydrogen bonded to the polycarbonate surface at the ester sites in the backbone. One can also clearly notice that the smaller amine groups are close to the polymer "surface" while the bulkier triethoxysilanes are pointed away from the "surface". Figure 12 plots both the instantaneous and the average hydrogen bond energies in the system against the simulation time. At approximately 5 ps the first primer molecule formed a hydrogen bond with the polymer surface. The attractive hydrogen bonding energy increased to −42 kcal/mol around 70 ps when the second primer molecule also found the acceptor oxygen atom on the polycarbonate substrate. Once hydrogen bonded, these molecules remained close to polymer surface for the entire simulation. The third 3-APS molecule interacted with the polymer surface but did not satisfy the hydrogen bonding criteria during the simulation period. Had a longer simulation time been utilized, it is expected that this third 3-APS molecule would have "docked" with the polycarbonate substrate.

The above analysis strongly suggests that hydrogen bonding interactions are sufficiently strong to influence the orientation and coverage of the polymer surface. The amino group interacts with the ester group on the polycarbonate substrate through hydrogen bonding. The alkoxy group can hydrolyze to silanols (SiOH), which then chemically bond to the coating through cocondensation with the alkoxy groups in the coating. As a result, the primer can act as a bridge to bond the coating with the substrate. It should also be pointed out that the amino group in 3-APS may possibly chemically react with hydroxyl or carboxyl groups (at the

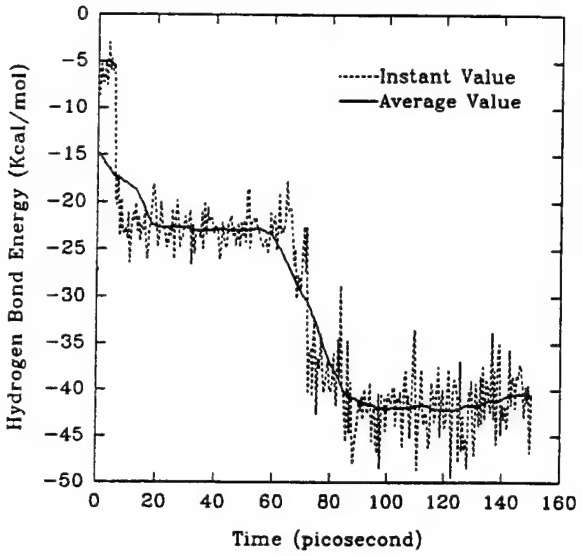

Fig. 12. Plot of hydrogen bond energy in the system against the simulation time.

end of polymer chains) on the polycarbonate surface during the curing.

SEM Investigations

Due to the extensive discussion in this issue and the similar surface texture between the new coatings and the previous coatings [22–24], only three SEM micrographs are presented in this paper. The SEM micrographs in Fig. 13 show the surface texture for polycarbonate coated with IMPA-TMOS, RSOL-TMOS and PEI-TMOS coatings. Polycarbonate is abraded through a mechanism where the surface is gradually roughened by scratches as we have reported earlier [22–24]. The IMPA-TMOS and RSOL-TMOS coatings appear to be abraded more by the same chipping mechanism reported earlier for the DETA-TMOS coatings [14]. However, due to the more severe test conditions, i.e. higher loadings on the abrader wheels, the surface of the coating between major scratches is no longer scratch free. For the PEI-TMOS coating, more damage is observed due to its poorer abrasion resistance.

Conclusions

Novel abrasion resistant coating materials prepared by the sol-gel method have been developed and applied on the polymeric substrates

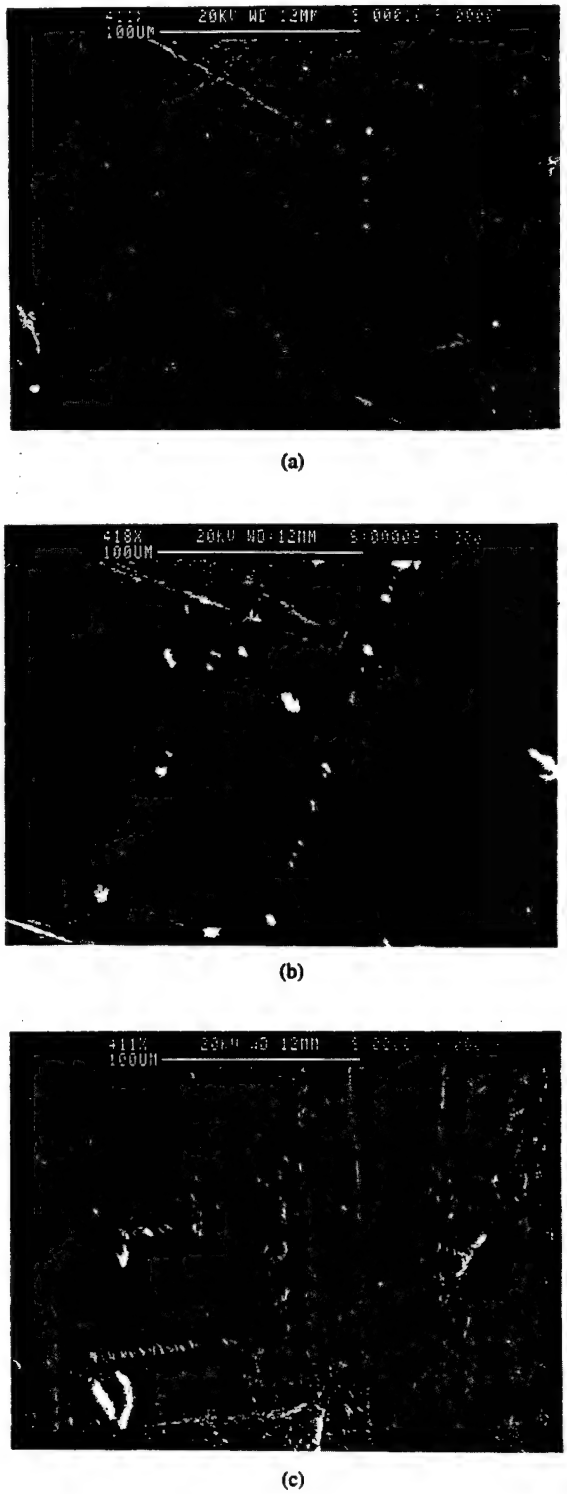

Fig. 13. SEM micrographs of wear track of coated polycarbonate samples: (a) IMPA60-TMOS40, 500 cycles; (b) RSOL60-TMOS40, 500 cycles; (c) PEI60-TMOS40, 500 cycles.

of either bisphenol-A polycarbonate or diallyl diglycol carbonate resin (CR-39). These coatings are inorganic/organic hybrid materials synthesized from 3-isocyanatopropyltriethoxysilane functionalized organics and metal alkoxide. These materials are spin coated onto bisphenol-A polycarbonate and CR-39 sheet and thermally cured to obtain a transparent coating of a few microns in thickness. Following the curing, the abrasion resistance is measured and compared between uncoated and different coating systems. It was found that the abrasion resistance of inorganic/organic hybrid coatings in the neat form or containing metal alkoxide alkoxide can be very effective to improve abrasion resistance. The adhesion tests show that the adhesion between coating and substrate can be greatly improved by treating the polymeric substrate surface with a primer solution of isopropanol containing 3-aminopropyltriethoxysilane. The interaction between 3-APS and the polycarbonate surface was investigated by a molecular dynamics simulation and the analysis strongly suggest that the hydrogen bonding between the amino group of 3-APS and the ester group in the polycarbonate backbone was sufficiently strong to influence the orientation of the primer molecules.

Acknowledgments

The authors acknowledge the financial support of the Air Force Office of Research. The support of the National Science Foundation Science and Technology Center for High Performance Adhesives and Composites at Virginia Polytechnic under contract number DMR8809714 is greatly appreciated. The authors would also like to thank Dr. Jim Tonge (Dow Corning Corporation) for performing the microhardness tests.

References

1. J. Kasi, JPn. Kokai Tokkyo Koho, JP6335, 633 (88,35,633).
2. R. Nass, E. Appac, W. Glaubitt, and H. Schmidt, J. Non-Cryst. Solids **121**, 370 (1990).
3. H. Schmidt and H. Walter, J. Non-Cryst. Solids **121**, 428 (1990).
4. H. Schmidt, Mat. Res. Soc. Symp. Proc. **32**, 327 (1984).
5. G.L. Wilkes, B. Orler, and H.H. Huang, Polymer Preprints **26**(2), 300 (1985).
6. H. Huang and G.L. Wilkes, Polymer Bulletin **18**, 455 (1987).
7. H. Huang, R.H. Glaser, and G.L. Wilkes, ACS Symp. Ser. **360**, 354 (1988).
8. H. Huang and G.L. Wilkes, Polymer **30**, 2001 (1989).
9. Y. Hu and J.D. Mackenzie, Mat. Res. Soc. Symp. Proc. **271**, 681 (1992).
10. Y. Hu and J.D. Mackenzie, J. Mat. Sci. **27**, 4415 (1992).
11. J.D. Machenzie, Y.J. Chung, and Y. Hu, J. Non-Cryst. Solids, **147 & 148**, 271 (1992).
12. J.E. Mark and S.-J. Pan, Makromol. Chem. Rapid Commun. **3**, 681 (1982).
13. J.E. Mark, C.-Y. Jiang and M.-Y. Tang, Macromolecules **17**, 2613 (1984).
14. J.E. Mark, J. Appl. Polym. Sci., Appl. Polym. Symp. **50**, 273 (1992).
15. J.E. Mark, *Frontier of Polym. & Advanced Mater.*, edited by P.N. Prasad (Plenum Press, New York, 1994), p. 403.
16. B.M. Novak, Advanced Materials **5**, 422 (1993).
17. H. Schmidt, Mat. Res. Soc. Symp. Proc. **171**, 3 (1990).
18. B.M. Novak and R.H. Grubbs, J. Am. Chem. Soc. **110**, 7542 (1988).
19. S. Wang, Z. Ahmad, and J.E. Mark, Macromol. Reports **A31**, 411 (1994).
20. J.L.W. Noell, G.L. Wilkes, D.K. Mohauty, and J.E. McGrath, J. Appl. Polym. Sci. **40**, 1177 (1990).
21. C. Betrabet and G.L. Wilkes, Polymer Preprints **32**(2), 286 (1992).
22. B. Tamami, C. Betrabet, and G.L. Wilkes, Polymer Bulletin **30**, 39 (1993).
23. B. Tamami, C. Betrabet, and G.L. Wilkes, Polymer Bulletin **30**, 393 (1993).
24. B. Wang and G.L. Wilkes, J. Macromol. Sci-Pure Appl. Chem. **A31**, 249 (1994).
25. B. Wang, G.L. Wilkes, C.D. Smith, and J.E. McGrath, Polymer Commun. **32**, 400 (1991).
26. J. Wen and G.L. Wilkes, J. Inorganic & Organometallic Polymers **5**, 000 (1995).
27. C. Betrabet and G.L. Wilkes, J. Inorganic & Organometallic Polymers **4**, 343(1994).
28. M. El-Shabsy, Period. Polytech. Electr. Eng. **25**, 283 (1981).
29. Y. Zhan and W.L. Mattice, Macromolecules **27**, 7056 1994.
30. A. Selwood, Wear **4**, 311 (1961).
31. W.D. Bascom, *Eng. Mater. Handbook* (ASM International EDS., 1990) **V3**, p. 254.
32. E.P. Plueddemann, *Adhesion Aspects of Polymeric Coatings*, edited by K.L. Mittal (Plenum Press, New York, 1983), p. 319.
33. S.L. Mayo, B.D. Olafson, and W.A. Goddard III, J. Phys. Chem. **94**, 8897 (1990).

Appendix 2

Journal of Inorganic and Organometallic Polymers, Vol. 5, No. 4, 1995

Synthesis and Characterization of Abrasion Resistant Coating Materials Prepared by the Sol-Gel Approach: I. Coatings Based on Functionalized Aliphatic Diols and Diethylenetriamine

J. Wen[1] and G. L. Wilkes[1, 2]

Received February 10, 1995; revised June 14, 1995

The synthesis of inorganic/organic hybrid materials has been undertaken and used as abrasion resistant coatings for polymeric substrates by the sol-gel method. The organic components are diethylenetriamine (DETA), glycerol, and a series of aliphatic diols which are functionalized by 3-isocyanatopropyltriethoxysilane. The inorganic components are tetramethoxysilane (TMOS), aluminum tri-*sec*-butoxide, titanium *sec*-butoxide and zirconium *n*-propoxide. Solutions of these materials are spin coated onto bisphenol-A polycarbonate sheet and thermally cured to obtain a transparent coating of a few microns in thickness. Following the curing, the abrasion resistance is measured and compared with a control having no coating. It was found that the abrasion resistance of inorganic/organic hybrid coatings in the neat form or containing additional silicon, titanium, zirconium, and aluminum alkoxides can be very effective to improve abrasion resistance. The adhesion tests show that the adhesion between coating and substrate can be greatly improved by treating the polymeric substrate surface with an oxygen plasma or a primer solution of isopropanol containing 3-aminopropyltriethoxysilane. Other experiments, such as the abrasion resistance tests following conditioning in a "hot-wet" condition (boiling water treatment), microhardness tests, UV absorption behavior, and the observation of abraded surfaces, were also undertaken in order to evaluate these coating materials.

KEY WORDS: Polycarbonate; abrasion resistance; sol-gel hybrid coatings; metal alkoxide; diethylenetriamine; inorganic–organic polymers.

[1] Department of Chemical Engineering, Polymer Materials and Interfaces Laboratory, Virginia Polytechnic Institute and State University, Blacksburg, Virginia 24061.
[2] To whom correspondence should be addressed.

1053-0495/95/1200-0343$07.50/0

INTRODUCTION

Many materials with suitable bulk properties often can not be utilized for a specific application because of their poor surface properties. For example, transparent synthetic thermoplastics, such as polycarbonate and polymethylmethacrylate, offer excellent optical clarity and mechanical properties, and have been widely used in many applications. However, their optical quality decreases rapidly with surface wear because the abrasive resistance of these materials is poor. As a result, application of these and related optically clear materials is greatly limited by their non-abrasive resistant surface. The abrasive resistance of these polymers can be greatly improved by coating them with a hard coating. Many of these coatings are based on the use of metal alkoxides or organosiloxanes and generated by the sol-gel process [1–4].

Recently, organic/inorganic hybrid materials known as "Ceramers" [5–9], or "Ormocers" [10–12], prepared by a sol-gel approach, have been developed and studied. Depending on the chemical structure of the organic component and inorganic content, the resulting composite can vary from soft and flexible to brittle and hard materials. Many of these materials exhibit optical clarity. More recently, similar hybrid materials based on low molecular weight organics have been developed in our laboratory and successfully used as optical abrasion resistant coating materials for a polymer substrate [13–17]. Two kinds of coating systems have been studied. One is the organic/inorganic hybrid system based on triethoxysilane endcapped low molecular weight polyethyleneimine while other examples include functionalized di- and tri- aliphatic and aromatic amines, and bis and tris maleimides [13–16]. These coating materials were prepared through a sol-gel process and showed optical clarity and improved abrasion resistance. The high abrasive resistance has been attributed to the Si–O–Si inorganic backbone structure along with the level of crosslinking. In addition, the organics can often provide improvement in the adhesion between coating and polymer substrate by increasing the polarity of the coating materials, reduce the shrinkage of sol-gel coating, and offer some flexibility relative to a pure brittle sol-gel coating. Another coating system reported earlier was obtained by incorporating metal alkoxides (e.g., titanium and zirconium) with triethoxysilane endcapped trifunctional aliphatic amine, diethylenetriamine, also through a sol-gel process [16, 17]. The final properties of the resulting hybrid coating materials were found dependent upon the molecular weight of the starting organic, their structure and the type and content of any added metal alkoxide. The coating systems containing additional metal alkoxide were also found to be optically transparent. As an aside, the incorporation of metal alkoxides can also offer

some other advantages to the coating materials. For example, high refractive index transparent materials can be obtained when using titanium tetraisopropoxide as the metal alkoxide [18, 19]. High toughness and thermal shock resistance can be achieved by using zirconium alkoxide [20].

The starting organic components utilized for the work presented in this paper were 3-isocyanatopropyltriethoxysilane functionalized DETA, glycerol and a series of aliphatic diols. The inorganic components were tetramethoxysilane (TMOS), aluminum tri-*sec*-butoxide, titanium *sec*-butoxide, and zirconium *n*-propoxide. All coating materials were spin coated onto bisphenol-A polycarbonate and thermally cured to obtain a transparent coating. The optical abrasion behavior, the adhesion between coating and substrate and some other properties will be discussed.

EXPERIMENTAL

Materials

Diethylenetriamine (DETA), ethyl acetoacetate, titanium butoxide, zirconium *n*-propoxide, aluminum tri-*sec*-butoxide, dibutyltin dilaurate, glycerol, ethylene glycol, butanediol, 3-aminopropyltriethoxysilane (3-APS), isopropanol (IPA) and hexanediol were obtained from the Aldrich Chemical Company and used without further treatment. 3-isocyanatopropyltriethoxysilane and tetramethoxysilane (TMOS) were purchased from Hüls America Company. HPLC grade N, N-dimethylformamide (DMF). Bisphenol A polycarbonate (1/16 inch Lexan®) sheets were obtained from the General Electric Company and used as the polymeric substrate.

Sample Preparation Procedure

Substrate Surface Treatment

In some cases, the polycarbonate substrate was treated with an oxygen plasma to enhance the adhesion between coating and substrate. The surface of the polycarbonate substrate was first cleaned with IPA and dried. The sample was then placed in the plasma chamber which was flushed with oxygen for several minutes. Oxygen plasma gas (generated by a March Plasmod apparatus) was then utilized to treat the substrate under a vacuum of 1 torr for two minutes at a power of 100 watts and a radio frequency of 13.56 MHz. As an alternative to plasma treatment, a primer solution, 0.5 wt.(%) 3-aminopropyltriethoxysilane in IPA, was used to treat the substrate surface in order to achieve good adhesion between coating and substrate. The substrates were cleaned with the primer solution

and dried in room temperature for a few minutes before applying the coating.

Preparation of Triethoxysilane Functionalized DETA

Five grams of DETA and 19.6 g IPA were mixed together in a 100 ml flask after which the solution was kept in an ice bath. Then, 39.4 g of 3-isocyanatopropyltriethoxysilane was slowly added to the above solution and stirred for six hours. Infrared spectroscopy was used to monitor the reaction. The loss of isocyanate functionality (2273 cm^{-1}) as endcapping takes place was confirmed by FTIR. This solution was stored under nitrogen before use.

Preparation of Triethoxysilane Functionalized Glycerol and Diols

In the preparation of functionalized glycerol and diols, 5 g of glycerol and 19.6 g DMF were mixed together in a 100 ml flask after which the solution was kept in a 80°C oil bath. Then 39.4 g of 3-isocyanatopropyltriethoxysilane were slowly added to the above solution and stirred for 2–4 days. Again infrared spectroscopy was used to monitor the functionalization reaction. The loss of isocyanate functionality (2273 cm^{-1}) as reaction takes place through the formation of urethane linkages (1700 cm^{-1}) was confirmed by FTIR. This solution was then stored under nitrogen before use. These reactions can also be carried out at lower temperature in the presence of a catalyst (i.e., dibutyltin dilaurate).

Preparation of Coatings

A typical coating recipe consisted of adding aqueous HCl solution (0.5 N or 1 N) and IPA to a solution of functionalized DETA (or glycerol, diols) and metal alkoxide (if necessary) under brisk stirring. The mixture was allowed to stir for 1–2 min before being spin-coated onto a polycarbonate substrate. The substrate used was a Lexan® grade 3.5″ × 3.5″ square polycarbonate with a thickness of 1/16″. The polycarbonate was cleaned with isopropanol before being spin-coated at a speed of 3600 rpm. The spin-coated polycarbonate was then, placed in a 60°C oven where the coating was allowed to dry until it became non-tacky. The coating was then allowed to cure at 60°C for 1 hr and 130°C for 10 hr. Other curing times and temperatures have also been used in order to study their effects on abrasion resistance. The coating thickness was found to be between 2–4 μm from SEM (scanning electron microscopy) measurements.

The zirconium and aluminum alkoxide containing systems are very reactive for both the hydrolysis and condensation reactions relative to those based on silicon. Therefore a ligand, ethyl acetoacetate, was used to reduce the reactivity and avoid undesirable precipitation of zirconium or

aluminum oxide particulates. The ligand was added into the systems before adding aqueous HCI solution. The molar ratio of ligand to metal alkoxide was kept at 0.5 in all cases. Finally, an aqueous HCI (0.5M) solution was mixed with isopropanol before being added into the system.

For the results presented in this paper, the sample designation will be denoted as MX-NY where M represents functionalized organics such as DETA, GLYL (for glycerol), ETGL (for ethylene glycol), BUOL (for 1,4-butanediol), HXOL (for 1,6-hexanediol), and N represents metal alkoxides such as TMOS, Ti (for titanium butoxide), Zr (for zirconium *n*-propoxide), Al (for aluminum tri-*sec*-butoxide). X indicates the weight percent of the functionalized organics relative to the weight of precursor metal alkoxide and Y the weight percent of precursor metal alkoxide relative to the weight of the functionalized organics. For example, DETA60-TMOS40 means that the ratio of DETA to TMOS is 60 to 40 (in weight) in the starting solution.

Characterization

Optical Abrasion Testing

The coated substrate was subjected to a Taber abrasion test in which standard CS-10 abrader wheels with an extra load of 250 g on each wheel were utilized as reported in our previous studies [13–17]. The pure and coated substrates were, allowed to be abraded cumulatively to 500 cycles. A flowing air stream was used to remove the abraded particles from the coating surface during the entire period of the test. A wear track is created by the rotating wheels. A Shimadzu CS-9000 UV-VIS spectrometer was used for a light transmittance test to measure the percent transmittance change in the wear track area relative to the unabraded materials. At intervals of 50, 100, 150, 200, 300, 350, 400, 500 cycles (up to 1500 in some cases), light absorbance through the wear track was measured at a wavelength of 420 nm using a beam size of 10×0.4 mm. The transmittance can be calculated as described elsewhere [16]. The results were plotted as percent of transmission versus number of wear cycles. For comparison, an uncoated substrate served as the control. While it is realized that this method does not provide all features of abrasion wear rate or level of adhesion of the coating, it does provide a practical and sensitive quantitative index of optical clarity as influenced by uneven disruption of the coating layer (or control substrate).

Other Measurements

X-ray photoelectron spectra (XPS) were recorded by using a Kratos XSAM800 spectrometer with Mg Kα excitation (260 w). Spectra were obtained with the analyzer position 80° from the sample surface. Atomic

composition were determined with programmed instructment sensitivity factors: C_{1s}, 389.945; O_{1s}, 667.441; N_{1s}, 552.978; Si_{2p}, 457.914.

SEM (Scanning Electron Microscopy) was performed on a Cambridge Stereoscan 200 apparatus at 30 kv.

UV spectra were obtained on a Hitachi U-2000 spectrophotometer.

Microhardness tests were performed on a Fischerscope H-100 microhardness tester with a Vicker indenter.

Adhesion Measurement by Direct Pull Method

The so-called "direct pull method" was used to provide a quantitative index of adhesion of the thermally cured coating on the substrate. This technique is based on first forming a bond with the coating and then applying a force normal to the coating-substrate interface to determine a value for practical adhesion. The principle of this technique is shown in Fig. 1. If the force required to pull the film off the substrate is F, the stress of adhesion, σ, per unit area is defined by

$$\sigma = F/A \tag{1}$$

where A (0.785 cm^2 in this study) is the cross-sectional area of the bar. It is assumed by applying Eq. (1) that the pulling force is normal to and uniformly distributed across the area A (i.e., no shear stress) and fracture occurs at the film–substrate interface. To meet this criteria, samples must be prepared carefully to maintain a flat surface. Also, good alignment of the stress–strain crosshead elements must be utilized.

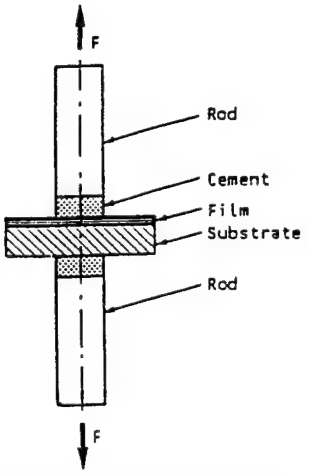

Fig. 1. Schematic of the direct pull-off test (application of a normal pulling force).

The coated polycarbonate substrates were cemented to aluminum rods using an epoxy resin adhesive (special *F* epoxy, Devcon corp.) for the adhesion between rod and coated surface and a methacrylate ester adhesive (plastic welder, Devcon Corp.) for the adhesion between rod and uncoated surface. After the adhesives were cured at room temperature for 16 hr (instructions of adhesive manufacturer), the samples were tested in a Instron (Model 1122).

RESULTS AND DISCUSSION

Synthesis

The functionalization of DETA, glycerol, and diols by isocyanatopropyltriethoxysilane was monitored by FTIR spectroscopy. The reaction was complete when the characteristic absorption band due to the isocyanate group at 2270 cm^{-1} disappeared. As is well known, the reaction rate between amino and isocyanate groups is much higher than the rate between hydroxyl and isocyanate groups. As a result, the reaction time and temperature for functionalizing DETA (ca. 3 hr at 0–4°C) was much less than for the hydroxyl terminated reactants (ca. 3 days at 70–80°C).

Following spin-coating of the polycarbonate substrate, the protective layer was obtained by curing at 130°C. When aqueous HCl solution was added, the hydrolysis and condensation reactions of functionalized DETA (or glycerol, diols) and metal alkoxides (if desired) took place. During this procedure, siloxane bonds were formed by the condensation of hydroxyl as well as methoxy groups which led to the formation of an inorganic backbone incorporated with organics as shown in Fig. 2. In order to obtain some information about the extent of condensation and minimum curing time, the total weight loss of the reaction solution during curing was

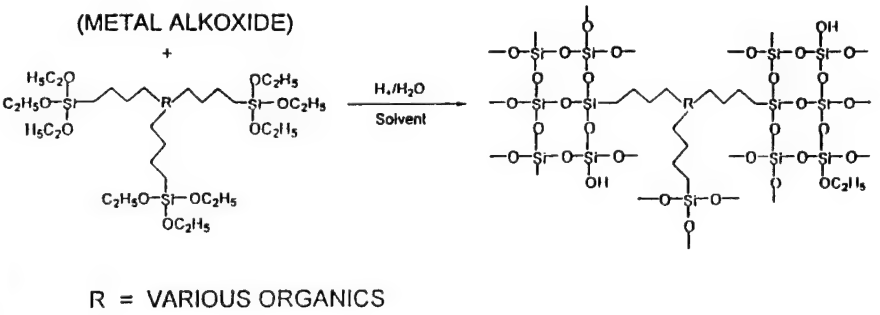

Fig. 2. Generalized reaction scheme for the conversion of functionalized organics into a cured network coating.

Table I. The Weight Loss and Condensation Extent

Sample	Extent of reaction (%)		Time to reach final weight at 130°C (hours)
	Weight loss	NMR[19]	
DETA	65	65	3.5
	70	65	3.5
Glycerol	75	—	4.0

measured. It was determined from the results in Table I, that the maximum weight loss was reached after ca. 3–4 hr in 130°C. The extent of reaction was estimated by using the weight loss data. This method is based on the assumption that the extra weight in the final product was due to the unreacted groups left in the final product. According to this method, the extent of reaction can be calculated as follows;

$$\text{Extent of reaction} = (W_I - W_A)/(W_I - W_T) \times 100 \quad (2)$$

where W_I, W_A, and W_T are initial weight, actual final weight and theoretical final weight respectively. As shown in Table I the extent of reaction obtained by this method is in good agreement with data obtained from earlier ^{29}Si NMR measurements on similar materials by Betrabet and Wilkes from this same laboratory [19].

Abrasion Resistance

Functionalized DETA Systems

In a previous study it was shown that with regard to the abrasive resistance, the best performer was based on triethoxysilane endcapped DETA [13–15]. The incorporation of zirconium *n*-propoxide and titanium butoxide only had a slight influence on the abrasive resistance [16, 17]. Figure 3 shows the typical plot of percent transmission as a function of the number of Taber abrader cycles. In the present study, the number of cycles was increased to 500 from 200 as previously reported, in order to better separate coating performance. It was found that all the coating systems discussed here had much better abrasive resistance than uncoated polycarbonate, and for the coated substrates, all the damage caused by the abrader wheels remained within the coating layer up to at least 500 cycles. In Fig. 4, the scale for percent transmission was enlarged so that the abrasive resistance between different systems could be easily compared. The data show that DETA, DETA62-Ti38, DETA62-Zr38, and DETA62-Al38 all

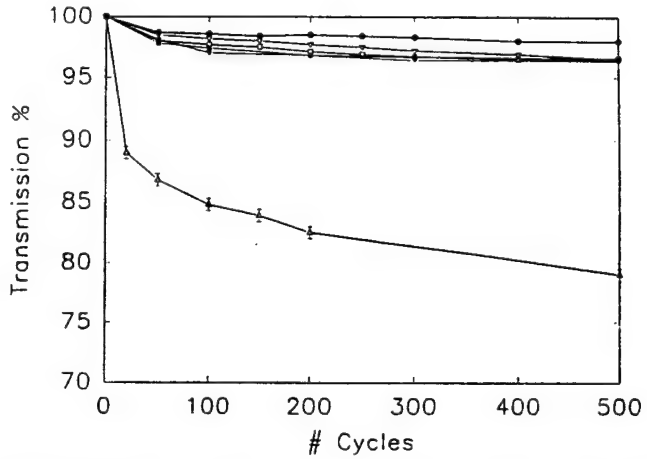

Fig. 3. Light transmittance as a function of number of wear cycles for uncoated and coated polycarbonate samples. The coating temperature was 130°C: (△) PC control (no coating), (▽) DETA, (●) DETA 60–TMOS40 (plasma treated substrate), (▼) DETA62–Al38, (□) DETA62–Zr38, (■) DETA62–Ti38. Typical error bar behavior for all samples is marked in the curve for the PC control.

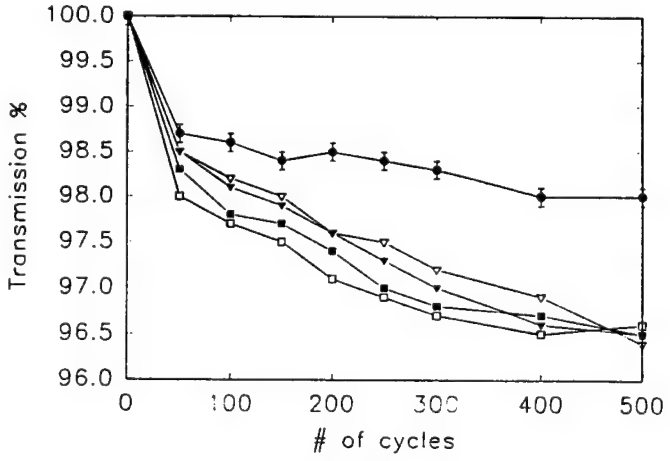

Fig. 4. Light transmittance as a function of number of wear cycles for coated polycarbonate samples. The coating temperature was 130°C: (▽) DETA, (●) DETA60–TMOS40 (plasma treated substrate), (▼) DETA62-Al38, (□) DETA62-Zr38, (■) DETA50 Ti38. The error bar behavior for all samples is marked in the curve for DETA60 TMOS40.

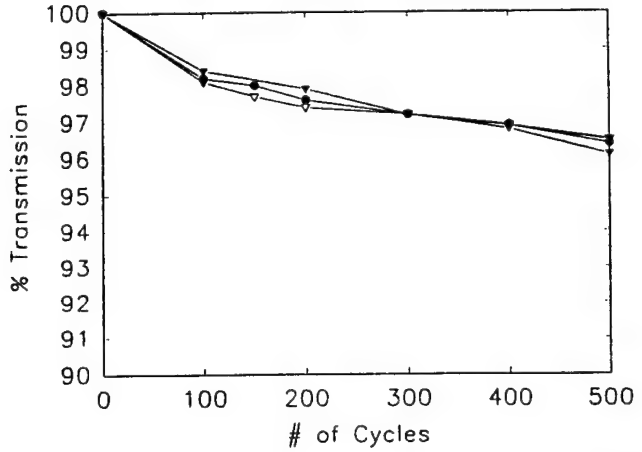

Fig. 5. Light transmittance as a function of number of wear cycles for coated polycarbonate samples. The coating temperature was 130°C: (●) DETA with plasma treatment, (▽) DETA without plasma treatment, (▼) DETA with primer treatment.

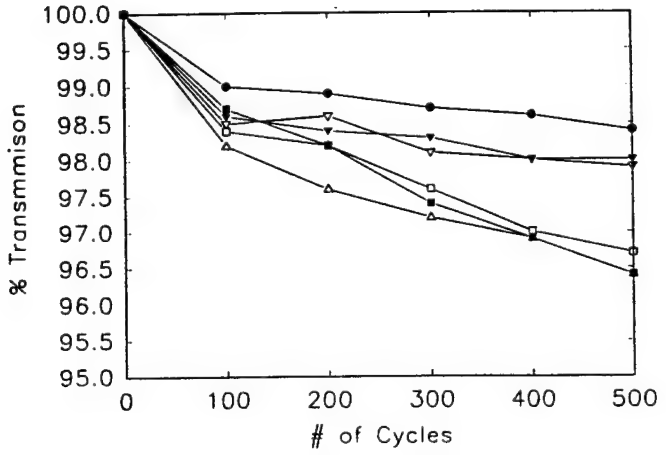

Fig. 6. Light transmittance as a function of number of wear cycles for coated polycarbonate samples. The coating temperature was 130°C: (●) DETA40–TMOS60, (▽) DETA50–TMOS50, (▼) DETA60–TMOS40, (□) DETA70–TMOS30, (■) DETA80–TMOS20, (△) DETA. All the coatings containing TMOS were on a primer-treated substrate.

have similar abrasive resistance. The abrasive resistance of the DETA-TMOS system, however, was distinctly higher than for the other systems. Also, due to the incompatibility between TMOS and the polycarbonate substrate, the adhesion between the DETA-TMOS coating and the polycarbonate substrate is poor. As a result, a surface treatment by oxygen plasma was used in this case in order to improve the adhesion. In all other cases, an oxygen plasma treatment was not necessary because the adhesion between coating and substrate was sufficient so that all the damage caused by the abrader wheels remained within the coating layer during the first 500 cycles. If all the damage caused by the abrader wheels was confined within the coating layer at the end of the test, then the surface treatment of the substrate appeared to have little influence on the abrasive resistance. This has been confirmed by the results in Fig. 5. As shown in this figure, for the DETA coating, the abrasion resistances are very close no matter how the substrates are treated before applying the coating. Similar results were also obtained in the other coating systems. Figure 6 shows the influence of TMOS content on abrasive resistance. It was found that the abrasion resistance increased as the amount of TMOS increased. The high abrasive resistance is attributed to the increase of Si–O–Si inorganic backbone structure introduced by TMOS. At least 40 wt.(%) of TMOS in the starting solution is necessary to obtain enhanced abrasive resistance. However, the increase of TMOS amount also increases the coating shrinkage during the drying and curing processes. As a result, a crack-free

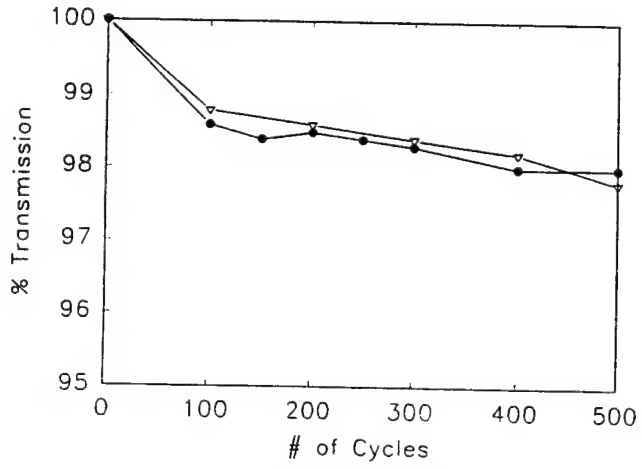

Fig. 7. Light transmittance as a function of number of wear cycles for coated polycarbonate samples. The coating temperature was 130°C: (●) DETA–TMOS with plasma treatment, (▽) DETA60–TMOS40 with primer treatment.

coating is unable to be obtained when the TMOS content is higher than 70 wt.(%) in the starting solution. According to our results, crack-free coatings with high abrasion resistance can be obtained when the TMOS content is between 40–60 wt.(%).

As discussed above, the achievement of a high abrasion resistant DETA-TMOS coating is not without expense. It can only be obtained by first treating the substrate with an oxygen plasma. It would be much better for a direct application if the same abrasion resistance could be achieved without a plasma treatment. As a result, other surface treatment methods which can improve the adhesion in a simpler way, were considered. It was found that a substrate surface treatment with a primer solution of 0.5 wt.(%) 3-aminopropyltriethoxysilane in IPA can also achieve the same effect as oxygen plasma treatment. Figure 7 shows that high abrasion resistance of the DETA–TMOS coating was also achieved on the primer treated substrate.

Functionalized Glycerol and Diol Systems

To study the influence of the structure of the organic species in these coating systems on the abrasive resistance, DETA was replaced by glycerol and a series of aliphatic diols. Due to the poor adhesion between coating and polycarbonate substrate, oxygen plasma and primer treatments were used in all cases to make sure that the adhesion between coating and substrate is strong enough so that all the damage caused by the abrader wheels remained within the coating layer for at least 500 cycles. As stated earlier,

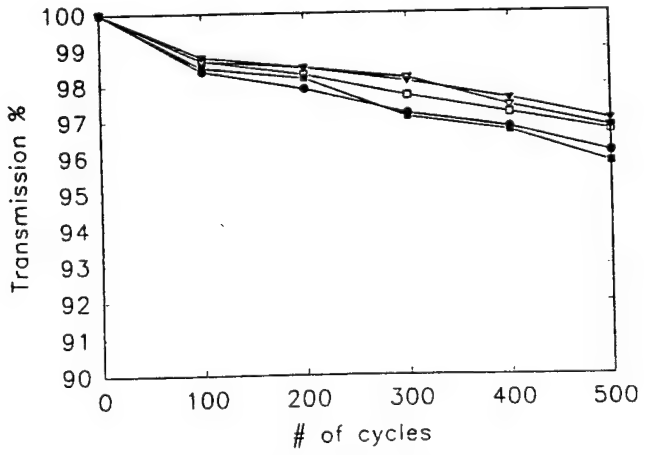

Fig. 8. Light transmittance as a function of number of wear cycles for coated polycarbonate samples. The coating temperature was 130°C: (●) DETA, (■) Hexanediol, (□) Butanediol, (▼) Ethylene glycol, (▽) Glycerol. All the coatings were on a primer-treated substrate.

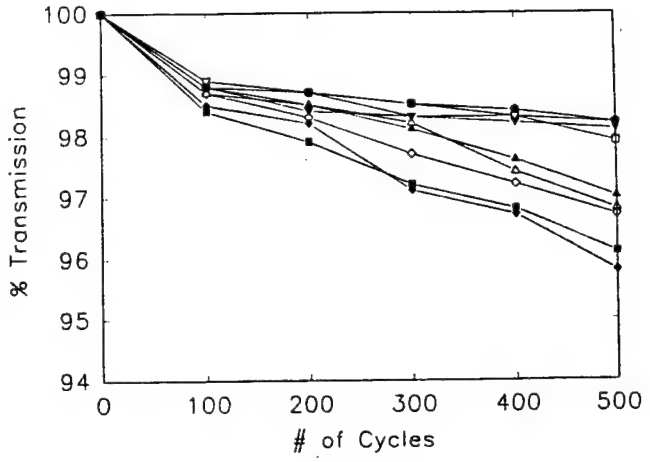

Fig. 9. Light transmittance as a function of number of wear cycles for coated polycarbonate samples. The coating temperature was 130°C: (●) BUOL60–TMOS40, (▽) ETGL60–TMOS40, (▼) GLYL60–TMOS40, (□) HXOL60–TMOS40, (■) DETA, (▲) GLYL, (△) ETGL, (◇) BUOL, (◆) HXOL. All the coatings were on a primer-treated substrate.

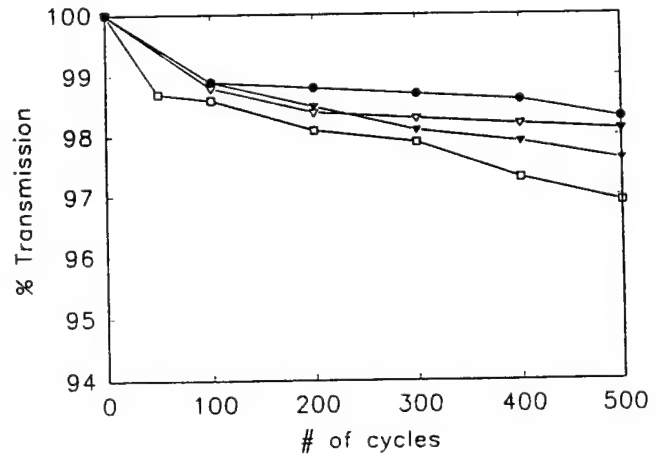

Fig. 10. Light transmittance as a function of number of wear cycles for coated polycarbonate samples. The coating temperature was 130°C: (●) GLYL50–TMOS50, (▽) GLYL60–TMOS40, (▼) GLYL80–TMOS20, (□) GLYL. All the coatings were on a primer-treated substrate.

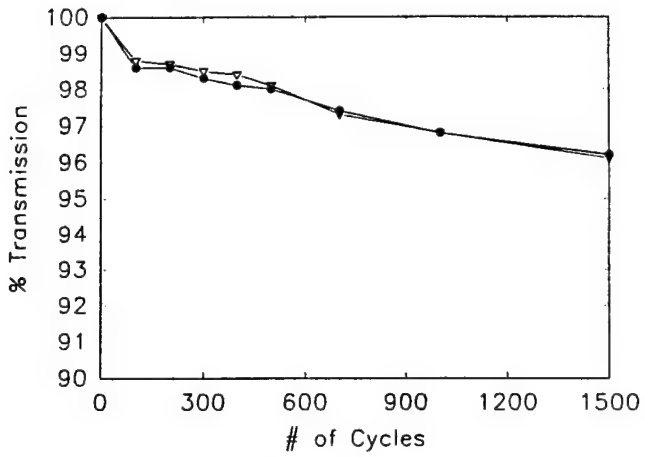

Fig. 11. Light transmittance as a function of number of wear cycles for coated polycarbonate samples. The coating temperature was 130°C: (●) DETA60–TMOS40, (▽) GLYL60–TMOS40. All the coatings were on a primer treated substrate.

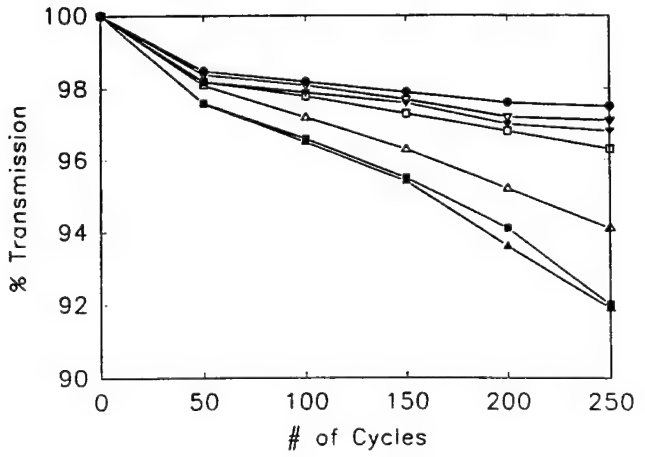

Fig. 12. Light transmittance as a function of number of wear cycles for coated polycarbonate samples. The coating temperature was 130°C and loading is 500 g: (●) BUOL60–TMOS40, (▽) ETGL60–TMOS40, (▼) GLYL60–TMOS40, (□) DETA60–TMOS40, (△) GLYL, (■) BUOL, (▲) DETA. All the coatings were on a primer-treated substrate.

it appears that since all the damage caused by the abrader wheels was confined to the upper portion of the coating layer, the surface treatment of the substrate had little influence on the abrasive resistance. Figure 8 compares the abrasive resistance of these functionalized glycerol and diol coatings with that of the DETA coating. Glycerol, ethylene glycol, and butanediol coatings were as good as the DETA coating. The abrasive resistance of the hexanediol coating, however, was slightly lower. This may be due to the fact that the average crosslink density of the coating decreases with increase in diol chain length between crosslink sites thereby providing a less brittle coating.

Because of the higher abrasive resistance of the DETA–TMOS coating, when compared to DETA without TMOS, TMOS was also incorporated into these diol systems and Fig. 9 shows the results. Again, excellent abrasive resistance was obtained when TMOS was used. Figure 10 shows the influence of TMOS content on the glycerol coating. It is noted that at least 40 wt.(%) of TMOS was necessary to obtain good abrasive resistance. Again, the increase of TMOS amount also increases the coating shrinkage during the drying and curing processes. For the GLYL–TMOS system, crack-free coatings with high abrasion resistance can still be obtained when the TMOS content is between 40–50 wt.(%) in the starting solution.

For the results shown above, the coating systems containing TMOS clearly possess a much higher abrasion resistance than the coatings without TMOS. However, the difference in abrasion resistance among these high performing coating systems containing TMOS can not be easily separated using the above test conditions. As a result, more severe test conditions, e.g., larger number of abrasion cycles (1500 instead of 500 cycles) and a heavier loading on each abrader wheel (500 g instead of 250 g), were used thinking that longer test times and heavier loads would create a larger difference in abrasion resistance. Figure 11 shows the abrasion behavior of DETA–TMOS and GLYL–TMOS coatings up to 1500 cycles. As can be easily seen, both of them still have excellent abrasion resistance for 1500 cycles. The abrasion resistance for these coating systems was also investigated using a 500 g loading. As might be expected, the same trend in abrasion resistance, using a 250 g loading, can be observed for these coating systems. The abrasion behavior of selected coating systems containing TMOS are shown in Fig. 12. Among all the coating systems, the BUOL–TMOS coating displayed the best abrasion resistance.

Influence of Reaction Time and Temperature

The effect of curing temperature on the abrasion resistance of the DETA coating has been addressed in the earlier study [17]. The results

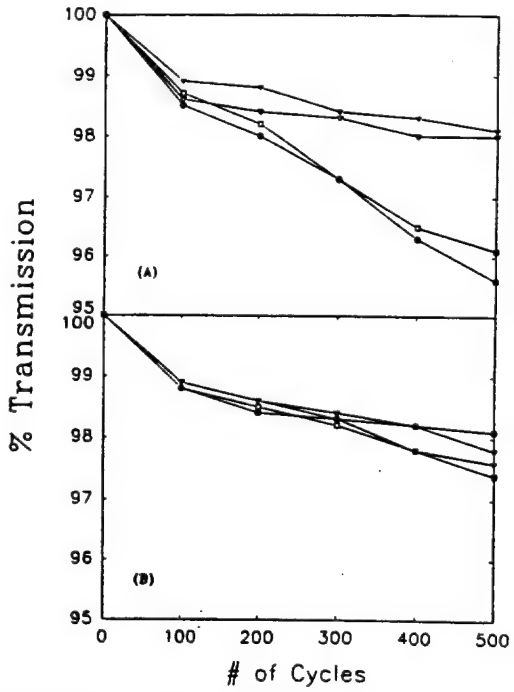

Fig. 13. Light transmittance as a function of number of wear cycles for coated polycarbonate samples cured at various temperatures for 10 hr: (A) DETA60–TMOS40. (●) 100°C, (□) 110°C, (V) 120°C, (▼) 130°C; (B) GLYL60–TMOS40, (□) 100°C, (▼) 110°C, (▽) 120°C, (●) 130°C. All the coatings were on a primer treated substrate.

show that increasing curing temperature improves abrasion resistance. The higher curing temperature is believed to promote an increased extent of network formation thus increasing abrasion resistance. However, the effect of reaction time was not studied at that time. Reaction time and curing temperature are very important parameters from a theoretical point of view as well as industrial application. Therefore, these two variables were systematically investigated. Figure 13 addresses the effect of curing temperature on the abrasion resistance of the DETA–TMOS and GLYL–TMOS coatings. A higher abrasion resistance at a higher curing temperature can be obtained and explained based on the above hypothesis. The effect of curing time on these coatings is addressed in Fig. 14. A longer curing time is also believed to lead to a higher extent of network formation which results in higher abrasion resistance. However, a curing time longer than 3 hr in 130°C is unnecessary.

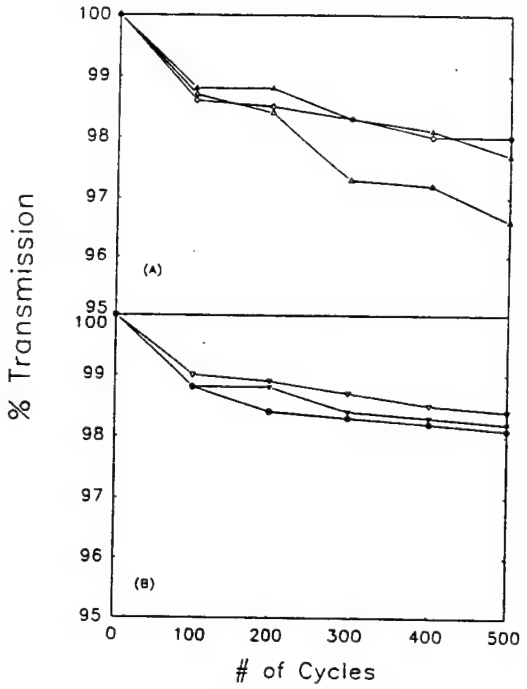

Fig. 14. Light transmittance as a function of number of wear cycles coated polycarbonate samples cured at various time at 130°C: for (A) DETA60–TMOS40, (△) 2 hr, (▲) 3 hr (◇) 10 hr; (B) GLYL60–TMOS40, (●) 2 hr, (▼) 3 hr, (▽) 10 hr. All the coatings were on a primer-treated substrate.

SEM Investigations

In order to obtain some insight into the wear mechanism by the Taber abrader, SEM studies were undertaken. The direct observation of a wear surface by SEM can often provide useful information about the wear mechanism, such as the mode of damage to the surface, the extent of damage, etc..

The SEM micrographs in Fig. 15 show the surface texture for uncoated polycarbonate, DETA, and DETA-Al coated polycarbonate (without surface treatment), and DETA–TMOS coated primer-treated polycarbonate. Polycarbonate is abraded through a mechanism where the surface is gradually roughened by scratches (or grooves) as reported earlier [13]. On the other hand, the coatings appear to be abraded more by a tearing mechanism as has been discussed in earlier publications

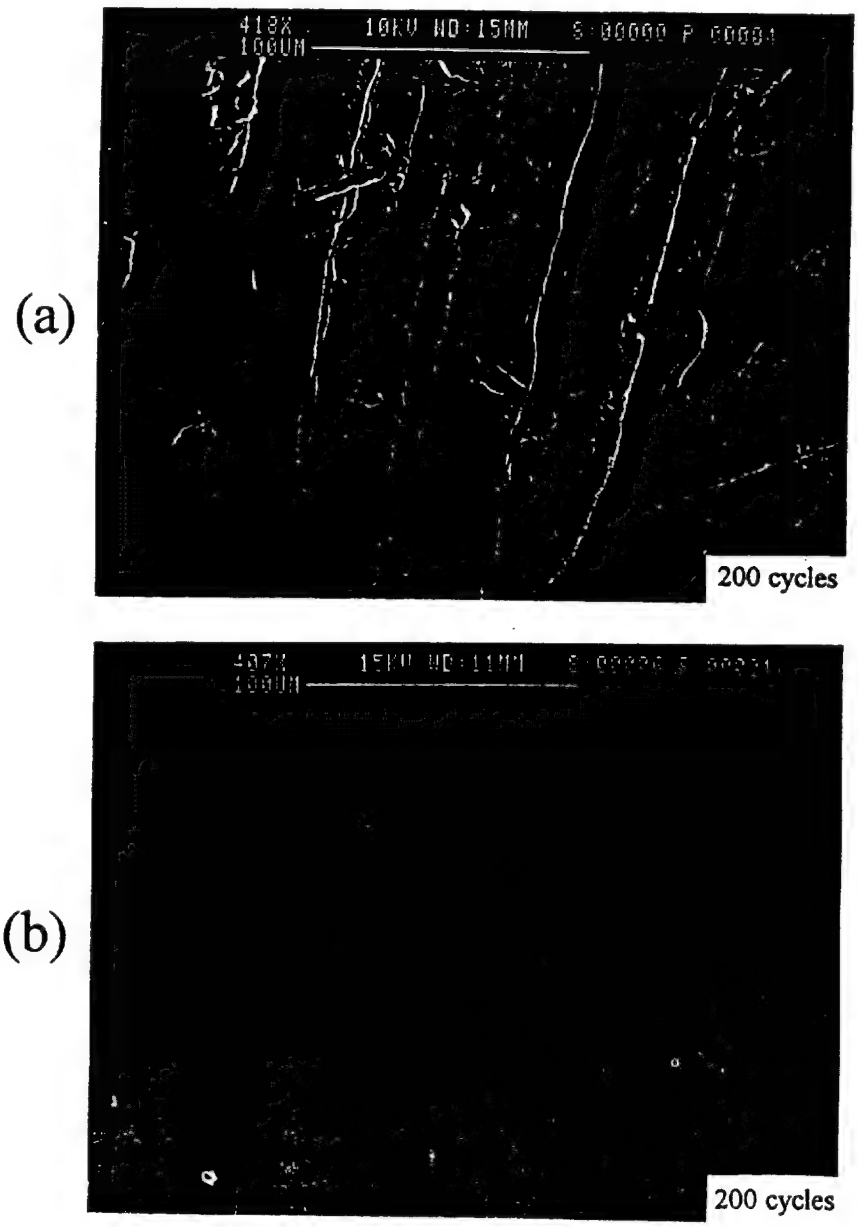

Fig. 15. SEM micrographs of wear track of uncoated and coated polycarbonate samples: (a) PC control, 50 cycles, (b) DETA, 200 cycles, (c) DETA60-TMOS40, 200 Cycles, (d) DETA60-TMOS40, 500 cycles. The sample was tilted at 60° in case of (d) also a higher magnification was used for this micrograph relative to a-c.

(c)

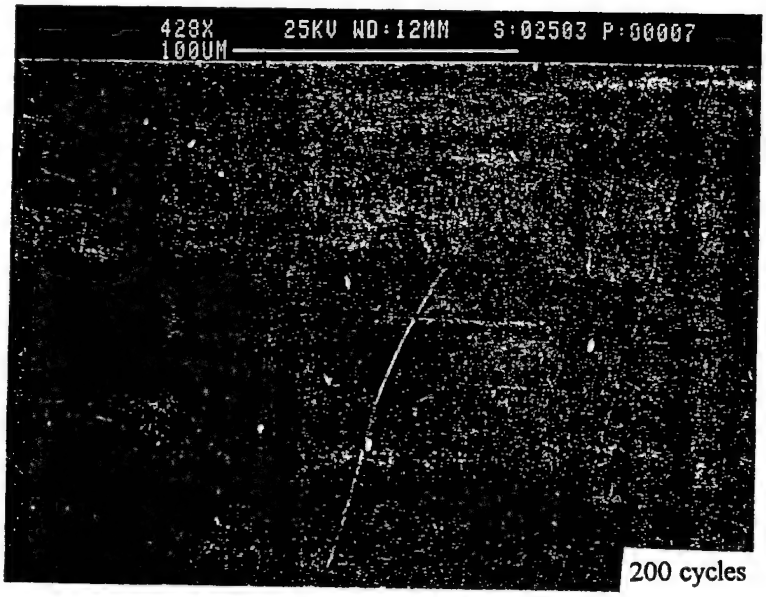

(d)

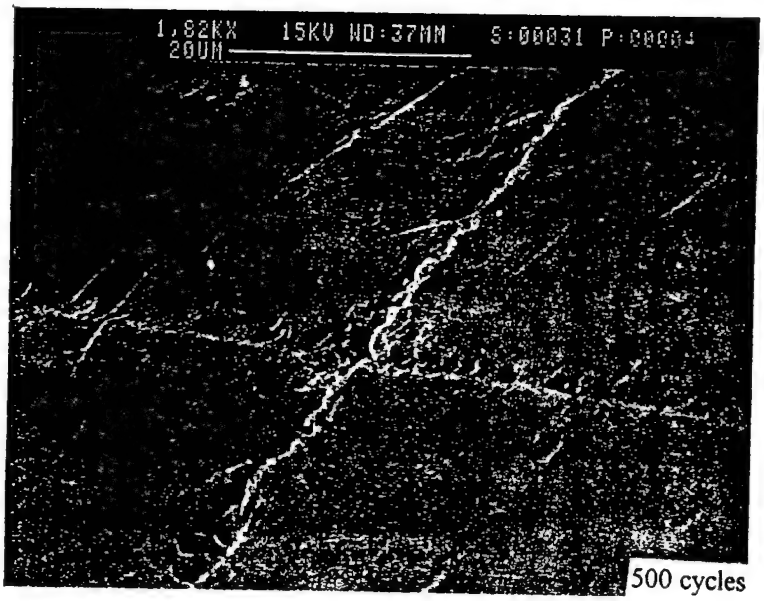

Fig. 15. Continued.

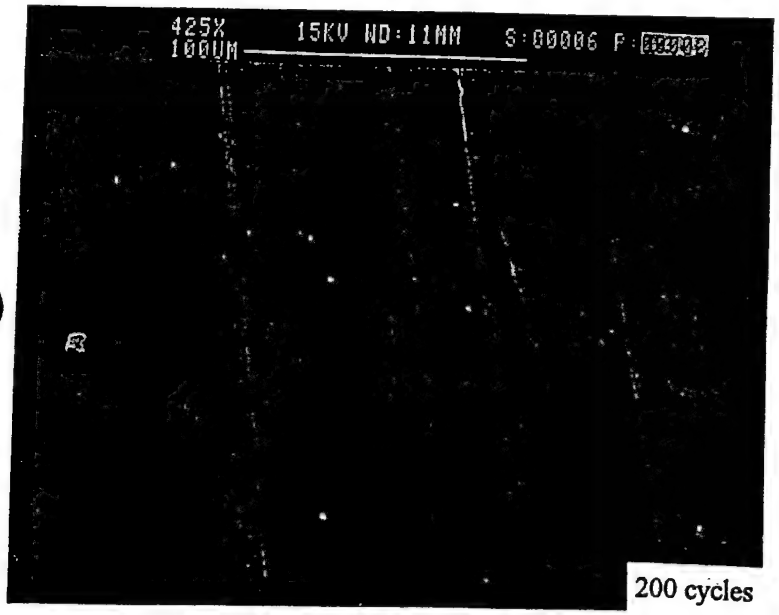

(a)

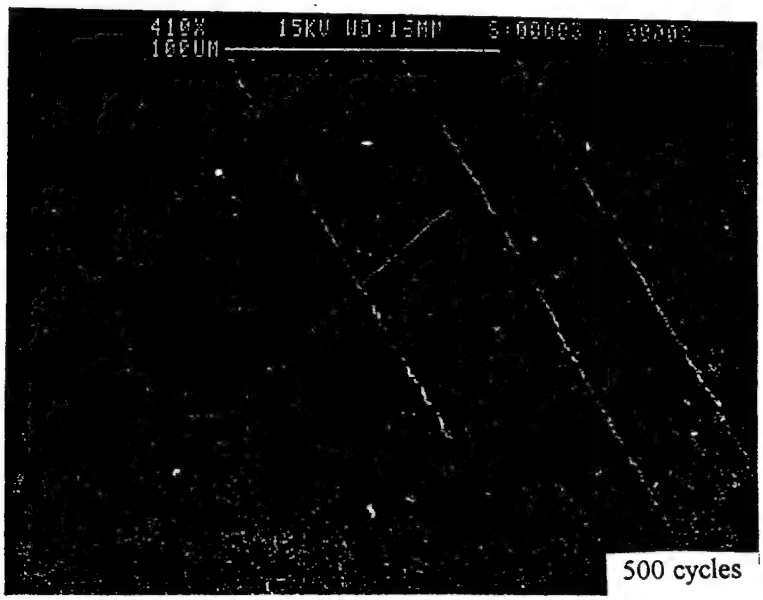

(b)

Fig. 16. SEM micrographs of coated polycarbonate samples as a function of Taber abrader cycles: (a) DETA, 200 cycles, (b) DETA, 500 cycles, (c) DETA60-TMOS40, 200 cycles, (d) DETA60-TMOS40, 500 cycles.

(c)

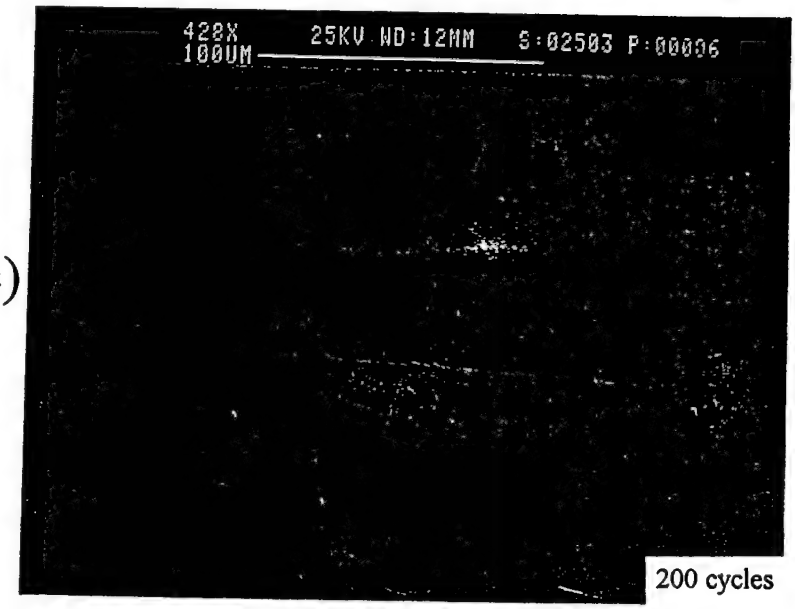

(d)

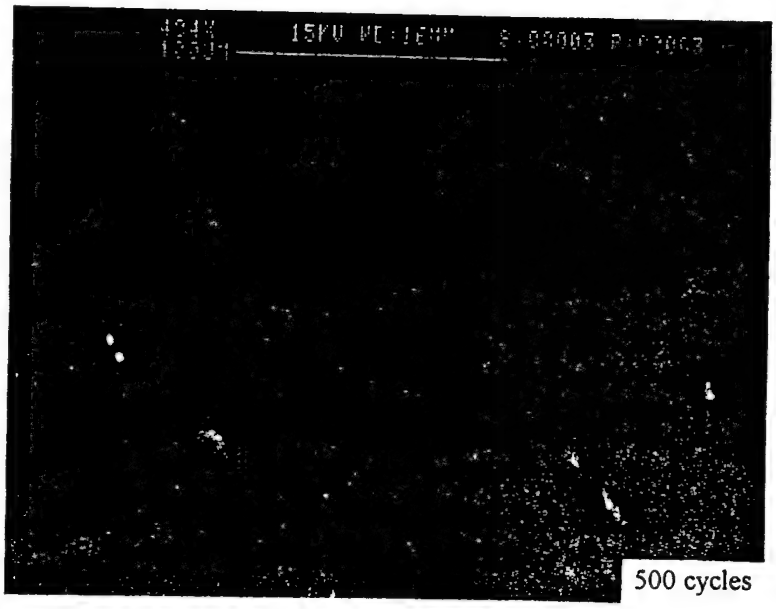

Fig. 16. Continued.

[13–15, 19]. Also, one notes that the scratches are few in Fig. 15b–d. The surface of the coating between these defects are relatively scratch free. It was also concluded, based on the SEM of different coatings, that all the coatings are abraded by a similar mechanism.

The SEM micrographs in Fig. 16 shows the progression of the surface texture as a function of abrader cycles for selected coatings. Compared to the DETA coating, the coatings containing TMOS have distinctly fewer scratches on the surface which confirm their excellent abrasion resistance. As expected, the number of scratches increases as the abrader cycle increases.

The other structural features of these sol-gel derived hybrid coatings, such as inhomogeneities and porosity, are also very important factors to their performance, and our investigation of this behavior is still underway.

Adhesion Measurement

The ability to change the surface properties of an engineering material by the use of a surface coating has opened up many new applications in a variety of technological areas. Adhesion between the coating and its substrate is another very important property. As a result, a quantitative or qualitative measurement of coating-substrate adhesion is necessary to evaluate the coating usefulness. There are at least nine different basic techniques for adhesion assessment [21, 22]: "scotch tape" test, abrasion test, bend and stretch test (qualitative); direct pull-off method, laser spallation test, scratch test, indentation test, acoustic imaging, ultracentrifuge test (quantitative). Of these methods, the direct pull-off method is geometrically simple and of practical interest. It is also the most widely used method and has already been standardized internationally [23]. In this research, it was used to give a quantitative index of adhesion for our coating systems and the results are listed in Table II. The scattering of the data is influenced by true random fluctuations in the force of adhesion. This difference may be due to local outgassing, and the differences in the surface conditions of a chemical nature. Misalignment problems during testing (recall Fig. 1) as well as the difference in epoxy thickness also introduce errors which always lead to a lower adhesion value [24]. Because of this, at least five measurements were taken for each coating. All these data, along with the maximum and the average values, are given in Table II.

The main purpose of the adhesion measurement here is to compare the adhesion between the different coating systems and different substrate surface treatments. As shown in Table II, the adhesion value for the DETA–TMOS coating was much lower than that of the DETA coating when the polycarbonate surface was not treated either by a plasma or

Table II. Results of Direct Pull-off Test

Sample	Strength $\sigma = F/A$ (kg/cm^2)						
	1	2	3	4	5	Average	Max.
DETA							
Without treatment	106	80	57	69	68	76	106
Primer treatment	159	93	100	120	85	112	159
DETA–TMOS							
Without treatment	39	42	26	40	37	37	42
Plasma treatment	117	104	144	128	135	126	144
Primer treatment						all > 207	
GLYL–TMOS							
Without treatment	27	52	33	39	31	36	52
Plasma treatment	118	139	149	101	104	122	149
Primer treatment						all > 207	
DETA–Zr						all > 186	
DETA–Al						all > 182	

primer solution before applying coating. The poor adhesion is apparently due to the incompatibility between the polymeric substrate and the inorganic metal alkoxide. The abrasion test confirmed that the "peel off" effect appeared long before 500 cycles was reached for the DETA–TMOS coatings. However, after the polycarbonate surface was treated with either an oxygen plasma or primer solution, the adhesion value *improved significantly*. The oxygen plasma and primer treatment also improved the adhesion between the GLYL–TMOS coating and polycarbonate substrate. In contrast, the DETA–Zr, DETA–Al, and DETA–Ti coatings display very good adhesion to polycarbonate substrate *even without* any surface treatment.

Plasma treatment is a rapid way to prepare the surfaces of polymeric substrates [25]. It is a very effective means of treating a polymer surface for bonding. The molecular characteristic of the polymer surface can be modified after exposure to a gas plasma, resulting in the formation of a wettable skin with good adhesion characteristics. For example, oxygen plasma can introduce functional groups such as carboxylic acids (-COOH) and increase the oxygen content on the polymer surface. As a result, the wettability and polarity of the surface can be greatly improved. As shown in Fig. 17, the amount of hydroxyl (peak 1) and carboxylic acid (peak 2) groups on the polycarbonate surface increased by a factor of 7 and 2 times, respectively, after exposure to an oxygen plasma for 2 minutes.

As indicated earlier, the use of a primer is another effective way to modify a substrate surface [26, 27]. Here, as was discussed in the

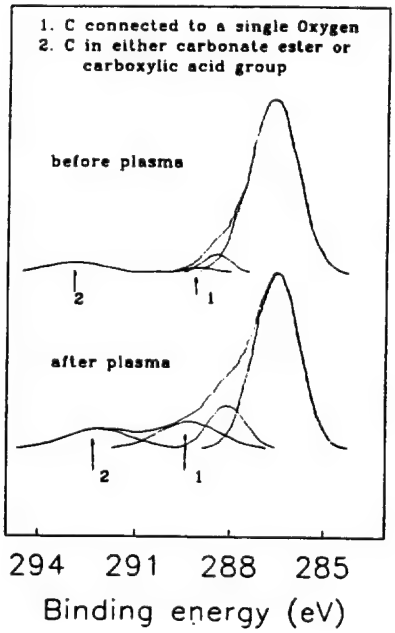

Fig. 17. C_{1s} region of XPS spectrum of polycarbonate surface before and after treatment.

experimental section, 3-APS was used to promote the adhesion between coating and polymeric substrate. Even though 3-APS is mainly used as the adhesion promoter for glass or mineral substrates, it is also effective in bonding coatings to some polymeric surfaces. The amino group may either interact with the ester group on polycarbonate substrate through hydrogen bonding, or possibly it can chemically react with hydroxyl or carboxyl groups (at the end of polymer chains) on the polycarbonate surface during the curing. The alkoxy group should also hydrolyze to silanols (SiOH), which then chemically bond to the coating through co-condensation with the alkoxy groups in the coating. As a result, the primer can act as a bridge to bond the coating with the substrate.

Boiling Water Treatment

The effect of water on coating adhesion has been extensively studied [28–31]. It depends on the bulk coating film properties, temperature, the properties of the interfacial region between coating and substrate, and the pH and salt content of water, etc. The adhesion loss upon exposure to water is often due to the presence of a water sensitive layer at the

coating–substrate interface. In many systems, a weak interfacial layer may form because of the absorption of water, which results in the reduction of adhesion. The rate of adhesion loss is often accelerated at high temperatures. Also, the pH and salt content of water are important factors, especially for the coatings containing readily hydrolyzable linkages. It is generally conceded that seawater is more aggressive than distilled water because it is more conductive and therefore corrosion and adhesion loss can take place at a more rapid rate.

Besides the abrasive resistance of these coating materials, consideration was also given to their thermal stability and water resistance. Some of the coating systems were therefore exposed to an extreme "hot-wet" condition by boiling in water for 1 to 24 hr. Most of the coatings stayed intact after the boiling water treatment. However, the abrasive resistance of many of the coatings decreased as shown in Fig. 18A and B and 19A. The Zr–DETA coating is an exception. Its abrasive resistance was found to be

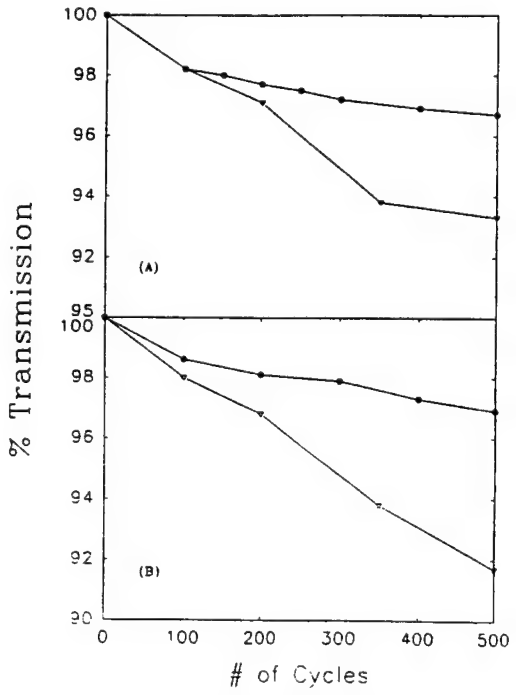

Fig. 18. Light transmittance as a function of number of wear cycles for coated polycarbonate samples. The coating temperature was 130°C: (A) Glycerol, (●) before water treatment, (▽) 1 hr in boiling water; (B) DETA, (●) before water treatment, (▽) 1 hr in boiling water. All the coatings were on a primer-treated substrate.

essentially the same after the boiling water treatment as shown in Fig. 19B. The surface texture of selected abraded coatings was investigated by SEM and the results are shown in Fig. 20. It was found that for the DETA and GLYL coatings, there was more damage compared to the abraded surface before boiling water treatment. The number and width of scratches increase after the hot-wet treatment. Many of the scratches are irregular and randomly oriented which implies that some of the damage occurs at points of weakness. The absorption of water may reduce the adhesion between coating and substrate, especially at weak points. The difference in the thermal expansion coefficient between coating and substrate may also create some points of stress concentration. All these factors contribute to the loss of abrasion resistance. Similar results have also been obtained for DETA–TMOS, GLYL–TMOS coatings. Further efforts to understand these effects are underway.

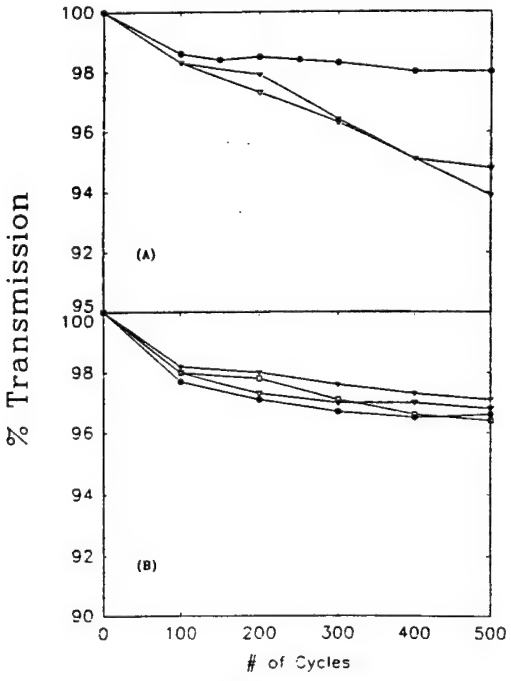

Fig. 19. Light transmittance as a function of number of wear cycles for coated polycarbonate samples. The coating temperature was 130°C; (A) DETA60-TMOS40, (●) before water treatment, (▽) 1 hr in boiling water (plasma treated substrate), (▼) 1 hr in boiling water (primer treated substrate). (B) DETA62–Zr38,: (●) before water treatment, (▽) 24-hr in boiling water (plasma treated substrate), (▼) 1 hr in boiling water (plasma treated substrate), (□) 1 hr in boiling water (primer-treated substrate).

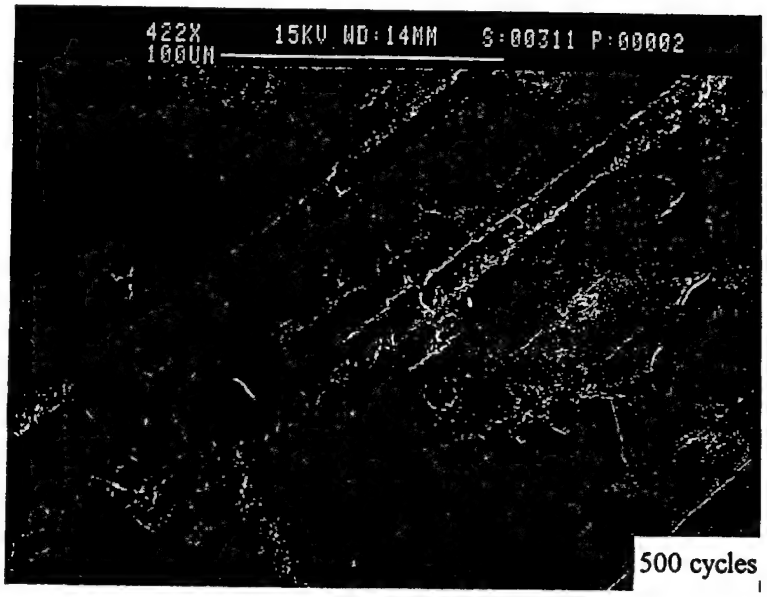

(a)

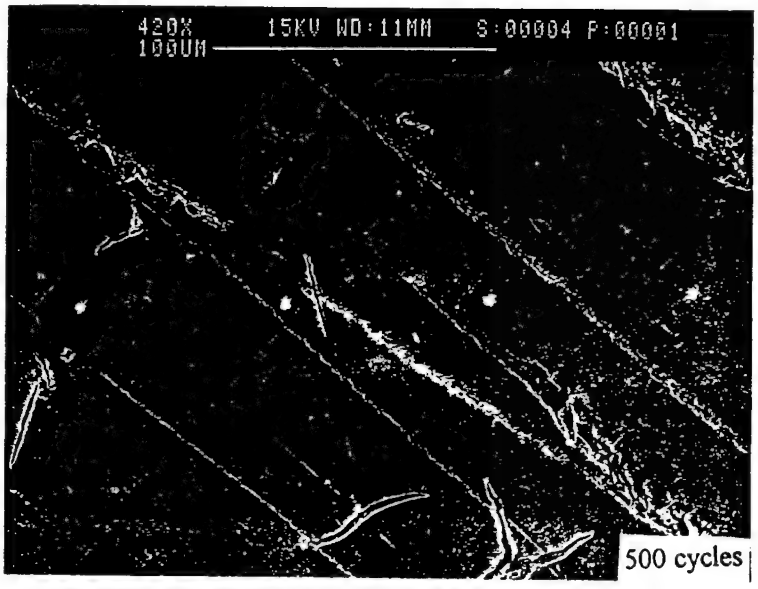

(b)

Fig. 20. SEM micrographs of wear track of coated polycarbonate samples after boiling water treatment: (a) DETA, 500 cycles, (b) GLYL, 500 cycles, (c) DETA62-Zr38, 500 cycles (before boiling water treatment), (d) DETA62-Zr38, 500 cycles (1 hr in boiling water).

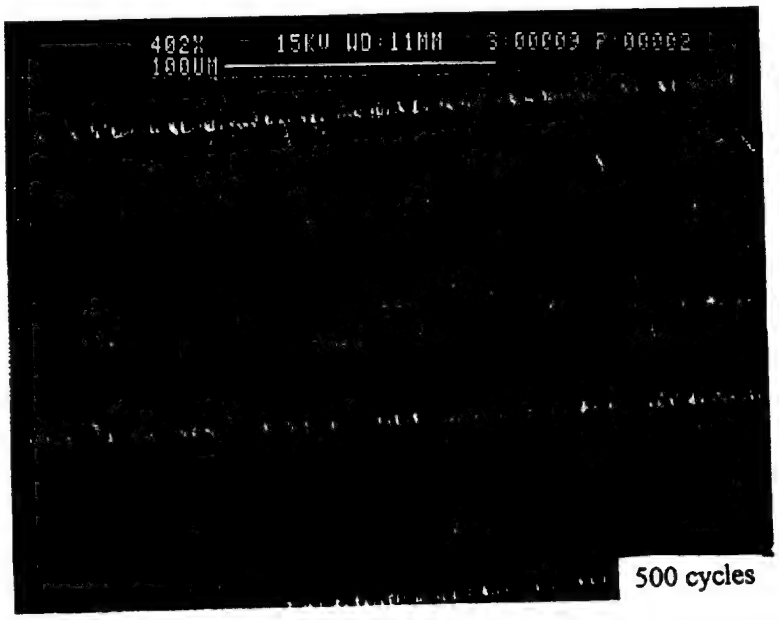

(c)

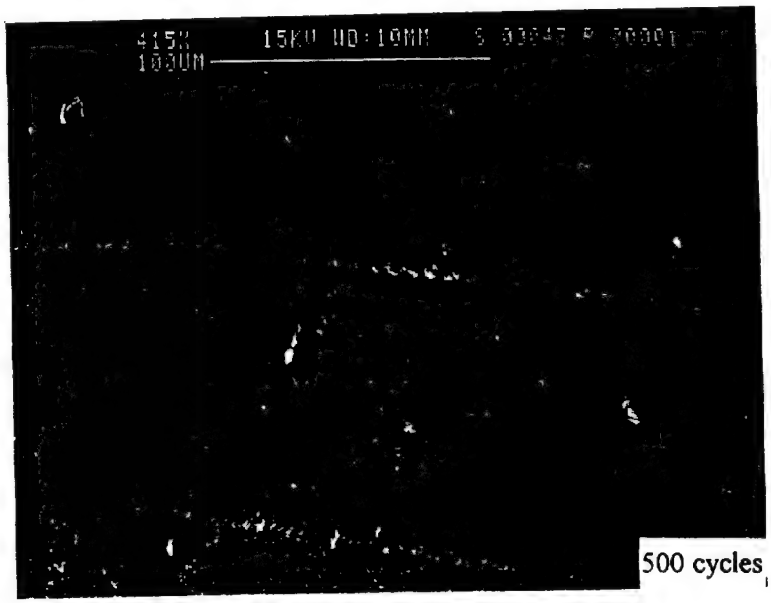

(d)

Fig. 20. Continued.

Table III. Direct Pull-off Test Results

Sample	Strength $\sigma = F/A$ (kg cm^2)								
	1	2	3	4	5	6	7	Average	Max.
DETA									
Before boiling water 1 hr	106	80	57	69	68			76	106
Plasma treatment	17	10	87	10	21	31		29	87
Primer treatment	21	31	22	26	109	41		42	109
DETA–TMOS									
Before boiling water 1 hr	117	104	144	128	135			126	144
Plasma treatment	33	52	44	31	27	10	14	30	52
DETA–Zr									
Before								all > 186	
1 hr in boiling water		33	81					> 186	

Table III compares the adhesion strengths before and after boiling water treatment. For the DETA and DETA–TMOS coatings, there is a significant decrease in the adhesion between coating and substrate. The values of adhesion strength become more scattered which implies that adhesion is more non-uniform. *However, the DETA-Zr coating still has good adhesion to substrate even though some weak points also exist. The SEM analysis shows no difference in surface topology before or after boiling water treatment.*

Microhardness Tests

The hardness of a coating is a very important property and results primarily from interatomic forces and complicated interactions caused by deformation mechanisms in the coating material [32]. Of the typical coating materials for plastics, the oxides show a higher hardness value than the other coating materials. The values for the coating materials studied within this report are listed in Table IV.

When comparing the microhardness of the coating materials made from glycerol and a series of diols, it is noted that the values of microhardness correlate to the expected crosslink densities of the inorganic network. The higher the crosslink density, the higher the microhardness. The incorporation of TMOS significantly increased the microhardness of the resulting coating materials for this reason.

The hardness of a coating generally has a significant effect on its abrasive or wear resistance. It is believed in some cases that the abrasion rate of a coating surface is inversely proportional to the hardness of the surface [32]. Indeed, if we compare the coating materials with TMOS and

Table IV. Microhardness Test Results

Sample	Modulus GPa	Plastic hardness N/mm^2	Universal hardness N/mm^2
GLYL	4.87	548	243
ETYL	4.31	451	210
BUTL	3.74	372	179
HEXL	3.58	333	167
GYTL60–TMOS40	6.22	1278	343
ETYL60–TMOS40	5.25	931	288
BUTL60–TMOS40	4.20	634	224
DETA	5.29	471	243
DETA60–TMOS40	5.47	656	277
DETA50–TMOS50	5.79	832	306
DETA62–Ti38	4.06	504	208
DETA62–Zr38	5.03	808	271
DETA62–Al38	6.07	962	325

their counterpart (without TMOS), such as GTYL–TMOS with GTYL, the coatings with higher value of microhardness also have better abrasion resistance. However, higher microhardness does not always result in better abrasion resistance. There are other factors, such as surface roughness, the coefficient of friction, fracture toughness, that also influence the abrasion resistance of the coating. For example, DETA62–Zr38 and DETA6–Al38 coatings have a much higher microhardness value than DETA, but their abrasion resistance behavior is similar. Therefore, great care should be taken when relating microhardness with abrasion resistance of the coating materials at least for this type of sol-gel hybrid coating.

The Absorption of UV Radiation by Coatings

Most commercial organic polymers undergo chemical changes upon exposure to UV light because they possess chromophoric groups capable of absorbing UV light. The absorption of UV light by polymers produces noticeable physical and chemical changes. As a result, many commercial polymers are discolored and lose mechanical strength when exposed to UV light [33, 34]. When polymers are coated, the behavior of the coating upon exposure to UV light also becomes important. Figure 21 shows the UV spectra of some of our coating materials. The wavelength range was chosen so that it represented the UV portion in sunlight. The DETA coating absorbed UV light with wavelength 350 nm and lower. The incorporation of Al and Zr has no appreciable effect on the UV absorption of DETA

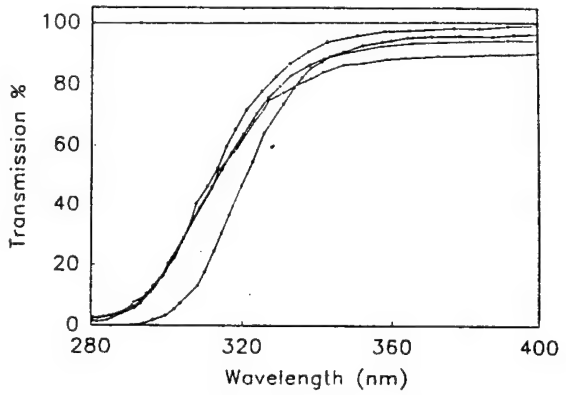

Fig. 21. UV spectra of selective coating materials. (▽) baseline, (●) DETA62–Al38, (■) DETA62–Zr38, (▼) DETA, (□) DETA62–Ti38.

coatings. However, the incorporation of Ti significantly increased the UV absorption of the DETA coating, which can be explained by the higher photoactivity of titanium oxide [35]. Because of its UV absorption, the DETA–Ti coating not only offers high abrasion resistance, but may also minimize the deleterious effects of UV weathering.

CONCLUSIONS

New transparent hybrid inorganic-organic coating systems have been synthesized and can be utilized as optical abrasive resistance coatings on polymeric substrates. The abrasion resistance of inorganic/organic hybrid coatings containing titanium, zirconium, and aluminum are competitive with our abrasion resistant DETA coating reported earlier [13–16]. The abrasion resistance of the coating systems containing TMOS is much better than that of the DETA coatings. The adhesion tests show that the adhesion between the coating and substrate can be greatly improved by treating the polycarbonate surface with an oxygen plasma or a primer solution. Other experiments, such as microhardness tests, UV absorption behavior, and the observation of abraded surface by SEM, were also undertaken. All these results show that these coating materials have excellent abrasion resistance and have potential applications as coating materials for lenses and other polymeric products. It is also noted the abrasion resistance of Zr–DETA coating remains the same after boiling water treatment while the other coatings suffer the loss of abrasion resistance.

ACKNOWLEDGMENTS

The authors acknowledge the financial support of the Air Force Office of Scientific Research. The authors would also like to thank Dr. Jim Tonge (Dow Corning Corporation) for performing the microhardness tests. Useful discussions with Dr. Neal R. Langley (Dow Corning Corporation) are also acknowledged.

REFERENCES

1. J. Kasi, *Jpn. Kokai Tokkyo Koho* **JP6335**, 633 (88, 35, 633).
2. M. Ishigaki, M. Inagaki, and M. T. Sakakibara, *Jpn. Kokai Tokkyo Koho* **JP6348**, 364 (88, 48, 364).
3. R. Nass, E. Appac, W. Glaubitt, and H. Schmidt, *J. Non-Cryst. Solids* **121**, 370 (1990).
4. H. Schmidt and H. Walter, *J. Non-Cryst. Solids* **121**, 428 (1990).
5. G. L. Wilkes, B. Orler, and H. H. Huang, *Polym. Preprints* **26**(2), 300 (1985).
6. H. Huang and G. L. Wilkes, *Polym. Bull* **18**, 455 (1987).
7. H. Huang, R. H. Glaser, and G. L. Wilkes, *ACS Symp. Ser.* **360**, 354 (1988).
8. H. Huang and G. L. Wilkes, *Polymer* **30**, 2001 (1989).
9. B. Wang, H. Huang, G. L. Wilkes, S. Liptak, and J. E. McGrath, *Polym. Mater. Sci. Eng.* **63**, 892 (1990).
10. H. Schmidt, *Mater. Soc. Symp.* **171**, 3 (1990).
11. H. Schmidt, *J. Non-Cryst. Solids* **73**, 681 (1985).
12. H. Schmidt and H. Wolter, *J. Non-Cryst. Solids* **121**, 428 (1990).
13. C. Betrabet and G. L. Wilkes, *Polym. Preprints* **32**(2), 286 (1992)
14. B. Tamami, C. Betrabet and G. L. Wilkes, *Polym. Bull* **30**, 39 (1993).
15. B. Tamami, C. Betrabet and G. L. Wilkes, *Polym. Bull.* **30**, 393 (1993).
16. B. Wang and G. L. Wilkes, *J. Macromol. Sci.-Pure Appl. Chem.* **A31**, 249 (1994).
17. B. Wang, G. L. Wilkes, C. D., Smith, J. E. McGrath, *Polym. Commun.* **32**, 400 (1991).
18. B. Wang, G. L. Wilkes, J. C. Hedrick, S. C. Liptak, and J. E. McGrath, *Macromolecules* **24**, 3449 (1991).
19. C. Betrabet, PhD thesis Chemical Engineering Department of Virginia Polytechnic Institute & State University (1993).
20. A. Tomasi, P. Scardi, and F. Marchetti, *Mater. Res. Soc. Symp. Proc* **271** 477 (1992).
21. D. S. Rickerby, *Surface Coatings Tech.* **36**, 541 (1985).
22. J. Valli, *J. Vac. Sci. Tech.* **A4**(6), 3007 (1986).
23. *International Standard ISO 4624.*
24. R. Jacobsson and B. Kruse, *Thin Solid Films* **15**, 71 (1973).
25. Adhesive Bonding, MIL-HDBK-691B, *Military Standardization Handbook* (U.S. Department of Defense, March 1987).
26. W. D. Bascom, *Eng. Mater. Handbook Vol.* 3 (ASM International eds., 1990), p. 254.
27. E. P. Plueddemann, in *Adhesion Aspects of Polymeric Coatings*, K. L. Mittal, eds. (Plenum Press, New York, 1983), p. 319.
28. P. Walker, *Paint Tech.* **31**, 22 (1967); ibid., **31**, 15 (1967).
29. M. Yaseen and W. Funke, *J. Oil Col. Chem. Assoc.* **61**, 284 (1978).
30. W. Funke and H. Zatloukal, *Farbe u. Lack* **84**, 584 (1978).
31. W. Funke and H. Haagen, *Ind. Eng. Chem. Frod Res. Dev.* **17**, 50 (1978).

32. H. K. Pulker, *Coatings on Glass* (Elsevier Sci. Publishing, New York, 1984).
33. P. Brennan and C. Fedor, in *Coatings Technology Handbook*, D.Satas, eds. (Marcel Dekker, New York, 1991), p. 85.
34. W. Schnabel, *Polymer Degradation* (Macmillan Publishing Co., New York, 1981).
35. G. Irick, Jr., G. C. Newland, and R. H. S. Wang, in *Photodegradation and Photostabilization of Coatings*, S. P. Pappas and F. H. Winslow, eds. (American Chemical Society, Washington, D.C., 1981).

Appendix 3

HYBRID ORGANIC/INORGANIC COATINGS FOR ABRASION RESISTANCE ON PLASTIC AND METAL SUBSTRATES

J. WEN, K. JORDENS AND G. L. WILKES
Department of Chemical Engineering and Polymer Materials and Interfaces Laboratory, Virginia Polytechnic Institute and State University, Blacksburg, VA 24061

ABSTRACT

Novel abrasion resistant coatings have been successfully prepared by the sol-gel method. These materials are spin coated onto bisphenol-A polycarbonate, diallyl diglycol carbonate resin (CR-39) sheet, aluminum, and steel substrates and are thermally cured to obtain a transparent coating of a few microns in thickness. Following the curing, the abrasion resistance is measured and compared with an uncoated control. It was found that these hybrid organic/inorganic networks partially afford excellent abrasion resistance to the polycarbonate substrates investigated. In addition to having excellent abrasion resistance comparable to current commercial coatings, some newly developed systems are also UV resistant. Similar coating formulations applied to metals can greatly improve the abrasion resistance despite the fact that the coatings are lower in density than their substrates.

INTRODUCTION

Transparent polymeric materials have been utilized in recent years as windows in aircraft and public buildings, and glazing for automobiles, buses and aircraft. However, while these polymeric materials may possess excellent optical clarity and many beneficial bulk mechanical properties, they show poor abrasion resistance which can often greatly limit their applications. This has promoted the need for developing abrasion resistant hard coatings for organic polymeric substrates. Many of these coatings have been developed and are based on the use of metal alkoxides or organosiloxanes and generated by the sol-gel process [1-2]. Such coatings may have utility for the protection of metallic surfaces as well. It is often desirable that such coatings for metals should provide good corrosion resistance in addition to good abrasion resistance because of the often rapid corrosion of metals.

Many inorganic/organic hybrid network materials prepared by a sol-gel approach, have been developed over the last decade and studied in our laboratory [3-5]. These materials were prepared from various metal alkoxides and functionalized organics with initial emphasis on functionalized oligomers such as poly(dimethylsiloxane) (PDMS), poly(tetramethylene oxide) (PTMO) and higher T_g components. Many of these materials exhibit high optical clarity. In light of the success of making inorganic/organic composites, hybrid materials based on low molecular weight organics have been more recently developed in our laboratory and successfully used as optical abrasion resistant coating materials. In the previous studies, a series of inorganic/organic coating materials were synthesized and tested [6-17]. In particular, the effect of reaction conditions, the use of metal alkoxide, and chemical structure of the organic component to the abrasion resistance have been principally examined in detail for the polymeric substrate coatings [14-16]. The adhesion behavior, coating durability in a "hot-wet" condition, microhardness tests, UV absorption behavior, and the observation of abraded surfaces by scanning electron microscopy (SEM) were also undertaken to evaluate these coatings. The Si−O−Si inorganic

Mat. Res. Soc. Symp. Proc. Vol. 435 1996 Materials Research Society

backbone structure, along with its level of crosslinking, promote the high abrasion resistance. The organics contribute some other advantages to the coatings, such as improved adhesion between coating and polymer substrate, reduced shrinkage upon curing, and flexibility relative to a pure brittle inorganic sol-gel coating.

The research summarized in this paper addresses the recent developments with regard to our studies of abrasion resistant coating materials. We particularly address the inorganic/organic coating materials that are based on 3-isocyanatopropyltriethoxysilane functionalized diethylene triamine (DETA) and 3,3'-iminopropyltriamine (IMPA) as the organic components and tetramethoxysilane (TMOS) and tetraethoxysilane (TEOS) as the inorganic components. The coating materials investigated and discussed in this paper have potential for wide application.

EXPERIMENTAL

Materials

Diethylenetriamine (DETA), 3,3'-iminobispropylamine (IMPA), tetraethoxysilane (TEOS), 3-aminopropyltriethoxysilane (3-APS), 3-(trimethoxysilyl)propylmethacrylate (MSi), benzoyl peroxide (BPO), and isopropanol (IPA) were obtained from the Aldrich Chemical Company and used without further treatment. 3-isocyanatopropyltriethoxysilane and tetramethoxysilane (TMOS) were purchased from the Huls America Company. Bisphenol A polycarbonate (3.5×3.5×1/16 inch Lexan®) sheets were obtained from the General Electric Company while CR-39 sheets (diallyl diglycol carbonate resin) were purchased from the Atlantic Plastic Company. These two sheet stock materials were used as the polymeric substrates. Aluminum (0.025 inch thick) and plain steel (0.020 inch thick, ASTM A-366) substrates were obtained from The Q-Panel Company. Norbloc 7966, which is a UV absorber (UVA) of the hydroxyphenylbenzotriazole class, was obtained from Noramco Inc. and Figure 1 shows its structure.

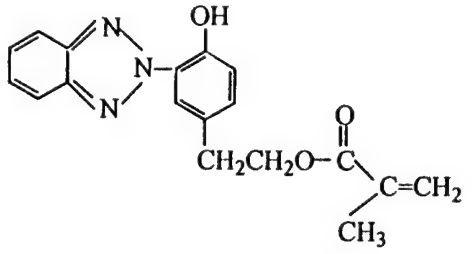

Figure 1. The chemical structure of UV absorber Norbloc 7966.

Coatings for Polymeric Substrates

The synthetic approach for coating preparation is demonstrated in Figure 2. In brief, the synthetic approach involves two major chemical reactions: functionalization of organics followed by the sol-gel reaction. The triethoxysilane functionalized organics in Figure 2 can be prepared through the reaction between the amino groups (or hydroxyl groups) in the organics and the isocyanate groups in 3-isocyanatopropyltriethoxysilane, as reported earlier [14-15]. The loss of isocyanate functionality as the reaction takes place was confirmed by FTIR (2273 cm^{-1}). The reaction was considered complete when this characteristic absorption band disappeared.

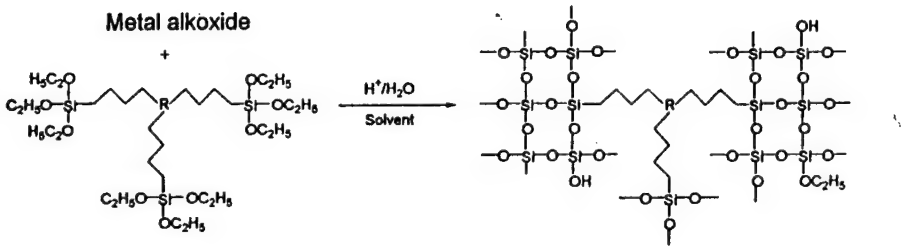

Figure 2. Generalized scheme for generating hybrid inorganic/organic coating materials through the sol-gel process.

During coating preparation, a portion of the resulting solution was mixed with 0.5-1 N aqueous HCl solution and metal alkoxide before being spin-coated at room temperature. The polymeric substrates were pre-treated with an isopropanol solution of a primer, 3-aminopropyltriethoxysilane (3-APS) in order to improve the adhesion between coating and substrate. The hydrolysis and condensation reactions of functionalized organics and metal alkoxides took place when aqueous HCl solution was added. During this procedure, siloxane bonds were formed by the condensation of hydroxyl as well as alkoxy groups which led to the formation of an inorganic backbone incorporated with organics as shown in Figure 2. The extent of reaction was estimated by using the weight loss data and ^{29}Si NMR measurements and found to be around 75% although the value is cure temperature dependent [14,15]. The coatings on the polycarbonate substrates were cured at 120-130°C for three to 12 hours. The coating thickness on the polymeric substrates was found to be either 3-5 microns at higher spin rate (3500 rpm) or 8-12 microns for slower spin rate (1000 rpm) by the surface texture measurement apparatus Talysurf 4 from Rank Talyor Hobson Company. In the case of UVA containing coatings, initiator BPO (1 wt% of MSi) and the desired amount of UVA (see Figures 4 and 5 for detail) were first dissolved in the mixture of MSi, TEOS, and IPA. Then 2 N aqueous HCl solution (H_2O:alkoxy = 2:1) were added to the above solution under brisk stirring for 15 minutes before adding silane functionalized IMPA. The UVA-containing coatings can then be prepared according to the same spin coating and curing procedure described above. The polymerization of the vinyl groups in UVA and MSi has been confirmed by FTIR.

The coated polymeric substrates were then tested for their optical abrasion resistance using the Taber Abraser with CS-10 wheels and 500g loading on each wheel. An index of abrasion was obtained by measuring the intensity of transmitted light through the abraded regions. A monochromatic light source (λ=420 nm) on a Shimadzu-9000 Flyscan spectrometer was used to measure the transmittance through the abraded substrates [6,14-16]. The UV absorption spectra of the coatings were measured by a Hitachi U-2000 Spectrophotometer. The "direct pull method" was used to provide a quantitative index of adhesion of the thermally cured coating on the substrate [14-16].

For the results presented in this report, the sample designation will be denoted as MX-NY where M represents the organic component such as IMPA, and N represents the metal alkoxide such as TMOS. The value of X indicates the weight percent of the precursor functionalized

organics in the coating formulation, and Y represents the weight percent of precursor metal alkoxide.

Coatings for Metallic Substrates

Pretreatment of the aluminum and plain steel substrates involved sanding with emery paper followed by washing with IPA. The method of generating coatings on metals is similar to that shown in Figure 2. However, curing has been carried out at a higher temperature of 175°C for 20 minutes to two hours. Using SEM, the coating thickness on aluminum and steel was found to be ca. two microns, but this can be controlled through either turntable spin rate or solution viscosity at the time of spin coating.

Analogously to the coated polymeric substrates, abrasion tests were performed on a Taber Abraser with CS-10 wheels and 500g of load on each arm. Because of the opaqueness of the metals, transmittance methods for evaluating abrasion performance could not be utilized. Instead, coating performance was evaluated visually and with SEM. Corrosion behavior was studied by immersion in 3.5 wt.% NaCl solution. Both full immersion and half immersion tests were performed. Control samples were then compared to coated counterparts. A similar attempt to quantify the adhesive strength between the coatings and metal substrates was made by the "direct pull-off method".

RESULTS AND DISCUSSION

Abrasion Coatings for Polymeric Substrates

The abrasion resistance of uncoated bisphenol-A polycarbonate, uncoated CR-39, and two selected coating systems is shown in Figure 3 as the plot of percent transmission as a function of the number of Taber abrader cycles. As shown in this plot, the abrasion resistance of uncoated bisphenol-A polycarbonate drops quickly at lower number of cycles but levels off at higher number of cycles. On the other hand, the abrasion resistance of CR-39, which is a more highly scratch-resistant crosslinked polymer and has been widely used for eyeglass lenses, decreases in a much slower rate in the beginning although this decrease continues. It was also found that all the coating systems discussed here had much better abrasive resistance than uncoated polycarbonates, and for the coated substrates, all the damage caused by the abrader wheels remained within the coating layer up to at least 500 cycles.

Figure 4 compares the abrasion resistance of two of our coatings with one of the current top commercial abrasion resistant coating Lexan MR5®. It was found that coating IMPA35-TEOS65 has the best performance in terms of abrasion resistance while coating IMPA32-TEOS65-MSi3-UVA1.1wt% has both excellent abrasion resistance and UV-protection.

An important area that has not been addressed in our previous studies is that of promoting ultraviolet stability through incorporation of an appropriate UV absorber. In addressing this issue it may be useful to recall that most commercial organic polymers undergo chemical changes upon exposure to UV light (290 to 400 nm) because they possess chromophoric groups capable of absorbing UV light. The absorption of UV light by many polymers produces noticeable physical and chemical damages. In order to avoid the UV degradation of polymeric materials, the protective coatings utilized should not only offer good abrasion resistance, but also have good durability upon exposure to UV light. Therefore it is a part of our research plan to enhance the UV resistance and sorption characteristics of these coatings without losing optical abrasion resistance and optical clarity. The most common approach is to blend UV absorbers in the coatings. A more desirable route is to covalently bond the UV absorber into the coating which could minimize problems such as incompatibility, migration, volatility, and solvent

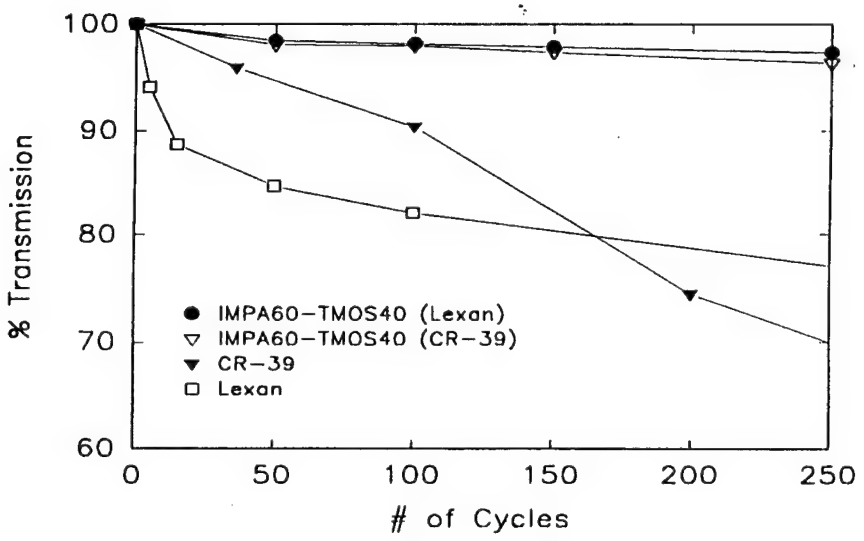

Figure 3. Light transmittance as a function of number of wear cycles for uncoated and coated polycarbonate samples. The cure temperature was 130°C and all the coatings were on a 3-APS primer treated substrate.

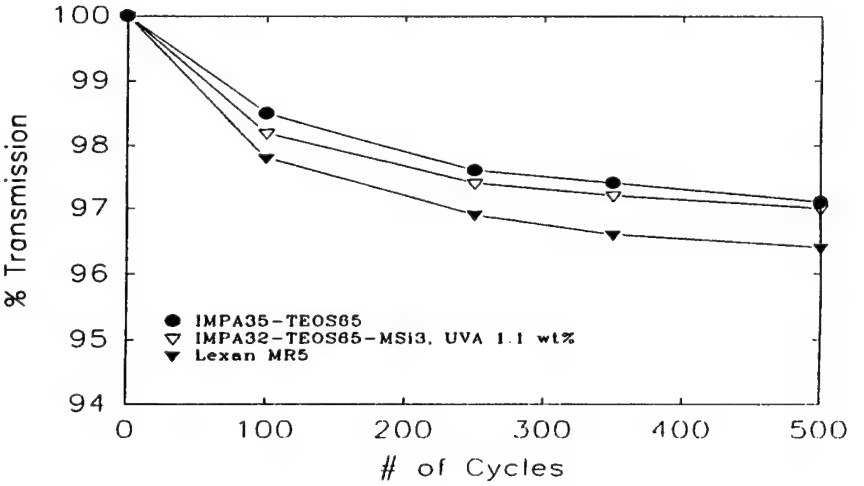

Figure 4. Light transmittance as a function of number of wear cycles for two coated bisphenol-A polycarbonate samples and commercial Lexan MR5® hard coating. Note the scale difference in the % transmission relative to Figure 3.

extraction. In this work, a commercially available UV absorber (Norbloc 7966), was utilized which contains a double bond. It has been successfully bonded into the coating network through the copolymerization with 3-(trimethoxysilyl)propylmethacrylate. Figure 4 clearly shows that the coating containing UV absorber still has excellent abrasion resistance.

Figure 5 shows the UV spectra of the same coating with different amounts of UV absorber on a glass substrate, and shows that the coatings with UVA are capable of absorbing long wavelength UV near 390 nm and the UV absorption ability is dependent, as expected, on the amount of UVA and coating thickness.

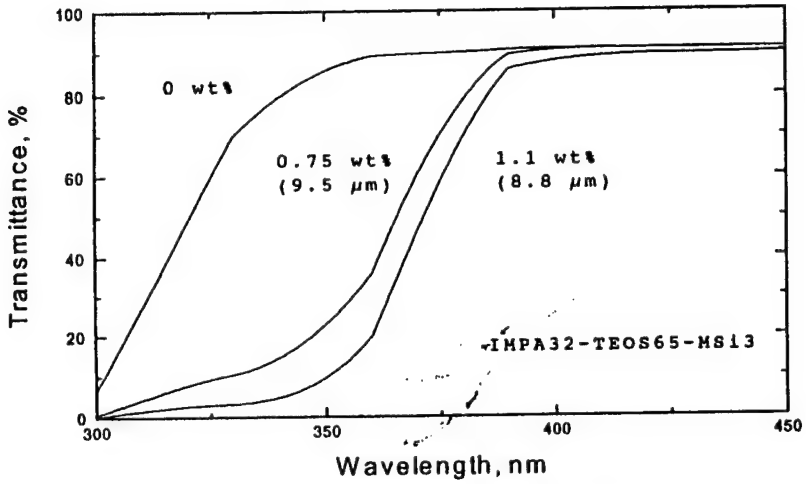

Figure 5. UV spectra of coatings IMPA32-TEOS65-MSi3 with different amounts of UVANorbloc 7966 (wt% in the starting coating solution) coated on glass.

Coatings for Metallic Substrates

One of the best performing abrasion resistant coating on aluminum studied to date is DETA50-TMOS50. After 350 cycles on the Taber abraser, little damage can be discerned visually [15]. A coating produced from neat functionalized DETA is not as abrasion resistant due to the lower content of inorganic material and lower crosslink density. Both coatings have shown good adhesion in the pull-off test (greater than 11.1 MPa). Adhesion of our sol-gel coatings to aluminum substrates may be enhanced by direct covalent bonding between the coating and surface hydroxyls on this metal. Unfortunately, the DETA50-TMOS50 coating performs poorly on steel substrates. Within 350 Taber cycles, pieces of the coating fragment off exposing the bare steel surface. Interestingly, results from the direct pull-off test show that the adhesion between this coating and the steel substrate is significant (greater than 20.9 MPa), and the exact reason for its poor performance is as yet uncertain. Neat DETA performs better in abrasion tests on steel.

Not surprisingly, the coated metal substrates show much better corrosion resistance than uncoated control samples. Both aluminum and steel coated with both neat functionalized DETA

and DETA50-TMOS50 display little visual change after 24 hour exposure to salt water, however, the bare metal surfaces show discoloration and pitting. No performance distinction could be made between the neat DETA and DETA50-TMOS50 coatings on either substrate by visual observation.

CONCLUSIONS

Novel transparent abrasion resistant coating materials prepared by the sol-gel method have been developed and applied to bisphenol-A polycarbonate, diallyl diglycol carbonate resin (CR-39), aluminum, and plain steel substrates. It was found that these hybrid organic/inorganic networks afford excellent abrasion resistance to polymeric substrates. In addition to having excellent abrasion resistance comparable to current commercial coatings; some newly developed systems are also UV resistant. Some extent of corrosion inhibition is afforded to aluminum and steel through these coating systems.

ACKNOWLEDGMENTS

The authors acknowledge the financial support of the Air Force Office of Research under grant number F49620-94-1-0149DEF. One of the authors (KJ) greatly appreciates the support of the Adhesive and Sealant Council and the Center of Adhesive and Sealant Science at VPI&SU.

REFERENCES

1. J. Kasi, JPn. Kokai Tokkyo Koho, JP6335, 633 (88,35,633).
2. H. Schmidt, H. Walter, J. Non-Cryst. Solids **121**, 428, (1990).
3. G. L. Wilkes, B. Orler, H. H. Huang, Polymer Preprints **26(2)**, 300, (1985).
4. H. Huang, R. H. Glaser, G. L. Wilkes, ACS Symp. Ser. **360**, 354, (1988).
5. H. Huang, G. L. Wilkes, Polymer **30**, 2001, (1989).
6. C. Betrabet, G. L. Wilkes, Polymer Preprints **32(2)**, 286, (1992).
7. B. Tamami, C. Betrabet, G. L. Wilkes, Polymer Bulletin **30**, 39, (1993).
8. B. Tamami, C. Betrabet, G. L. Wilkes, Polymer Bulletin **30**, 393, (1993).
9. B.Wang and G.L.Wilkes, J. Macromol. Sci.-Pure Appl. Chem. **A31**, 249, (1994).
10. B. Wang, G. L. Wilkes, C. D., Smith, J. E. McGrath, Polymer Commu. **32**, 400, (1991).
11. C. Betrabet and G. L. Wilkes, J. Inorganic & Organometallic Polymers **4**, 343, (1994).
12. Wang, B; Wilkes, G. L. US patent 5,316,855.
13. Betrabet, C. S.; Wilkes, G. L. J. Inorganic & Organometallic Polym. **4**, 343, (1994).
14. J. Wen and G. L. Wilkes, Journal of Inorganic & Organometallic Polymers **5**, 343, (1995).
15. J. Wen, V. J. Vasudevan, and G. L. Wilkes, J. Sol-Gel Science & Technology **5**, 115, (1995).
16. J. Wen and G. L. Wilkes, PMSE Preprints **73**, 429, (1995).
17. K. Jordens and G. L. Wilkes, PMSE Preprints **73**, 290, (1995).

Appendix 4

PREPARATION OF HIGHLY POROUS SILICA GEL FROM POLY(TETRAMETHYLENE OXIDE) (PTMO)/SILICA HYBRIDS

J. Wen, B. Dhandapani, S. T. Oyama*, G. L. Wilkes*

Department of Chemical Engineering, Virginia Polytechnic Institute and State University, Blacksburg, VA 24061-0211

* To whom correspondence should be addressed.

ABSTRACT

Porous silica gels with high surface area were prepared by calcination of silica/poly(tetramethylene oxide) (PTMO) hybrid network materials. The variation of surface area of these silica gels with PTMO/silica composition and molecular weight of PTMO was investigated. BET surface area analysis showed that for all oligomeric molecular weights of PTMO, high values in the range of 700-900 m^2g^{-1} could be obtained. The opimum PTMO/TEOS weight ratio was 30-50. Pore size analysis indicated that samples with high surface areas were mesoporous, while samples with low or medium surface areas were nonporous. The hysteresis in the adsorption-desorption isotherms indicated that the pores were cylindrical in shape.

INTRODUCTION

Inorganic/organic hybrid materials known as "ceramers" or "ormosils", prepared through the combination of inorganic metal alkoxides and polymers by the sol-gel approach, have been developed and studied since the early 1980s [1-6]. The incorporation of polymeric or oligomeric materials into inorganic networks by the sol-gel process offers an opportunity to optimize specific properties independently. An important characteristic of inorganic/organic hybrid materials is the homogeneous dispersion of the organic species at the molecular level in the inorganic network, which has lead to the development of novel hybrid materials that have or will have potential applications in many fields. One such application is the preparation of highly porous metal oxides having microscale pores. This can be readily done by calcination of the hybrid materials at temperatures below the fusion temperature of the metal oxide, normally 500 to 600 °C. At these temperatures, the

organic species will decompose, leaving the inorganic component with nanoscale or microscale pore size.

For porous materials, the control of pore size and structure is very important for their applications such as adsorbents, separation membranes, and catalyst supports [7]. While limited in number, some different types of hybrid materials have been prepared with different synthetic approaches by various researchers and utilized as the precursors for high surface area porous materials, mostly porous silica [8-15]. Chujo and Saegusa prepared inorganic/organic hybrid materials with silane endcapping poly(N-acetylethyleneimine) (POZO) as the organic component and tetraethoxysilane (TEOS) as the inorganic component, and subsequently produced a porous silica material with surface area as high as ca. 810 m^2/g [8-9]. They indicated in their work that it is possible to control the pore size by using so-called starburst dentrimers as the organic component. Nakanishi et al., also prepared a porous silica gel using poly(acrylic acid) as the organic component [12]. In this work, the structure of the hybrid was controlled by utilizing the competition between polymerization and phase separation in the mixed solution, and the porous silica gel was obtained using solvent extraction of the organic polymer instead of pyrolysis. Other polymers that have been used as organic components include poly(ethylene glycol) (PEG) [13-14], polymer electrolytes and proteins [15], and poly(vinyl alcohol) (PVA) [10]. Besides porous silica gel, microporous silica/zirconium oxide materials have also been prepared utilizing the calcination approach.

The synthesis and structure of poly(tetramethylene oxide) (PTMO)/silica hybrid network materials have been extensively studied in one of our laboratories over the last ten years [16-22]. This paper addresses the preparation of highly porous silica gel from PTMO/silica hybrid network materials through the calcination approach and characterization of these materials by measurements of the Brunauer, Emmett and Teller (BET) surface area, pore size, and pore volume. Adsorption-desorption isotherms are analyzed in terms of the classification scheme discussed in reference [23] which

distinguishes between materials with different pore structures: microporous, mesoporous and macroporous [23].

EXPERIMENTAL

Materials

3-Isocyanatopropyltriethoxysilane was purchased from Huls America, Inc. Hydroxyl-terminated poly(tetremethylene oxide) (PTMO) with number average molecular weight 650, 1000, 2000, and 2900 g/mol were obtained from Polysciences, Inc. Tetraethoxysilane (TEOS), hydrocloride (HCl), isopropanol (IPA) were obtained from the Aldrich Chemical Company.

Preparation of PTMO/silica hybrids

The hydroxyl-terminated PTMO was first functionalized with 3-isocynatopropyltriethoxysilane by our standard route reported earlier [24] . The triethoxysilane end-capped PTMO oligomers were in crystalline form prior to the reactions, therefore, were heated in a beaker at ca. 70 °C before mixing with desired amount of TEOS and solvent IPA. The mixture was stirred for about 20 minutes at room temperature. To this mixture was added water and acid catalyst. The molar ratio of H_2O/ethoxy/HCl was 4/1/0.04 in all cases. The contents of the beaker were stirred for an additional 2 minutes before being poured into polyethylene sample vials (20 mm (D) x 20 mm (H)) and left at room temperature to cure. The reaction usually proceeded rapidly at ambient temperature and the system turned into a gel within 30 minutes. However, depending on initial composition, the drying period varied from one week to one month. A material indicated by TEOS60-PTMO(2000)40 contains 40 wt% of PTMO (Mw = 2000) with respect to the total weight of TEOS and PTMO.

Calcination of PTMO/silica hybrids

The inorganic/organic composites were calcinated at 540 °C in air for 24 hours to dehydrate them thoroughly and remove PTMO. The heating rate from ambient was 1 °C/min and the cooling rate was 10 °C/min.

Apparatus

Thermogravimetric analysis (TGA) was carried out on a Seiko Simultaneous TGA/DTA analyzer (Model TG/DTA200) under air. BET surface area, pore size, pore volume and adsorption-desorption isotherm measurements were done on a Micromeritics ASAP 2010 Chemi system. Prior to nitrogen physisorption experiments the samples were degassed at 473 K for 2 h.

RESULTS AND DISCUSSION

Chemistry

The general sol-gel reaction of the PTMO-TEOS system is illustrated in scheme I. As shown, the PTMO oligomer is chemically bonded into the SiO_2 network. The high transparency of the final products, along with the large difference in refractive index between the two components demonstrated that no macroscale phase separation occurs. However, they tend to undergo some microphase separation similar to segmented or block polymers. Indeed, structural analysis from previous studies demonstrated that the scale of localized phase separation was also found to be dependent on reaction condition, composition, and molecular weight of PTMO. Typically the scale length for this microphase or domain texture is ca. 10 nm [4].

Evolution of surface area and pore size

The evolution of the surface area and pore size of silica was studied by following these properties at different stages of the sample preparation as shown by the TGA and

DTA results. Figure 1 shows typical results obtained by TGA and DTA. TGA showed that most of the weight loss occurred between 155 °C and 340 °C when the heating rate was 1 °C/min. There were two distinct weight loss stages within this temperature range, 155 to 230 and 230 to 340 °C, each being associated with a thermal degradation process as shown by the two endothermic peaks in the DTA curve. The first weight loss stage is associated with the oxidative degradation of PTMO when heated in contact with air. During this stage, the backbone of the PTMO which contain ether linkages are subject to oxidation and forms hydroperoxides which subsequently undergoes thermal degradation. Under these conditions thermal decomposition starts at ca. 155 °C with the evolution of tetrahydrofuran, and the formation of aldehydes and ketones[25]. The second weight loss stage is conjectured to be due to the thermal degradation of N-C-C-C structure associated with isocyonatopropyltriethoxysilane based on the fact that there is no second weight loss stage for pure PTMO.

Figure 2 and Table 1 show the evolution of surface area and pore size for sample TEOS60-PTMO(2000)40. The reaction was stopped at the following temperatures: 240 (held for 1 min), 340 (held for 1 min), 540 °C (held for 1 min, 10 h and 24 h). The BET surface area, pore volume, pore size were obtained from the adsorption-desorption isotherm measurements. According to Figure 1, surface area did not start to increase until the temperature reached 240 °C. At this point, the sample had lost 33 percent of its original weight although its surface area was only 1.7 m^2/g. Following this initial stage, the surface area started to increase and reached 592 m^2/g when the temperature reached 540 °C and the sample had lost 64 percent of its original weight. It can be noted from Figure 2 that surface area increased as the samples were held at 540 °C for 24 hours. There is no weight loss after 10 hours under this temperature. This clearly suggests that under these conditions, there is no significant sintering of silica.

From Figure 3 and Table 1 it can be seen that at 240 °C, the isotherm is Type II in the classification of reference [23], which is typical of either a non-porous material or a

material with pore diameters larger than micropores [23]. Pores with diameters less than 2 nm are in the micropore range, pores with diameters between 2 to 100 nm are mesopores, and pores larger than 200 nm are macropores. By comparing the pore size and the pore volume from Table 1, it can be inferred that there are probably very few pores whose dimensions are in the mesopore range. However, based on the pore volume the material is likely non-porous in nature. In the second stage, at 340 °C, the surface area increases considerably but still a Type II isotherm is observed. This is due to a decrease in the particle size. The particle size can be calculated from the surface area, $d_p=6/\rho S_g$, where d_p is the diameter of the particle, ρ the density of silica and S_g the BET surface area of the sample. These voids are of the same size as the particles, 6 nm. In the third stage at 540 °C (held for 1 min), the surface area increases further but a Type II isotherm is still observed, which matches with the particle size analysis, shown in Table 1. The fifth and sixth stage at 540 °C (held for 10 h and 24 h respectively), shows that the surface area increases further and a Type IV isotherm is observed, indicating pores in the range of mesopores which compares well with the pore size, shown in Table 1. The hysteresis of the Type IV isotherm indicates Type A which corresponds to cylindrical pores.

Effect of Composition

Figure 5 shows the dependence of the BET surface area and pore size on the composition ratio of PTMO and TEOS. The surface area is a maximum at an intermediate ratio of PTMO/ TEOS. For all of the molecular weights of PTMO studied, high surface areas were obtained with an optimum PTMO/TEOS ratio of 30-50 %. The pore sizes of the samples with high surface areas were in the range of mesopores and the samples with low surface areas were nonporous. The types of adsorption-desorption isotherms of the samples studied are summarized in Table 2. Figure 4 shows the isotherms for PTMO MW of 2900 and PTMO/TEOS ratio between 30-70. The samples with low PTMO/TEOS ratio are Type II and with an increase in the ratio of PTMO/TEOS the isotherm changes to

Type IV, and with further increase in the ratio the isotherm remains Type IV. This trend was seen for all the different PTMO molecular weight samples. This corresponds well with the pore sizes measured as shown in Table 2. The Type IV isotherm shows hysteresis of Type A which indicates cylindrical pore structures [23]. In summary, for each molecular weight of PTMO with an increase in the ratio of PTMO/TEOS the pore structure changes from nonporous to mesoporous.

Effect of Molecular Weight of PTMO

Figure 6 shows the effect of molecular weight of PTMO for a PTMO/TEOS ratio of 40/60. No clear trend is observed from Figure 6 due to the limited data available. It is evident that silica gels with high surface area can be obtained from the samples with both low and high PTMO molecular weight. It may be that the templating effect of the PTMO on the silica exerts its influence at the scale of the lowest PTMO molecular weight. Thus, there is no effect of further increasing the PTMO chain length.

CONCLUSIONS

Porous silica with high surface area were prepared by calcination of silica/poly(tetramethylene oxide) (PTMO) hybrid network materials. The BET surface area analysis showed that for all oligomeric molecular weights of PTMO, high surface areas in the range of 700-900 m^2g^{-1} can be obtained with an optimum PTMO/TEOS ratio of 30-50. The pore size analysis indicated that for samples with high surface areas the pores are mesoporous, and for samples with low or medium surface areas the pores are nonporous. The hysteresis of the adsorption-desorption isotherm indicated that the pores are cylindrical in shape.

ACKNOWLEDGMENTS

The authors greatly acknowledge the financial support of the Air Force Office of Scientific Research under grant number F49620-94-1-0149DEF, and the Exxon Education Foundation.

REFERENCES

1. Wilkes, G. L.; Orler, B.; Huang, H. *Polymer Prep.* **1985**, *26*, 300.
2. Schmidt, H. *J. Non-Cryst. Solids* **1985**, *73*, 681.
3. Schmidt, H; Philipp, G. *J. Non-Cryst. Solids* **1984**, *63*, 283.
4. Sanchez, C.; Ribot, F. *New J. Chem.* **1994**, *18*, 1007.
5. Wilkes, G. L.; Huang, H.; Glaser, R. H. "*Silicon-Based Polymer Science: A Comprehensive Resource*", Advances in Chemistry Ser. 224, American Chemical Society, Washington, DC, 1990; p207.
6. Wen, J.; Wilkes, G. L. *Chem. Mater.* **1996**, in print.
7. Richardson, J. T. *Principles of Catalyst Development*, Plenum Press, New York, 1992.
8. Saegusa, T. *J. Macromol. Sci. - Chem.* **1991**, *A28(9)*, 817.
9. Saegusa, T. *PMSE Polym. Prep.* **1994**, *70*, 371.
10. Suzuki, F.; Iwakura, K.; Kuroume, K.; Onozato, K. *J. Colloid Interface Science* **1994**, 167, 424.
11. Nakane, K.; Suzuki, F. *Transaction* **1996**, 52, 143.
12. Nakanishi, K.; Komura, H.; Takahashi, R.; Soga, N. *Bull. Chem. Soc. Jpn.* **1994**, *67*, 1327.
13. Uo, M.; Yamashita, K.; Suzuki, M.; Tamiya, E.; Karube, I.; Makishima, A. J.*Ceram.Soc. Jpn.* **1992**, *100*, 426.
14. Yazawa, T.; Miyake, A.; Tanaka, H. *J. Ceram. Soc. Jpn.* **1991**, *99*, 1094.
15. Sato, S.; Murakata, T.; Suzuki, T.; Ohgawara, T. *J. Mater. Sci.* **1990**, *25*, 4880.
16. Wilkes, G. L.; Huang, H. H.; Glaser, R. H. *Macromolecules* **1987**, *20*, 1322.
17. Huang, H. H.; Wilkes, G. L.; Carlson, J. G. *Polymer* **1989**, *30*.
18. Wilkes, G. L.; Brennan, A. B.; Huang, H.; Rodrigues, D.; Wang, B. *Mat. Res. Soc.Symp. Proc.*, **1990**, *171*.
19. Brennan, A. B.; Wilkes, G. L. *Polymer* **1991**, *32*.

20. Brennan, A. B.; Wang, B.; Rodrigues, D. E.; Wilkes, G. L. *J. Inorganic and Organometallic Polymers* **1991**, *1*.

21. Rodrigues, D. E.; Brennan, A. B.; Betrabet, C.; Wang, B.; Wilkes, G. L. *Chem. Mater.*, **1992**, *4*, 1437.

22. Rodrigues, D. E.; Wilkes, G. L. *J. Inorganic and Organometallic Polymers* **1993**, *3*.

23. Lowell, S.; Shields, J. E. *Powder Surface Area and Porosity*, Chapman and Hall, New York, 1991.

24. Huang, H. H; Wilkes, G. L; Carlson, J. G., *Polymer* **1989**, 30, 2001.

25. Dreyfuss, P.; Pruckmayr, G. *Encyclopedia of Polymer Science and Engineering* Vol 16, 2nd ed., John Wiley & Sons Limited, New York, 1989, pp. 656-669.

Hydrolysis

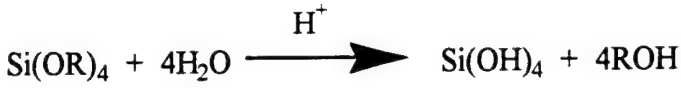

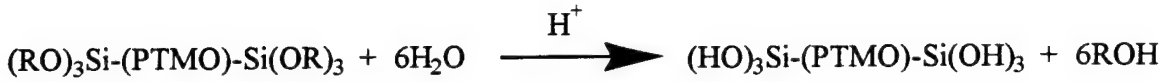

Condensation

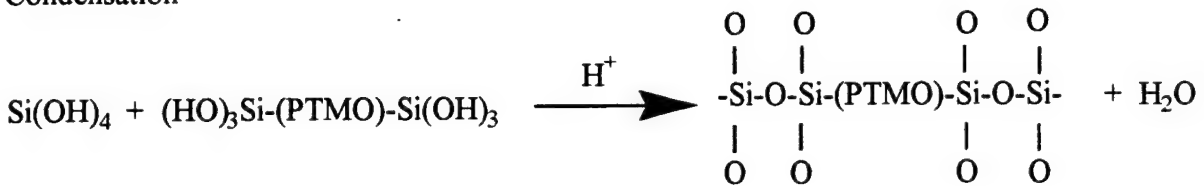

Scheme 1

List of Tables

List of Figures

Table 1. Summary of surface area, pore size, pore volume and isotherm type at different stages of thermal degradation of the organic PTMO (MW 2000), at a weight ratio of 40/60 PTMO/TEOS.

Temp (°C)	BET area (m^2g^{-1})	Particle Size (nm)	Pore Volume (cm^3g^{-1})	Pore Size (nm)	Isotherm Type
240	1.7	1477	0.002	4.4	II
340	395	6.4	0.16	2.0	II
540	592	4.3	0.23	1.9	II
540 (10 h)	625	4.0	0.33	2.2	IV
540 (24 h)	803	3.1	0.61	3.1	IV

Table 2. Summary of BET surface area, pore size, pore volume, and isotherm type of the samples

PTMO MW ($gmol^{-1}$)	Feed ratio (PTMO/TEOS)	BET area m^2g^{-1}	Pore size nm	Pore volume cm^3g^{-1}	Isotherm type
1000	15/85	309	1.8	0.13	II
1000	30/70	760	1.8	0.34	II
1000	40/60	963	2.5	0.55	IV
1000	50/50	1031	2.6	0.66	IV
1000	70/30	725	1.9	0.35	II
2000	15/85	233	1.8	0.10	II
2000	30/70	420	1.8	0.17	II
2000	40/60	803	3.0	0.61	IV
2000	50/50	573	3.5	0.41	IV
2000	70/30	450	2.0	0.19	II
2900	15/85	365	1.8	0.17	II
2900	30/70	531	1.8	0.20	II
2900	40/60	980	3.9	0.95	IV
2900	50/50	760	2.8	0.40	IV
2900	70/30	702	3.3	0.49	IV

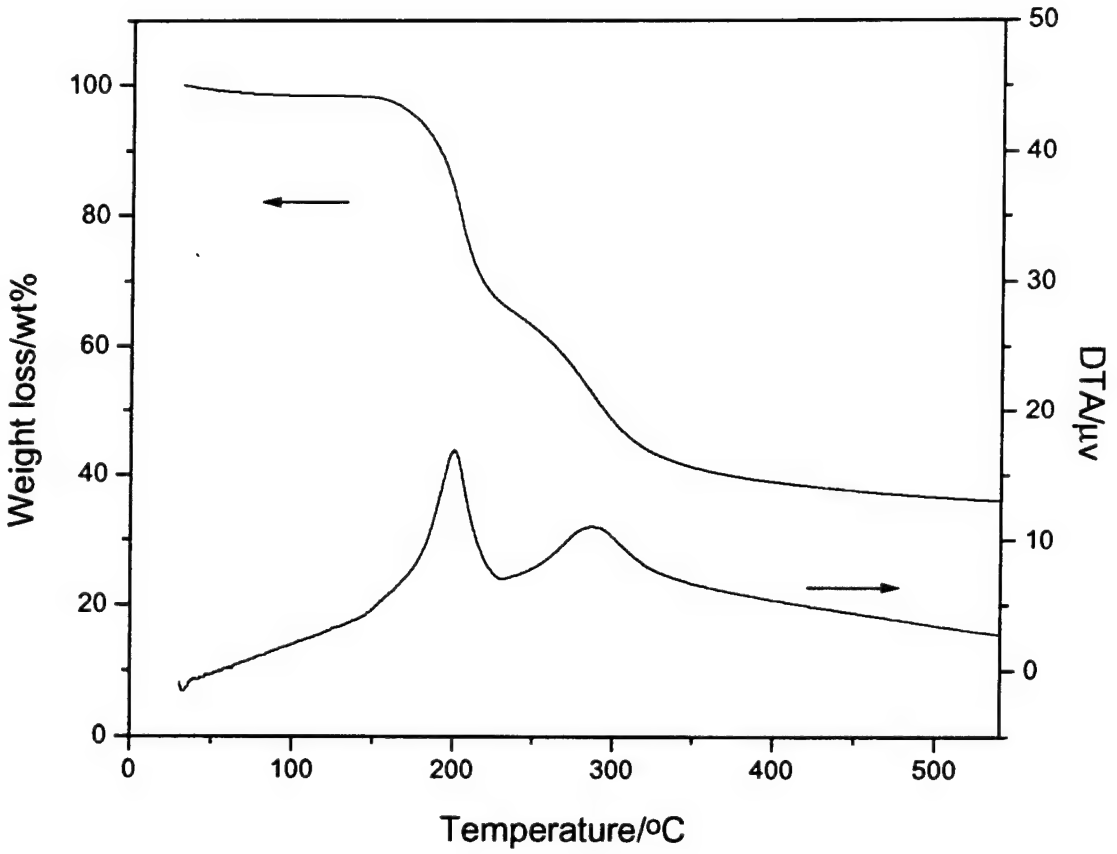
Weight loss/wt%
DTA/μv
Temperature/°C
0
20
40
60
80
100
0
10
20
30
40
50
0
100
200
300
400
500

Figure 1.

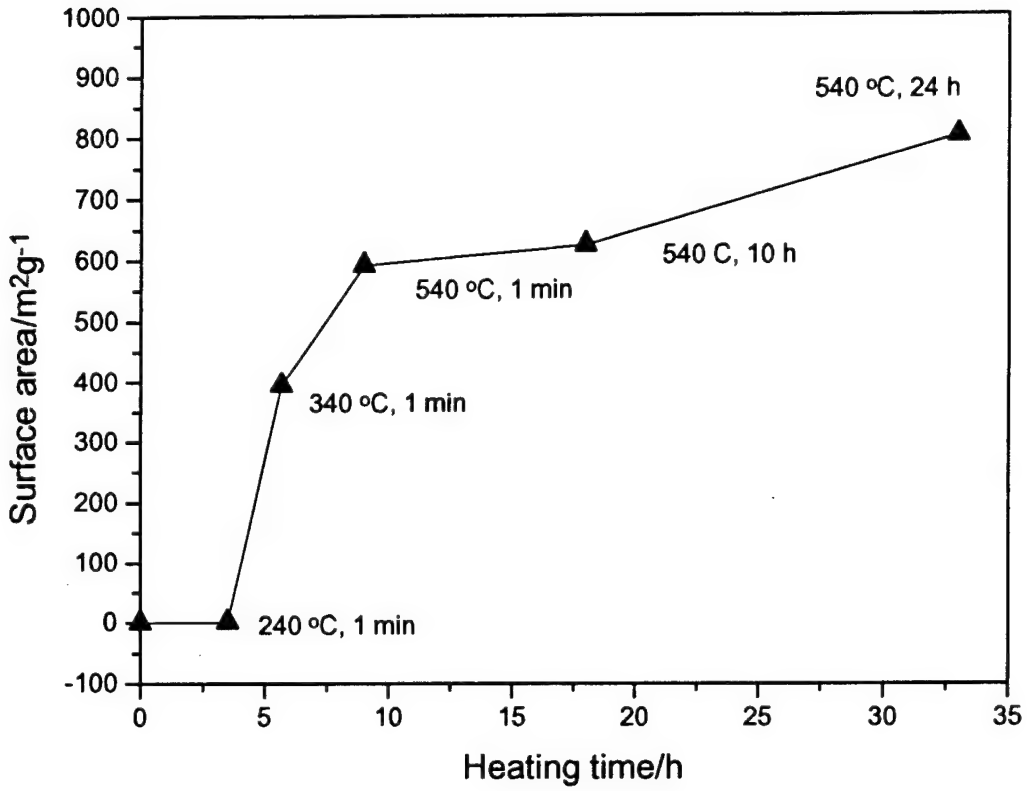
Surface area/m²g⁻¹
Heating time/h
1000
900
800
700
600
500
400
300
200
100
0
-100
0
5
10
15
20
25
30
35
540 °C, 24 h
540 C, 10 h
540 °C, 1 min
340 °C, 1 min
240 °C, 1 min

Figure 2.

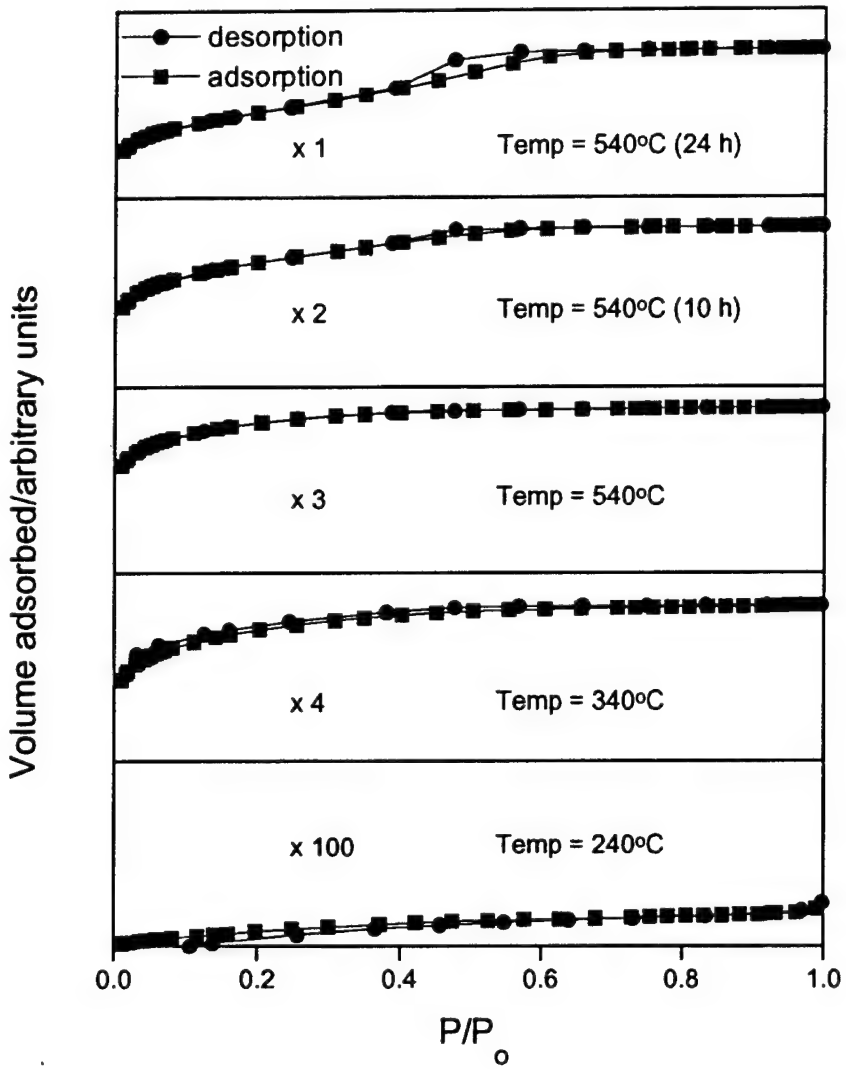
desorption
adsorption
x 1
Temp = 540°C (24 h)
x 2
Temp = 540°C (10 h)
x 3
Temp = 540°C
x 4
Temp = 340°C
x 100
Temp = 240°C
Volume adsorbed/arbitrary units
0.0
0.2
0.4
0.6
0.8
1.0
P/P o

Figure 3.

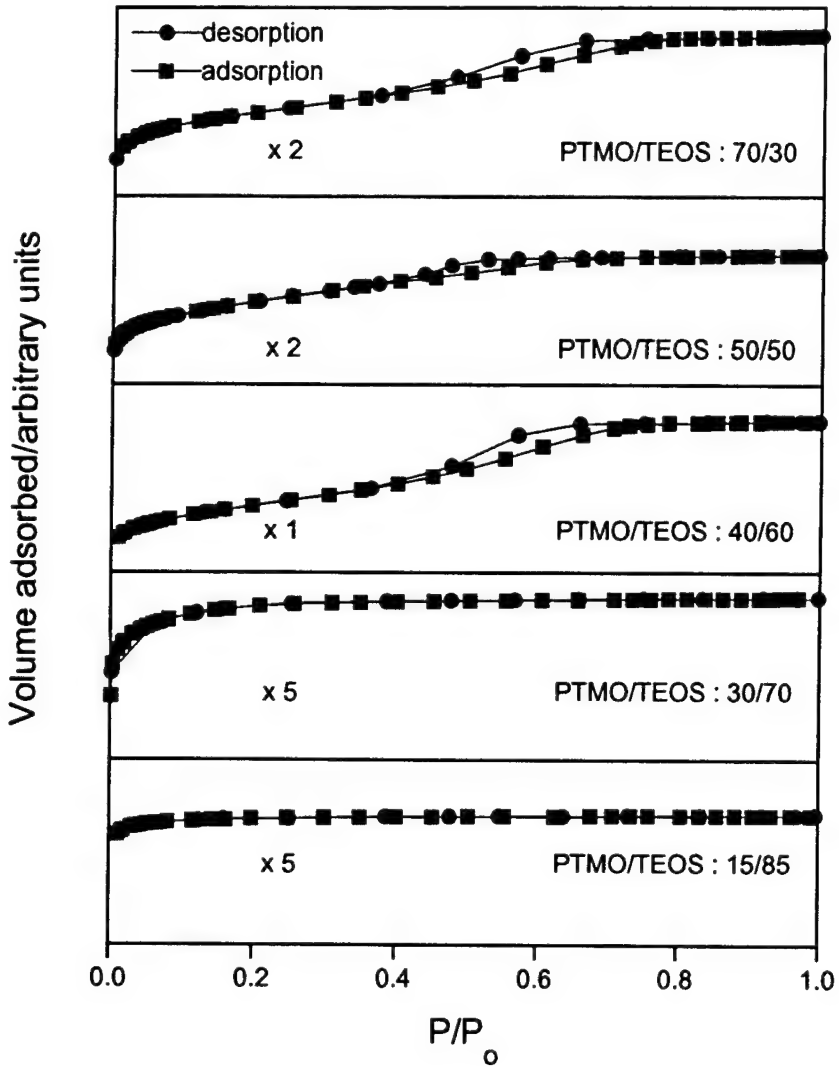
desorption
adsorption
x 2
PTMO/TEOS : 70/30
x 2
PTMO/TEOS : 50/50
x 1
PTMO/TEOS : 40/60
x 5
PTMO/TEOS : 30/70
x 5
PTMO/TEOS : 15/85
Volume adsorbed/arbitrary units
0.0
0.2
0.4
0.6
0.8
1.0
P/P o

Figure 4.

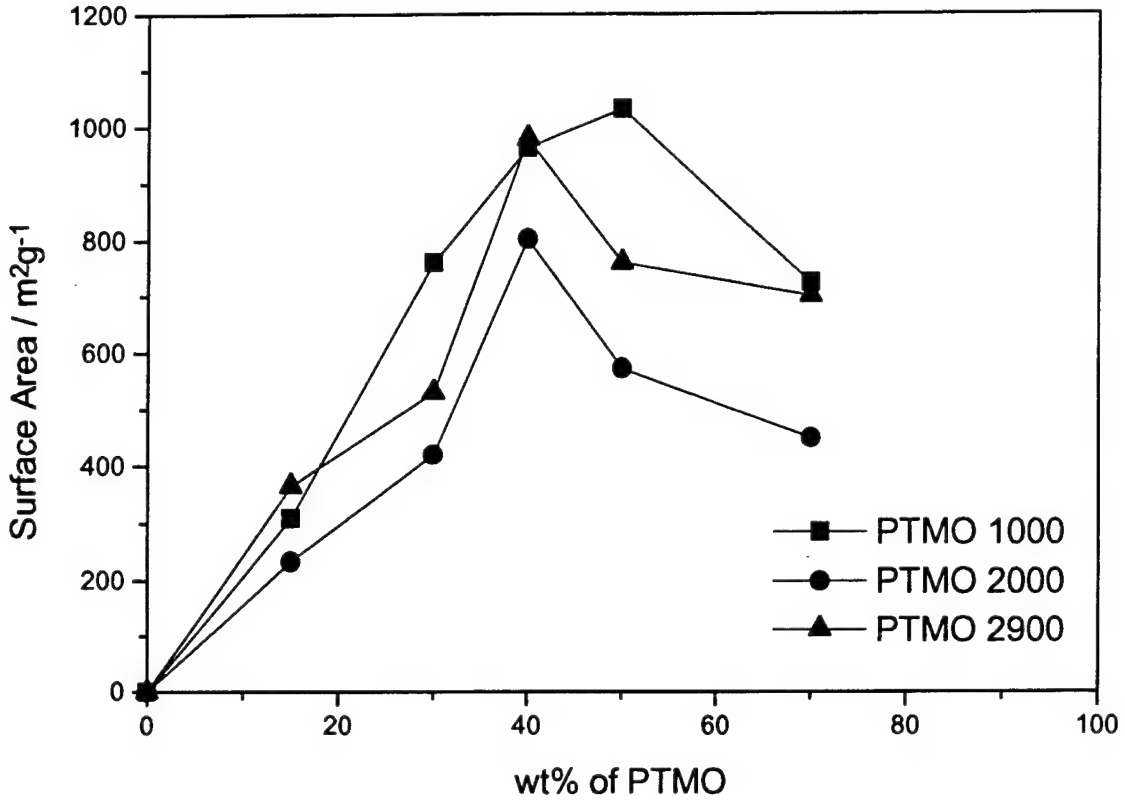
1200
1000
800
600
400
200
0
Surface Area / m²g⁻¹
0
20
40
60
80
100
wt% of PTMO
PTMO 1000
PTMO 2000
PTMO 2900

Figure 5.

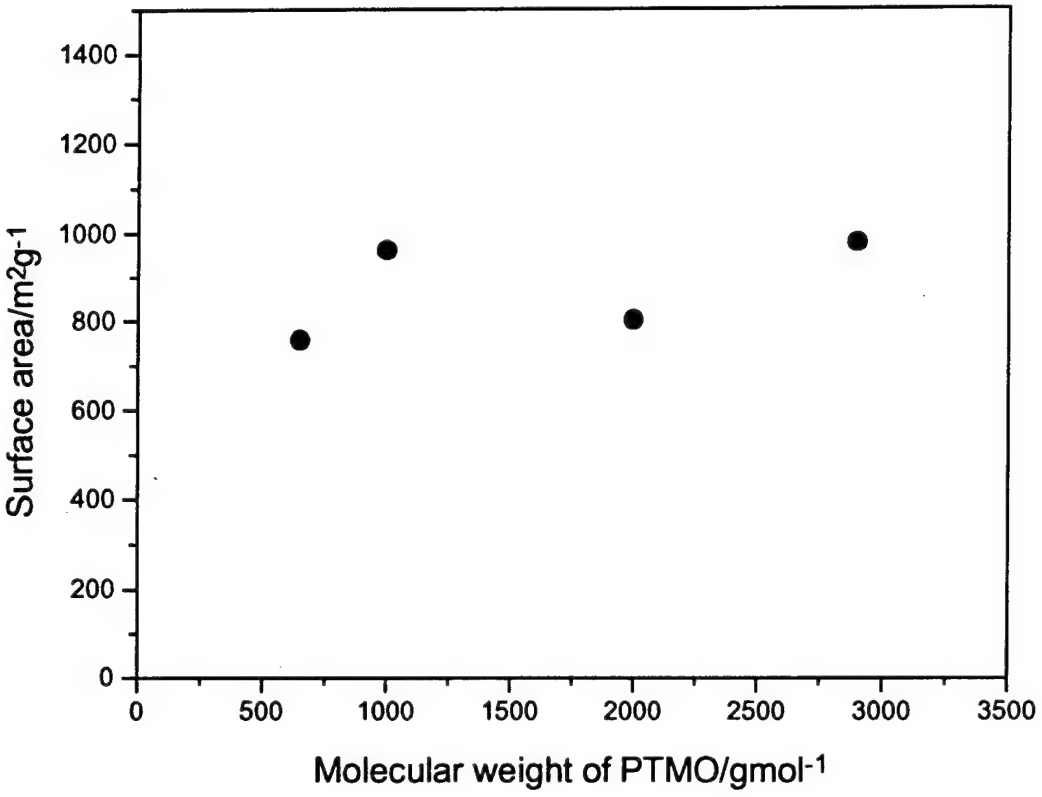
Surface area/m2g-1
1400
1200
1000
800
600
400
200
0
0
500
1000
1500
2000
2500
3000
3500
Molecular weight of PTMO/gmol-1

Figure 6.

Appendix 5

Organic/Inorganic Hybrid Network Materials by the Sol–Gel Approach

Jianye Wen and Garth L. Wilkes*

Department of Chemical Engineering, Polymer Materials and Interfaces Laboratory, Virginia Polytechnic Institute and State University, Blacksburg, Virginia 24061

Received February 9, 1996. Revised Manuscript Received June 19, 1996[⊗]

Organic/inorganic hybrid materials prepared by the sol–gel approach have rapidly become a fascinating new field of research in materials science. The explosion of activity in this area in the past decade has made tremendous progress in both the fundamental understanding of the sol–gel process and the development and applications of new organic/inorganic hybrid materials. In this review, a brief summary of the research activities in the field of organic/inorganic nanocomposite materials and a general background of the sol–gel chemistry are first given. The emphasis of this report, however, is placed on the synthesis, structure–property response, and potential applications of the organic/inorganic hybrid networks that possess chemical bonding between the organic and inorganic phases, particularly those systems that were developed in our laboratory since 1985.

Introduction

The sol–gel process, which is mainly based on inorganic polymerization reactions, is a chemical synthesis method initially used for the preparation of inorganic materials such as glasses and ceramics. Its unique low-temperature processing characteristic also provides unique opportunities to make pure and well-controlled composition organic/inorganic hybrid materials through the incorporation of low molecular weight and oligomeric/polymeric organic molecules with appropriate inorganic moieties at temperatures under which the organics can survive. The organic/inorganic hybrid materials made in this way, which have been termed "ceramers" by Wilkes et al.[1] and "ormosils" or "ormocers" by Schmidt et al.,[2] are normally nanocomposites and have the potential for providing unique combinations of properties which cannot be achieved by other materials. For the past decade, organic/inorganic nanocomposites prepared by the sol–gel process have attracted a great deal of attention, especially in the fields of ceramics, polymer chemistry, organic and inorganic chemistry, and physics. The preparation, characterization, and applications of organic/inorganic hybrid materials have become a fast expanding area of research in materials science. The major driving forces behind the intense activities in this area are the new and different properties of the nanocomposites which the traditional macroscale composites and conventional materials do not have. For example, unlike the traditional composite materials which have macroscale domain size of millimeter and even micrometer scale, most of the organic/inorganic hybrid materials are nanoscopic, with the physical constraint of several nanometers, typically 1–100 nm, as the minimum size of the components or phases. Therefore, they are often still optically transparent materials although microphase separation may exist. Through the combinations of different inorganic and organic components in conjunction with appropriate processing methods, various types of primary and secondary bonding can be developed leading to materials with new properties for electrical, optical, structural, or related applications.

Organic/inorganic hybrid materials prepared by the sol–gel process can be generated using different synthetic techniques by incorporating various starting inorganic and organic components with varied molecular structure:

(1) Hybrid networks can be synthesized by using low molecular weight organoalkoxysilanes as one or more of the precursors for the sol–gel reaction in which organic groups are introduced within an inorganic network through the ≡Si–C– bond.[2-5]

(2) Organic/inorganic hybrid network materials can also be formed via the co-condensation of functionalized oligomers or polymers with metal alkoxides in which chemical bonding is established between inorganic and organic phases.[1,6-7]

(3) A hybrid material can also be synthesized through the in situ formation of inorganic species within a polymer matrix.[8-15] Specifically, inorganic species, generally in the form of particles with a characteristic size of a few hundred angstroms, can be generated in situ within the polymers by first swelling cross-linked, ionomeric, or crystalline polymeric host with a compatible solution containing metal alkoxides followed by the promotion of the sol–gel reaction of the inorganics. Various inorganic particles with extremely homogeneous particle size have been prepared in this manner within elastomeric or plastic matrixes.[16-29] The concept of such "in situ" generation of fillers is novel and of practical importance in terms of elastomer reinforcement.[11,12,30]

(4) Starting from the opposite direction of (3), organic/inorganic composites can be obtained by either the infiltration of previously formed oxide gels with polymerizable organic monomers or the mixing of polymers with a single or mixture of metal alkoxides in a common solvent. In the first approach, the impregnation of porous oxide gels with organics is followed by an in situ

[⊗] Abstract published in *Advance ACS Abstracts*, August 1, 1996.

S0897-4756(96)00114-7 CCC: $12.00

polymerization initiated by thermal or irradiation methods.[31-33] In the second approach, polymers can be trapped within the oxide gel network if the hydrolysis and condensation of metal alkoxide are carried out in the presence of preformed polymers.[34-42] Optically transparent composite materials can be obtained if there is no macro- or microphase separation during both the gel forming and drying process.

(5) Similar to approach (4), organics can also be simply impregnated or entrapped as a guest within inorganic gel matrixes (as a host). This approach has been extensively used in the incorporation of enzymes, proteins, and various organic dyes such as luminescent dyes,[43] photochromic dyes,[44] and nonlinear optical (NLO) dyes[45] into an inorganic network. The main driving force behind the intensive research activity in preparation of these types of materials is the development of new optical and bioactive materials in the application of photophysical, electrical, biotechnical, and nonlinear optical (NLO) devices.[43,46-51]

(6) Hybrid networks can also be formed by interpenetrating networks and simultaneous formation of inorganic and organic phases. By using triethoxysliane $R'Si(OR)_3$ as the precursor with R′ being a polymerizable group such as an epoxy group, an organic network can be formed within the inorganic network by either photochemical or thermal curing of such groups, as Schmidt has demonstrated in 1984.[4,52,53] Novak and Grubbs[54] also developed an interesting convenient method to form inorganic/organic simultaneous interpenetrating networks (SPINs), where both inorganic glass and polymer formation occur concurrently. These transparent composites are synthesized through a synchronous application of the aqueous ring-opening metathesis polymerization (aqueous ROMP) of cyclic alkenyl monomers and the hydrolysis and condensation of metal alkoxides.

(7) Other new synthetic strategies have also been developed in recent years.[55-63] For example, by employing polymerizable monomers as the cosolvent such that all mixture components contribute either to the silica network or to the organic polymer to avoid large scale shrinkage, a "nonshrinking" sol–gel composite materials can be obtained.[56,57] A different kind of inorganic/organic nanocomposite material has been developed by exploiting the unique intercalation and self-assembling characteristics of layered ceramics, particularly those based on the 2:1 layered silicates.[58-62] These 2:1 layered silicates consist of two-dimensional layers formed by sandwiching two SiO_2 tetrahedral sheets to an edge-shared octahedral sheet. Single chains of the polymer alternately stacked with the layers of the host can be obtained by intercalative polymerization of various monomers in the silicate galleries. Researchers[63] are also exploring novel processing strategies to produce organic/inorganic composite biomimetically—taking inspiration from the fact that biological systems fabricate complex multicomponent, multiphase materials using assembly, and processing strategies that are unique but reproducible.

The incorporation of organic/oligomeric/polymeric materials into organic/inorganic networks by the sol–gel process makes it possible to optimize selected properties independently. Specifically, the introduction of organic groups into an inorganic network leads to new structure–property variation, thereby promoting new potential applications for the resulting composite materials. As examples:

(1) Flexibility can be introduced by the incorporation of organic/oligomeric/polymeric materials into the inorganic networks.

(2) New electronic properties, such as conductivity, redox properties, etc., can be achieved by introducing conductive polymers along with transition-metal alkoxides.

(3) By incorporating organic dyes or π-conjugated polymers into the inorganic networks, the optical properties can be systematically altered in both the linear as well as nonlinear optical properties (NLO).

Even though many of the network systems are comprised of components having very different refractive indexes, the resulting material can often be prepared optically transparent due to the small scale lengths over which phase separation may exist. As a result, these composite materials can find applications in many fields which are far beyond the scope of application of traditional composite materials and this is one important reason for the strong interest in the application of organic/inorganic hybrid materials. To date, the number of commercial sol–gel hybrid products is still comparatively small, but the promise of new technological uses remains. Some potential applications for these materials are as follows:

(1) Scratch and abrasive-resistant hard coatings and special coatings for polymeric materials, metal, and glass surfaces.[64-74]

(2) Electrical and NLO materials.[42,43,47,48,75,76]

(3) Adhesives and contact lens materials.[65,77]

(4) Reinforcement of elastomers and plastics.[8,12,25-27,60-62]

(5) Catalyst and porous supports, adsorbents.[5,36]

(6) Tunable solid-state lasers[78,79] and chemical/biomedical sensors.[80,81]

On the basis of the connection between the inorganic and organic phases, the organic/inorganic composite materials can be also conveniently divided into two general classes: those with chemical bonding between the two phases and those without.[82] *Following a brief introduction to the sol–gel chemistry, this review principally addresses the synthesis, structure–property response, and applications of organic/inorganic nanocomposites with chemical bonding between the organic and inorganic phases, with some emphasis on the research carried out in our laboratories that was initiated in 1985.* As can be imagined, it is impossible to completely review this field and omissions to the other workers has not been by design but is due to space limitations. In this regard the interested reader is referred to some other recent reviews[49,82-91] to allow a complete view of the history and recent development of organic/inorganic hybrid materials.

General Background of Sol–Gel Chemistry

Considering the key role of the sol–gel reaction in the preparation of organic/inorganic hybrid materials, it is difficult to understand their preparation without a basic knowledge of the sol–gel process. Over the past 2 decades numerous studies have been carried out in the field of sol–gel chemistry, and great progress has been made in understanding the reaction mechanisms although many questions remain. However, a brief review of the most basic sol–gel chemistry, especially

Scheme 1

drolysis

$$Si(OR)_4 + H_2O \longrightarrow (HO)Si(OR)_3 + ROH$$
$$(OH)Si(OR)_3 + H_2O \longrightarrow (HO)_2Si(OR)_2 + ROH$$
$$(OH)_2Si(OR)_2 + H_2O \longrightarrow (HO)_3Si(OR) + ROH \quad (1)$$
$$(OH)_3Si(OR) + H_2O \longrightarrow Si(OH)_4 + ROH$$

cohol Condensation (Alcoxolation)

$$\equiv Si\text{–}OR + HO\text{–}Si \equiv \longrightarrow \equiv Si\text{–}O\text{–}Si \equiv + ROH \quad (2)$$

ater Condensation (Oxolation)

$$\equiv Si\text{–}OH + HO\text{–}Si \equiv \longrightarrow \equiv Si\text{–}O\text{–}Si \equiv + HOH \quad (3)$$

verall Reaction

$$Si(OR)_4 \xrightarrow[H^+,\ OH^-]{H_2O,\ solvent} \text{(silicate network)} \quad (4)$$

at related to the preparation of organic/inorganic mposites, is still appropriate here. Interested readers ay refer to other studies and reviews for a more mplete understanding of the entire sol–gel field.[92–100]

As stated earlier, the sol–gel reaction is a method to epare pure ceramic precursors and inorganic glasses relatively low temperatures. The reaction is generally vided into two steps: hydrolysis of metal alkoxides produce hydroxyl groups, followed by polycondensa- on of the hydroxyl groups and residual alkoxyl groups form a three-dimensional network. The general heme can be represented in Scheme 1 with silicone koxide as the example.

The sol–gel process generally starts with alcoholic or her low molecular weight organic solutions of mono- eric, metal or semimetal alkoxide precursors $M(OR)_n$, here M represents a network-forming element such s Si, Ti, Zr, Al, B, etc., and R is typically an alkyl group $_xH_{2x+1}$) and water. Generally, both the hydrolysis and ondensation reactions occur simultaneously once the ydrolysis reaction has been initiated. As can be seen om Scheme 1, both the hydrolysis and condensation eps generate low molecular weight byproducts such s alcohol and water. These small molecules must be emoved from the system, and such removal would lead, the limit, to a tetrahedral SiO_2 network if the species ere silicon. The removal of these byproducts also ontribute to the high shrinkage that occurs during the lassical sol–gel process.[100]

Both hydrolysis and condensation occur by nucleo- hilic substitution (S_N) mechanisms which involve three teps: nucleophilic addition (A_N), proton transfer within he transition states, and removal of the protonated pecies as either alcohol or water. For non-silicate netal alkoxides, generally no catalyst is needed for ydrolysis and condensation because they are very eactive. In the case of silicon based metal alkoxides, he hydrolysis and condensation reactions typically roceed with either an acid or base as catalyst. There- ore, the structure and morphology of the resulting etwork strongly depend on the nature of the catalyst.

Table 1. Electronegativity (χ), Coordination Number (N), and Degree of Unsaturation ($N - Z$) for Some Metals

alkoxides	χ	N	Z	$N - Z$
$Si(OPr^i)_4$	1.90	4	4	0
$Sn(OPr^i)_4$	1.96	6	4	2
$Ti(OPr^i)_4$	1.54	6	4	2
$Zr(OPr^i)_4$	1.33	7	4	3
$Ce(OPr^i)_4$	1.12	8	4	4
$Al(OPr^i)_3$	1.61	6	3	3

common silicon alkoxides, since the hydrolysis rate is high under an acidic environment relative to that of condensation, acid catalysis promotes the development of more linear or polymer-like molecules in the initial stages. For a pure metal alkoxide system, this will result in the formation of high-density, low fractal dimension structures. On the other hand, base catalysis results in a higher condensation rate. Therefore, this environment tends to produce more of a dense-cluster growth leading to dense, colloidal particulate structures.[98,100–102] In addition to the pH of the reaction, the size of the alkoxy group can also influence the hydrolysis and condensation reactions through a steric or leaving-group stability effect. For example, species such as tetramethoxysilane (TMOS) tends to be more reactive than tetraethoxysilane (TEOS).

Mixed-metal alkoxide systems are also of great interest because of the potential properties and applications they provide. In the case of different metal alkoxide combinations, the structure and morphology of the resulting network depend not only on the nature of catalyst but also on the relative chemical reactivity of metal alkoxides. The great difference in their reactivity can often cause phase separation.[103] Therefore, the control of the reactivity of metal alkoxides is necessary in order to be able to tailor the structure of the resulting materials. The hydrolysis and condensation reactions in the sol–gel process generally start with the nucleophilic addition of hydroxylated groups onto the electrophilic metal atoms which results in an increase of the coordination number of the metal atom in the transition state. As described by Sanchez and Ribot, the degree of reactivity of a given metal or semi-metal atom of an alkoxide is not due only to the electrophilic nature but rather is more a function of degree of unsaturation.[82] The extent of unsaturation is given as $(N - Z)$, where N is the coordination number of the atom in the stable oxide network and Z is the oxidation state. Table 1 lists the electronegativity and the degree of metal unsaturation for a few metal alkoxides. It is noted that silicon has a low electrophilicity and zero degree of unsaturation. Therefore, silicon alkoxides are less reactive. On the other hand, non-silicate metal alkoxides, including elements such as Ti, Zr, Al, and B with higher unsaturation, all have much higher reactivity than silicon. They are so sensitive to moisture, even in the absence of a catalyst, that precipitation of the oxide will generally occur as soon as water is present. For example, the hydrolysis and condensation rates of titanium butoxide are much faster than that of tetraethoxysilane (TEOS). As a result, titanium butoxide generally reacts rapidly with water and precipitates out of the reaction mixture before it can coreact with the TEOS into a network. The sequence of reactivity is expressed as follows:[103,104]

$$Zr(OR)_4, Al(OR)_3 > Ti(OR)_4 > Sn(OR)_4 \gg Si(OR)_4$$

There are several ways to control the coreactivity of two or more metal alkoxide species to avoid unnecessary phase separation. Chemical additives, such as glycols, organic acids (acetic acid), β-dicarbonyl ligands (ethyl acetoacetate (EACAC)), have often been used as chelating ligands to slow the hydrolysis and condensation reactions of non-silicate metal alkoxides.[105,106] After forming a complex with the chelating ligand, the species between metal and chelating agent is less easy to hydrolyze.[107] However, the chelating ligand will normally remain which alters the structure of the final network. Chemically controlled condensation (CCC), a procedure proposed by Schmidt and Seiferling,[108] has also been used to control the difference in reactivity of various metal alkoxides. Specifically, hydrolysis of a fast-reacting alkoxide species is slowly initiated by the controlled release of water from the esterification of an organic acid with an alcohol. Once the fast-reacting alkoxide has been partially hydrolyzed and condensed, water is added to complete the overall reaction and to incorporate the slower reacting alkoxide. Another useful method was used by Parkhurst et al.[109] to incorporate titanium butoxide into TEOS-based silica gel. In this procedure, the TEOS species is allowed to partially hydrolyze and condense in the presence of an acid catalyst and water. Then, fast-reacting titanium butoxide is added. Once introduced, it quickly hydrolyzes and at least partially condenses into the preexisting immature TEOS-based network rather than precipitating as titania.

Synthesis and Properties of Organic/Inorganic Nanocomposites

Both small organic moieties and polymeric/oligomeric species can be chemically bonded with inorganic components to produce organic/inorganic hybrid network materials. In this section, such hybrid materials with functionalized polymeric/oligomeric species as the organic component are reviewed first, with emphasis on the work from our laboratories. Following this, the incorporation of small organic groups is discussed.

Hybrid Materials Incorporating Polymeric/Oligomeric Species

A new range of material properties can be produced by combining the features of the inorganic sol–gel alkoxide moieties with those of oligomeric/polymeric species. The resulting composites can vary from soft and flexible to brittle and hard materials depending on the chemical structure of the organic components and the overall composition ratio of organic to inorganic. Modification of the structure of inorganic components also has a profound effect on the properties of the resulting composite materials although the majority of the research concern the sol–gel processing of silica.

Many polymeric/oligomeric species have been successfully incorporated within inorganic networks by different synthetic approaches. The chemical bond between inorganic and organic phases can be introduced mainly by three approaches: (1) functionalize oligomeric/polymeric species with silane, silanol, or other functional groups that can undergo hydrolysis and condensation with metal alkoxides; (2) utilize already existing functional groups within the polymeric/oligomeric species; (3) use alkoxysilanes ($R'Si(OR)_3$) as the sole or one of the precursors of the sol–gel process with R′ being a second-stage polymerizable organic group often carried out by either a photochemical or thermal curing following the sol–gel reaction. Table 2 lists many oligomers and polymers that have been incorporated into an inorganic network via this method. Table 2 is by no means comprehensive, and only these systems with chemical bonding between organic and inorganic phases will now be presented here.

Table 2. Oligomers/Polymers Used in the Preparation of Organic/Inorganic Hybrid Materials

oligomers/polymers	phase connection	ref
poly(dimethylsiloxane) (PDMS)	chemical bond	1, 6, 7, 109, 110–122
poly(tetramethylene oxide) (PTMO)	chemical bond	6, 7, 123–132
poly(methyl methacrylate) (PMMA)	chemical bond	3, 133
	no chemical bond	31–33
polystyrenes	chemical bond	134
polyoxazolines (POZO)	chemical bond	135
	no chemical bond	166
polyimides	chemical bond	130, 136–139
	no chemical bond	140
polyamide	no chemical bond	141
poly(ether ketone) (PEK)	chemical bond	158
poly(ethylene oxide)	chemical bond	142
poly(butadiene)	no chemical bond	116, 143
epoxy	chemical bond	5, 144
polycarbonate	no chemical bond	34
poly(vinyl alcohol)	no chemical bond	35, 37
poly(methyloxazoline)	chemical bond	36
poly(ethyloxazoline)	chemical bond	38
poly(vinyl acetate)	no chemical bond	34, 145, 146
poly(acrylic acid)	no chemical bond	41
poly(ethyleneimine)	chemical bond	147, 148
poly(2-vinylpyridine)	no chemical bond	39
poly(*p*-phenylenevinylene)	no chemical bond	74
poly(*N*-vinylpyrrolidone)	no chemical bond	36
poly(ϵ-caprolactam)	no chemical bond	149, 150
polyurethane	no chemical bond	149, 150
poly(*N*,*N*-dimethylacrylamide)	no chemical bond	34
cellulosics	no chemical bond	40
poly(silicic acid esters)	no chemical bond	57
polyacrylics	chemical bond	151
poly(arylene ether phosphine oxide)	chemical bond	152
poly(oxypropylene)	chemical bond	116
poly(arylene ether sulfone) (PSF)	chemical bond	153
cellulose acetate	chemical bond	154
poly(acrylonitrile)	no chemical bond	39
	chemical bond	155

1. Incorporation of Poly(dimethylsiloxane) (PDMS). As already mentioned, the low process temperature characteristic of the sol–gel reactions makes it possible to incorporate preformed oligomers or polymers that are often functionalized with trialkoxysilyl groups into the organic/inorganic networks via the cocondensation of functionalized oligomers or polymers with metal alkoxides. In 1985, work was initiated in our laboratory to develop novel organic/inorganic hybrid network materials by reacting metal alkoxides with functionalized polymeric/oligomeric species. The first successfully prepared system was that of the PDMS–TEOS system.[1,6,7] Low molecular weight (500–1700 g/mol) PDMS oligomers terminally functionalized with silanol groups were successfully coreacted into a network with TEOS, using an acid catalyst. The chainlike inorganic structures were promoted by using acidic catalysts. This system was studied later by other researchers[109,115–122] and PDMS with higher functionality and molecular weight have also been incorporated into the silica networks.[115]

The backbone of PDMS and the hydrolysis/condensation products of TEOS possess the same nature of chemical bonds (Si–O–Si) which help to make the organic and inorganic components more compatible. PDMS can also be maintained in solution with the reactive sol–gel components during reaction. If hydrolysis of the metal alkoxide is sufficiently rapid so as to provide hydrolysis products of the alkoxide for reaction with the silanol-terminated PDMS, a better dispersion of the functionalized PDMS in the final network can be achieved. Structural analysis by small-angle x-ray scattering (SAXS), dynamic mechanical spectroscopy (DMS), and other techniques did demonstrate that fine dispersion of PDMS was achieved by optimizing the reaction conditions even though some degree of localized microphase separation did occur and was influenced by reaction conditions and catalyst.[6,7] Systematic experiments were carried out to study the effects of the acid content, the content of PDMS, and the molecular weight of PDMS on the structure and properties of this material.[110–114] Depending on the amount and molecular weight of PDMS used, the final materials could be either flexible or brittle and all showed optical transparency clearly indicating that phase (domain) size was smaller than the wavelength of visible light. As expected, decreasing the PDMS content resulted in a system with higher modulus, but also led to cracking and greater shrinkage which made difficult to prepare thick monolithic materials as is also the case for pure sol–gel glasses. Less microphase separation and improved molecular uniformity was achieved with the use of PDMS of lower molecular weight. Of the three factors, however, the mineral acid content of the reacting system was particularly important in determining the structure of the final materials. A model was suggested to interpret the experimental results. At the beginning of the reaction, some self-condensation of the PDMS species was believed to take place, particularly if given sufficient time, because most of the silanol groups arose from the PDMS. As the hydrolysis reaction of TEOS occurs, the dominant type of reaction will shift from self-condensation of PDMS to co-condensation of PDMS and hydrolyzed TEOS because silanol groups are generated from TEOS. Finally, if the silanol functionalities from PDMS species become exhausted, some self-condensation of TEOS occurs. According to this reaction scheme, the relative length of these three reaction periods clearly will determine the structure of the final cast products. High acid content will result in a relatively short first period because the rate of the hydrolysis reaction of TEOS is increased. This suggests that less PDMS will be phase-separated and more will be incorporated into the network of TEOS. The reverse will be true if the first period is relatively long, as is the case for a low acid content. A better overall dispersion of PDMS could be achieved with a higher acid content. However, higher acid content can also promote backbone (–Si–O–) interchange within PDMS chains, i.e., the cleavage of Si–O skeletal bonds, formation of cyclic species, and recombination of PDMS chains. This may also alter the morphology and structure of the final materials by particularly influencing the molecular weight distribution of the initial PDMS oligomers.

Hybrid networks prepared from PDMS and titanium tetraalkoxide, TIP, was also studied by Joardar.[122] In this case, TIP end-capped PDMS instead of silanol-terminated PDMS was used to avoid possible PDMS chain degradation by additional TIP. Hybrid materials synthesized from varying PDMS–TIP compositions and different initial reaction conditions were then subjected to a systematic structure–property relationship study. Compared to the PDMS–TEOS systems, the PDMS–TIP materials showed less phase mixing and were of higher modulus for a comparable ratio of organic to inorganic components. At the 50/50 PDMS–TIP composition there was a rather distinct change in the mechanical properties which signified a morphological change in these materials. It was proposed that connectivity of the titanium oxide domains occurred at the 50/50 PDMS–TIP composition level which resulted in the changes in morphology and mechanical properties. SAXS and electron microscopy studies indicated that the domain sizes of the oxide phase in the PDMS–TIP material were smaller than those in the PDMS–TEOS material of equivalent composition, and these differences may be due to the reactivity difference between TIP and TEOS. Recently, Babonneau[121] prepared hybrid PDMS–oxide gels by cross-linking OH-terminated PDMS with Si, Ti, or Zr alkoxides. This researcher further investigated the influence of the alkoxide nature on the development of OH-terminated PDMS networks by ^{29}Si and ^{1}H MAS NMR, as well as Ti K edge X-ray absorption for titanium-containing gel. TEOS was found to serve as a cross-linking agent which prevents chain extension, i.e., self-condensation of the functionalized PDMS. On the other hand, titanium or zirconium alkoxides seem to behave mainly as a catalyst for condensation of PDMS and thus leads to the formation of long PDMS chains through self-condensation. In both cases, reactions occur between PDMS and the metal alkoxides during the hydrolysis process.

2. Incorporation of Poly(tetramethylene oxide) (PTMO). While the successful preparation of PDMS–TEOS systems did demonstrate the possibility to prepare organic/inorganic hybrid networks, these composites did not display high tensile strength and elongation which was attributed to remaining loose or dangling PDMS chain ends and the molecular weight "scrambling" or redistribution of PDMS chains caused by higher acid catalyst concentration.[6,7] The inherently poorer mechanical properties of pure PDMS along with these network defects were believed to lower the tensile strength of the resulting materials. To overcome these problems, hydroxyl terminated PTMO oligomers (650–2900 g/mol) with better mechanical properties were made. However, a different approach was utilized in functionalizing the PTMO oligomers. As mentioned above, a difference in the reactivity of the end groups of the selected oligomer and that of TEOS can result in poor incorporation of the oligomeric component. Therefore, the use of functional groups with reactivity comparable to those that exist on the alkoxide group certainly favors the preparation of hybrid systems with better component dispersion and network development. Often this can be achieved by endcapping the oligomeric or polymeric components with triethoxysilane groups.[7] For example, oligomers or polymers can be functionalized with triethoxysilane groups by allowing triethoxysilyl isocyanates to react with oligomers or polymers containing pendant amines or alcohols to form urea or urethane linkages, respectively. Triethoxysilane-func-

Scheme 2

Hydrolysis:

$$Si(OR)_4 + 4H_2O \xrightarrow{H^+} Si(OH)_4 + 4ROH$$

$$(RO)_3Si\text{-}(PTMO)\text{-}Si(OR)_3 + 6H_2O \xrightarrow{H^+} (HO)_3Si\text{-}(PTMO)\text{-}Si(OH)_3 + 6ROH$$

Co-condensation:

$$Si(OH)_4 + (HO)_3Si\text{-}(PTMO)\text{-}Si(OH)_3 \xrightarrow{H^+} \text{–SiOSi–(PTMO)–SiOSi–} + H_2O$$

tionalized PTMO oligomers are a typical example, and the reaction scheme is shown in Scheme 2 using various functionalized species in conjunction with a metal alkoxide such as TEOS.[6,7,123–132] It should be pointed out here that the extent of reaction is certainly not complete. The extent of reaction can be estimated by using ^{29}Si NMR and weight-loss methods as demonstrated for other hybrid network systems.[127] Depending on the reaction conditions and composition ratio of PTMO to TEOS, these resulting hybrid networks can again vary from soft and flexible to brittle and hard materials and still maintain optical transparency. Compared to the organic/inorganic hybrid materials prepared by using PDMS oligomers, the acid-catalyzed PTMO-containing hybrid materials generally provide an enhanced mechanical response for an equivalent oligomer content due to higher functionality and the nature of PTMO oligomers. For example, for the PTMO–TEOS materials with an initial weight percentage of TEOS ranging from 50 to 70 wt %, the tensile strength may be as high as 30 MPa and strain-at-break ranges from several percent to over 100%. In contrast, the tensile strength for its PDMS counterpart never exceeded 6 MPa, and the strain-at-break was less than 20%.[7]

The reaction scheme for PTMO–TEOS systems is different from the three-period reaction model for PDMS–TEOS systems.[6,7] The PTMO molecules have three functional groups at each end that can undergo hydrolysis and condensation together with TEOS. The PTMO oligomers are therefore certainly more likely to be chemically connected into the final network. In addition, phase separation is more likely to be suppressed due to the homogeneity of the solution of functionalized PTMO and TEOS, assuming there is no preferential condensation of either component. Therefore, the reaction model suggested by Brinker et al.[156] for acid-catalyzed pure TEOS network has been generalized to interpret the development of the PTMO–TEOS systems. When PTMO chains are incorporated into the TEOS network, their glass transition behavior can be changed if there is any mixing with the hard condensed TEOS segments. The movement of the neighboring PTMO chains will be restricted due to the local presence of the inorganic moieties. Thus, because more thermal energy will be required to mobilize the incorporated oligomeric chain, these restrictions will result in an increase of the glass transition temperature of the oligomeric chain as has been observed in the earlier PDMS–TEOS systems as well.

Utilizing the above analysis, the experimental results such as stress–strain response and DMS of PTMO–TEOS systems were rationalized. As the molecular weight of PTMO increases, the restrictions to the oligomeric chains decrease due to their coil-like nature. Also, there is poorer mixing. Consequently, the increase of T_g becomes less significant and the modulus of the final material decreases. As the TEOS content increases, the result is higher modulus, higher T_g, lower elongation at break, and higher tensile strength. In addition to the effects of the molecular weight of PTMO and TEOS content, the influence of the number of triethoxysilane functional groups along a given PTMO backbone was also investigated by replacing triethoxysilane-endcapped PTMO with branched PTMO systems. Unlike the triethoxysilane-endcapped PTMO, these branched PTMO systems were of somewhat higher molecular weight (5800 g/mol) and possessed a controlled number of triethoxysilane groups along the backbone of the chain. It was observed that the presence of additional pendant triethoxysilane groups did have a systematically significant effect on mechanical properties of final materials. Due to the additional constraints caused by the triethoxysilane groups along the backbone, the mobility of the oligomers decreased and T_g shifted to higher temperature as the number of functional groups per molecule increased (molecular weight of PTMO between cross-links decreased). This resulted in a final material of higher modulus and lower elongation at break. Furthermore, the materials produced also showed significant improvement in both tensile modulus and strength over previous PTMO–TEOS systems. Also, the tensile strength reached 50 MPa in some cases.

The high transparency along with the large difference in refractive index between the two components demonstrated that no macroscale phase separation occur. Indeed, the functionalized PTMO oligomers react well with the hydrolysis products of TEOS. However, they tend to undergo some microphase separation similar to segmented or block polymers. The same microphase separation behavior was also observed for PTMO–TiOPr (titanium alkoxide) and PTMO–ZrOPr (zirconium alkoxide) systems. SAXS[7,123] was utilized to gain further insight regarding the morphology of these materials, and an example of this data given in Figure 1 confirms the existence of microphase separation on a very localized scale. The single first-order interference peak in each of these SAXS profiles, although broad because of slit smearing, strongly indicates an interdomain spacing (correlation distance) over which a periodic fluctuation in electron density occurs. Since only a single scattering peak is noted, this also implies only short-range ordering exists. The observed correlation distance is on the order of about 10 nm for the PTMO–TEOS systems and shifts to slightly higher values as the metal alkoxide changes from TEOS to TiOPr to that of ZrOPr.[7,124,126,157,158] The intensity of the scattering maxima is significantly higher for the TiOPr and ZrOPr systems relative to that from a corresponding TEOS system due to the higher electron density of both of the latter metals compared with silicon. The high angular tail of the scattering curve also suggested that some level of mixing of the inorganic occurs within the oligomeric phase. This partial phase mixing was also supported by dynamic mechanical spectroscopy (DMS) data. The increase of interdomain spacing for these three systems in terms of SAXS behavior was due in part to the increase in rate of hydrolysis of the metal alkoxide used.

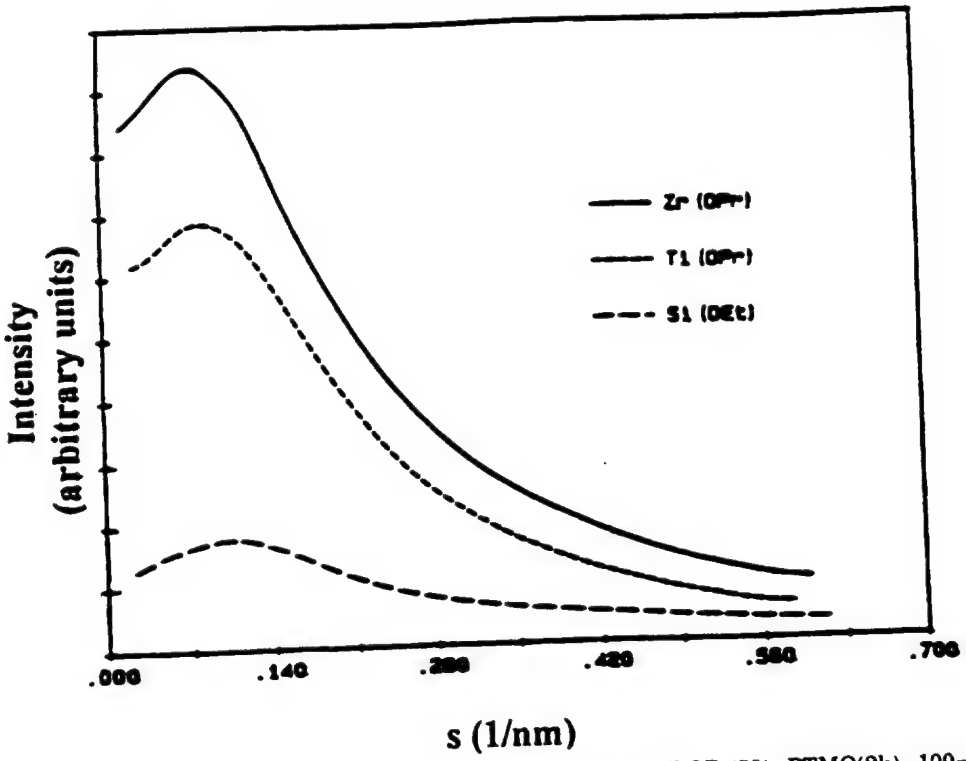

Figure 1. SAXS profiles for Ceramers TEOS(50)–PTMO(2k)–100–0.014–RT, TiOPr(50)–PTMO(2k)–100–0.014–RT, ZrOPr-50)–PTMO(2k)–100–0.014–RT. The sample nomenclature indicates that the material was prepared with 50 wt % of metal alkoxide and 50 wt % of triethoxysilane-functionalized PTMO with M_w of 2000, 100% of the stoichiometric amount of water for the hydrolysis reaction, 0.014 molar ratio of HCl/metal alkoxide, and cast at room temperature into film form from a 2-propanol solution (reproduced with permission from ref 126).

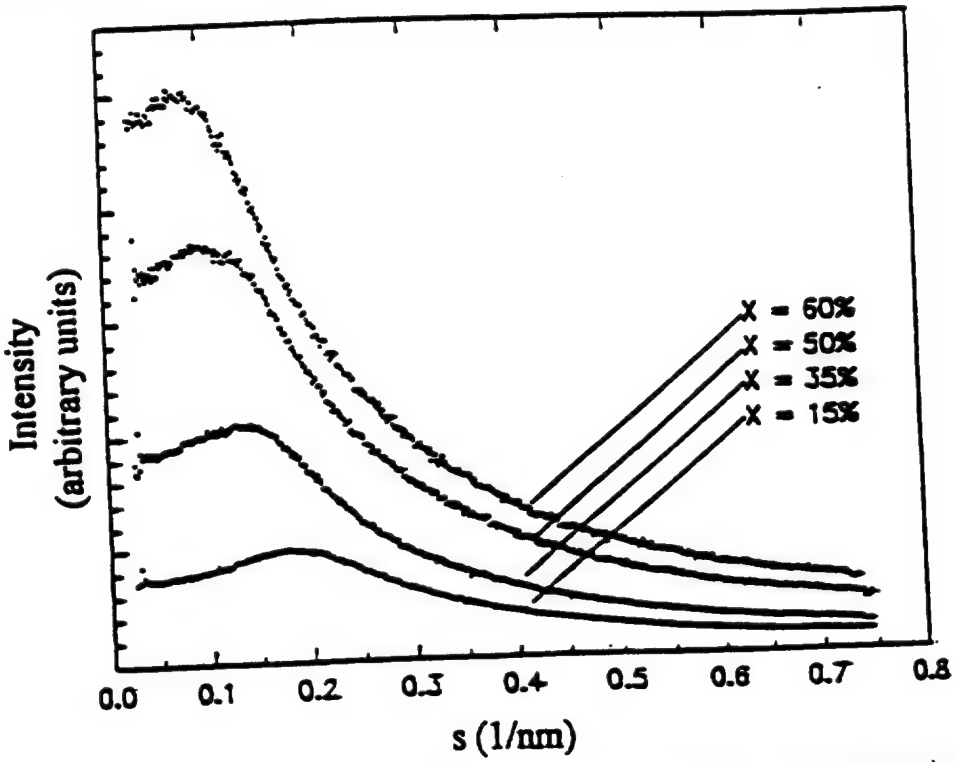

Figure 2. SAXS profiles of PTMO–TiOPr systems (PTMO molecular weight 2000 g/mol) containing varying amounts of TiOPr.

To further strengthen the concept behind the development of the microdomains of rich inorganic regions, Figure 2 shows the SAXS profiles from a series of TiOPr–PTMO hybrid network materials where the variable is that of composition ratio, i.e., the functionalized 2000 g/mol of PTMO molecular weight has been held constant.[128] The maximum scattering intensity as well as the interdomain spacing was found to systematically increase with an increase in metal alkoxide content. The correlation distance increased from ca. 7 to 17 nm as the initial reactant weight fraction of TiOPr was increased from 15% to 60%. This suggested that, as expected, as the inorganic domains became larger, but connected by the same organic spacer length, the interdomain distance would increase.

On the basis of a variety of related SAXS investigations, a simplified model was proposed and is schematically shown in Figure 3.[123] This very general model attempts to visually convey the types of structure present in the PTMO–metal alkoxide hybrid materials

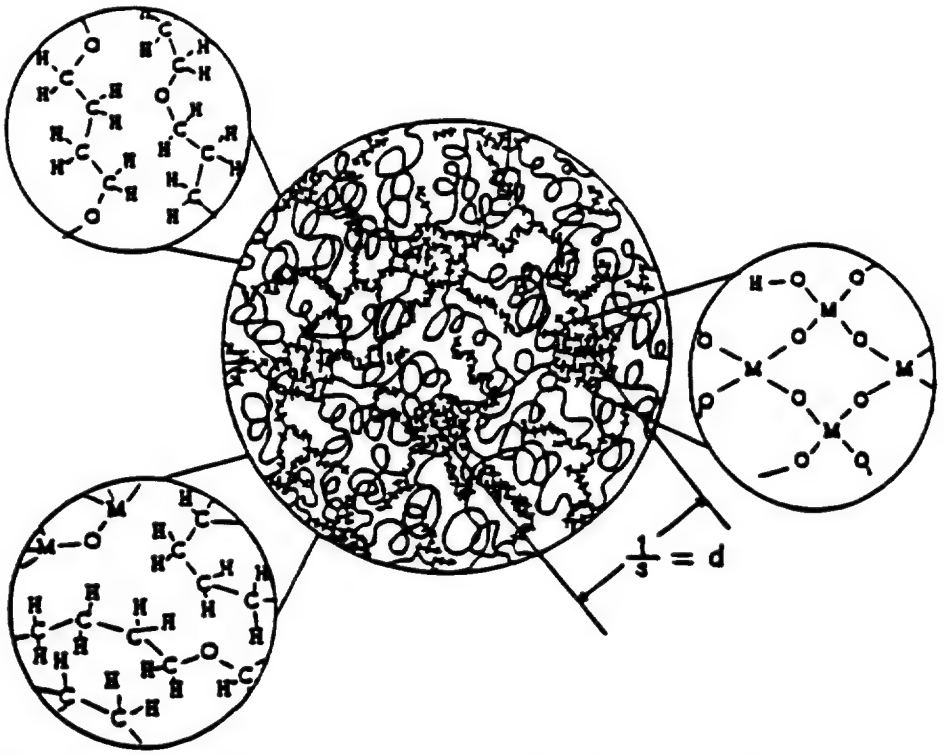

Figure 3. Generalized model of the local morphological structure in PTMO–TEOS hybrid systems, in which $1/s$ is an estimate of the correlation distance where the value of the scattering vector, s, is that at the first interference peak in the SAXS profile (reproduced with permission from ref 123).

when percolation of the inorganic phase is absent.[123] The model displays three generalized regimes or phases:

(1) The regime identified in the upper left circle represents the "lower electron density" organic–oligomeric-rich phases.

(2) The regime in the right-hand side circle indicates the "higher electron density" inorganic-rich regions.

(3) The third regime identified in the lower left circle represents the regions in which the two components display some level of mixing.

The correlation length (interdomain spacing) between two inorganic-rich regions can be approximated in terms of $1/s$, where s is the value of the scattering vector at the interference peak. This generalized model suggests the separation of a dispersed inorganic-rich phase chemically cross-linked at the interface with an oligomeric-rich matrix phase except at very high initial inorganic content. The interdomain spacing as well as the intensity of scattering has been found to depend on the nature of metal alkoxide, the molecular weight of oligomeric species, metal alkoxide content, temperature of processing, etc.

All the PTMO–metal alkoxide hybrid networks discussed so far were prepared with 2-propanol (IPA) as solvent. SAXS studies also showed that solvent type influenced the structure of the hybrid systems. When using a *N*,*N*-dimethylformamide (DMF)–IPA cosolvent system as the reaction medium, the SAXS scattering profiles became much sharper as the DMF content increased, indicating a narrower distribution of either domain sizes or interdomain spacings or both. This was believed to be attributable to the less acidic nature of the mixture when DMF was used as cosolvent which promoted less mixing between the two components.

The chemical stability of PTMO–TEOS and PTMO–TiOPr hybrid materials in neutral and alkaline aqueous solutions has also been investigated.[159] For PTMO–TEOS hybrids, the aging in 1 M NaOH for 24 h resulted in a better-defined two-phase microstructure because of the solubility of silicon oxide in the highly basic solution. The loss of silicon oxide resulted in a higher PTMO chain mobility to the extent that the PTMO chains could now undergo crystallization at low temperatures. The modulus of the treated network was also lower than untreated hybrids due to the loss of silicon oxide and hydrolysis of the alkali-treated networks. These results also supported the microstructural model proposed above. For PTMO–TiOPr hybrids, little change in the titanium oxide content was observed due to the lower solubility of titanium oxide in 1 M NaOH solutions. However, base treatment resulted in better phase separation between the inorganic and the organic phases which resulted in a higher mobility of the organic phase.

Besides the effects of the molecular weight of PTMO and influence of solvent effects, a substantial "aging effect" has also been noted in some cases.[7,124] If the ambient temperature cast films are later heated to a higher temperature (ca. 100 °C), the extent of reaction can be increased. Aging can also take place in the time period between gelation and vitrification of the "hard" regions and this aging effect can be easily interpreted by using the concept of the time–temperature–transformation (TTT) cure diagram established by Gillham.[160] Here, the isothermal cure of a system is usually characterized by gelation and vitrification and is complicated by the interaction of the chemical kinetics and the changing physical properties due to network development which influences the diffusivity of the reactive species. At a specific cure temperature, the T_g of the system will increase as the reaction proceeds and this will continue until the system reaches its new T_g which can often be the new higher cure temperature. Thus the cessation of the reaction is not necessarily an

indication that the reaction is complete but only quenched due to vitrification. Subsequent exposure of the system to a higher temperature that surpasses the original T_g can also result in further reaction.

Commenting briefly on acid catalysts, mineral and low molecular weight organic acids have been most used for the preparation of ceramers as well as conventional sol gels. However, the utilization of the polymeric acid catalyst poly(styrenesulfonic acid) (PSS), which is readily available in various molecular weight and degrees of sulfonation, has also been investigated.[132,161] The results demonstrate that PSS is an effective catalyst for the preparation of PTMO–TEOS hybrid materials that possess comparable properties to the same composition prepared with low molecular weight acid catalysts. An advantage of a polymeric acid catalyst is that it can be used as a rheological modifier to enhance processability yet also minimize fugitive acid moieties that are prominent from low molecular weight catalyst. Clearly, a similar approach could be followed but with a polymeric base catalyst such as a polyamine functionalized chain.

The effect of titanium(IV) tetraisopropoxide ($Ti(OPr)_4$) on the final properties of PTMO–TEOS hybrid systems was also investigated following the above studies. Due to the large difference in the reactivity of titanium(IV) tetraisopropoxide and TEOS, a new reaction scheme was developed to incorporate titanium(IV) tetraisopropoxide into PTMO–TEOS systems.[6,7] In this approach, TEOS and triethoxysilane-functionalized PTMO was first partially hydrolyzed and condensed by using a CCC system of glacial acetic acid and 2-propanol (no water). The titanium(IV) tetraisopropoxide is added later to avoid phase separation. With this approach, transparent hybrid materials were produced. The resulting materials develop a higher network density and high modulus, and the ultimate strength is improved with respect to the pure PTMO–TEOS hybrid systems.

Triethoxysilane functionalized PTMO has also been incorporated with titanium(IV) tetraisopropoxide, aluminum tris-*sec*-butoxide ($Al(OBu)_3$) and zirconium tetra-*n*-propoxide ($Zr(OPr)_4$) without the presence of TEOS.[113,162-164] Again, due to the fast reaction rate of these metal alkoxides, the direct addition of water will cause precipitation. Therefore, two new reaction approaches were developed to solve this problem:

(1) Chelating ligands, such as β-dicarbonyl ligand ethyl acetoacetate (EACAC), were first utilized.[163] The hydrolysis rate of metal alkoxides can be slowed by forming a complex with the chelating ligand so that no precipitation occurs and homogeneous sols or gels can be obtained. The functionalized PTMO species was added later. A drawback of using ligands is that they remain in the final products and may influence the structure–property behavior.

(2) A second approach was also developed by slowly adding water containing an acidified (HCl) alcohol solution to the metal alkoxide systems to avoid precipitation.[164] Transparent hybrid materials can be prepared by these approaches. SAXS and DMS analysis of these systems indicate a microphase-separated morphology similar in nature to that of previously described PTMO–TEOS systems.

Besides the normal solution casting and thermal curing technique, microwave curing processing has also been utilized to promote the sol–gel reaction of PTMO–TEOS, PTMO–TIP, and PTMO–zirconium propoxide systems. Microwave processing has the ability to potentially promote a higher rate of reaction due to specific interactions with the dipoles of the appropriate functionalized reacting groups. Indeed, it was found that gelation and near final properties of the PTMO–TEOS hybrid systems can be achieved in a matter of minutes.[165] The higher intensity and flat "tail region" from the SAXS scattering curve of microwave-processed PTMO–TEOS hybrid networks also indicated a higher extent of reaction and higher level of phase separation compared to ambient temperature casting or even conventional thermal (convection) cured systems.[6] The morphology for the ceramers made by microwave processing and thermal curing is nearly identical in that they all display an average correlation length of ca. 10 nm. There is no major change in morphology except that the intensity of scattering increases with the extent of curing and densification as expected. However, for PTMO–TiOPr systems, the differences in these hybrid materials cured thermally and by microwaves were not as great as observed in the PTMO–TEOS systems. The faster reaction rate of the titanium alkoxides was proposed to be the responsible factor.

3. Incorporation of Poly(ether ketone) (PEK). By utilizing a similar synthetic approach to that for the PTMO–TEOS systems, triethoxysilane-functionalized PEK oligomers (M_n = 3900 g/mol) were used to synthesize a hybrid network with TEOS.[158] PEK is an amorphous engineering thermoplastic material with good mechanical properties, thermal stability, and a relatively high glass transition temperature of ca. 150 °C in higher molecular weight form. A major difference between the PEK system and those of the PDMS or PTMO systems is that the high glass transition temperature of PEK can further limit the extent of cure caused by vitrification as gelation and network buildup occur. The gelation and vitrification occurred at low extents of reaction. However, by utilizing thermal postcure treatments at elevated temperature, further network development can be promoted. The final materials still maintain high transparency (but not water white) although local microphase separation does occur.

4. Incorporation of Polyoxazolines (POZO). Chujo et al.[135] synthesized polyoxazoline–silica hybrid materials by using a comparable synthetic approach. Triethoxysilane-terminated POZO with a molecular weight of 500–2000 was obtained by ring-opening polymerization of 2-methyl-2-oxazoline followed by termination with (3-aminopropyl)triethoxysilane—the same functionalizing agent as was utilized in the PTMO studies already reviewed. These silane-terminated POZOs were then subjected to acid-catalyzed cohydrolysis and condensation with TEOS to produce a homogeneous, transparent, and glassy inorganic/organic hybrid material. It should also be mentioned here that a hybrid without chemical bonding between inorganic and organic phases can also be prepared simply by utilizing the hydrogen-bond interactions between the silanol group and the POZO amide carbonyl group.[166]

An important application proposed for this latter hybrid material is the preparation of highly porous silica having micro- or nanoscale pores. This can be readily done by calcination of the hybrids at temperatures between 600 and 800 °C which are below the fusion temperature of metal alkoxide. The organic component

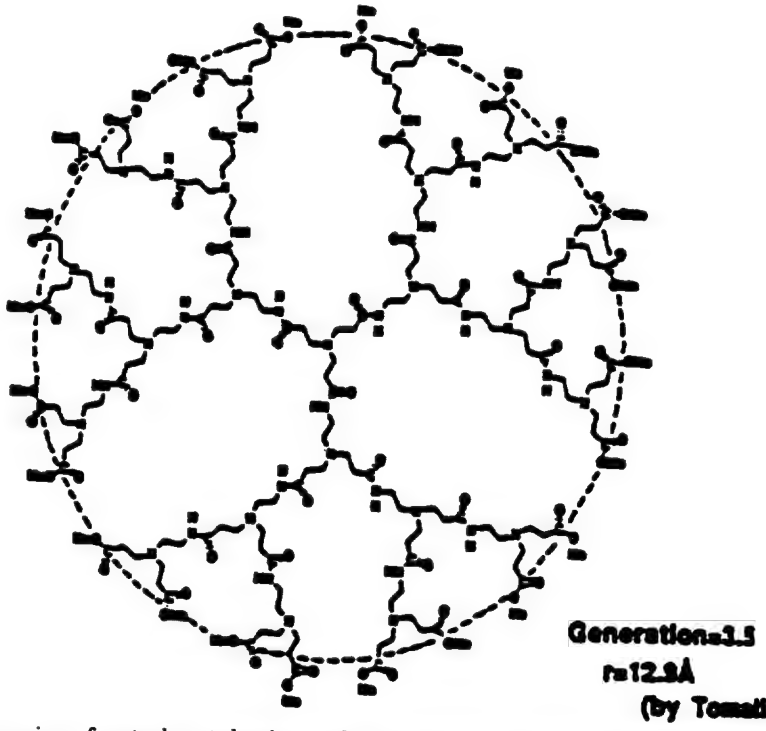

Figure 4. Schematic expression of a starburst detrimer of 3.5 generation (reproduced with permission from ref 168).

is decomposed at these temperatures, leaving behind a porous structure with surface areas varying between ca. 200 and 800 m^2/g depending on the composition and molecular weight of POZO.[36,166] The authors of this review have also obtained highly porous silica with surface area as high as over 1000 m^2/g through the calcination of PTMO–TEOS hybrid materials.[167] The influence of molecular weight and content of PTMO, reaction condition, and calcination temperature to the surface area of the resulting porous silica is still underway in our laboratory.

Control of the pore size in silica gels prepared by this hybrid approach can also be achieved by using so-called "starburst dentrimers" as the organic component.[168] These dentrimers, which are prepared with ammonia (core), methyl acrylate, and ethylenediamine, contain an *N*-alkylamide group as the repeating unit and possess a three-dimensional dentritic structure emanating from a central unit via a number of generations as shown in Figure 4. The number of generations determines the size of the dentrimer. In the case of dentrimer with 3.5 generations which has been employed to prepare hybrids, the radius of the dentrimer is ca. 12.9 Å which is found to be very close to the peak of the pore-size distribution curve of porous silica (13 Å).

5. Incorporation of Polyimides. Recent research work on organic/inorganic hybrids has been aimed to improve the properties of polymers with respect to better thermal stability and mechanical strength. So far, polyimides have drawn the most attention in this regard.[136–139] Unlike other high-performance polymers, such as Kevlar, polyimides are synthesized from a precursor molecule (poly(amic acid)) which is soluble in some organic solvents. This opens the possibility to produce polyimide–silica hybrid materials through the sol–gel approach.

By utilizing a comparable synthetic approach with PTMO–TEOS systems, Brennan[130] synthesized polyimide-containing hybrid network systems: titanium tetraisopropoxide (TiOPr)–polyimide in which the polyimide was based on 6F-benzophenone tetracarboxylic acid dianhydride (6F-BTDA) and bis(aminopropyl)-tetramethyldisiloxane (BisP). The oligomeric molecular weight ranged from 5000 to 13 000 g/mol. They were functionalized by either (aminophenyl)trimethoxysilane (AMP), (isocyanatopropyl)trimethoxysilane, or hydrosilyation of nadic anhydride. The SAXS behavior of these materials was similar to that of TiOPr/PTMO and TEOS/PTMO hybrid networks in that an interdomain spacing developed caused by a periodic fluctuation in electron density. It is generally believed that the introduction of inorganic components into organic materials can improve their thermal stability based on the fact that these species have good thermal stability and also enhance mechanical strength. Indeed, the hybrid networks described above exhibited relatively good thermal stability. However, thermal weight loss studies also indicated that the thermal stability of these hybrid systems was dependent upon the nature of the particular silane end group used to functionalize the polyimide with the order of thermal stability being (aminophenyl)-trimethoxysilane (AMP) > (isocyanatopropyl)trimethoxysilane > hydrosilyation of nadic anhydride.

Nandi et al.[137] reported the preparation of molecular level polyimide–silica and polyimide–titania composites by using a so-called "site isolation" method. In this method, metal alkoxide is maintained in isolated pockets in the polymeric matrix, and this can be achieved by prebinding the metal alkoxide precursor (tetraethoxysilane or titanium butoxide) to the carboxylic sites of the polyamic acid formed initially. The authors suggested that the metal alkoxide can be chemically bonded with the precursor polyamic acid through cohydrolysis of carboxylic groups and metal alkoxide. However, they did not confirm the formation of chemical bonding. The polyamic acid precursor was synthesized from 1,2,4,5-benzenetetracarboxylic acid dianhydride (PMDA) and 4,4′-oxydianiline (ODA). During the final curing step, imidization occurs, leading to ring closure which releases water that can then hydrolyze the metal alkox-

des to eventually generate the oxides. The rigidity of the polyimide backbone (as evidenced by the high T_g) slows the mobility of the metal alkoxide clusters and prevents agglomeration of large particles. Both TEM and SEM observations indicate the formation of a homogeneous dispersion of SiO_2 (and TiO_2) nanoclusters with a size of about 1.5 nm within the polyimide matrix. As a result, transparent and flexible polyimide-containing organic/inorganic films can be obtained in this way.

Morikawa et al.[136] also reported the preparation of polyimide–silica hybrid films by the hydrolysis and condensation of a metal alkoxide (TEOS) in a polyamic acid solution, followed by subsequent heating of the resulting film at high temperature. In this method, the polyamic acid was first prepared from PMDA and ODA in *N,N'*-dimethylacetamide (DMAc), and TEOS and water were then added to the solution of polyamic acid. The reaction between TEOS and water resulted in a homogeneous mixture which was then cast onto a glass plate. After this was heated to ca. 270 °C the polyimide–silica hybrid film was obtained. Hybrid films having silica content up to 70 wt % and silica size of approximately 5 μm could be obtained. This method was later modified by the same research group by introducing ethoxysilyl groups as the diamine monomer into the polyimide matrix, to connect the silica particles with the polyimide matrix and using methanol as the solvent, hybrid films containing up to 50 wt % silica with much smaller size (about 0.2–0.08 μm in diameter) were obtained.[136] In contrast to the other preparation method given above, the hybrid films made in this way show a higher storage modulus, a reduction in the decrease of the glass transition temperature, and low tan δ maximum.

The preparation and properties of additional polyimide–silica hybrid systems have also been investigated by several other research groups and only brief remarks will be made about this work here. Mascia and Kioul[139] studied the compatibility of polyimide–silica ceramers by adding a small amount of (γ-glycidyloxypropyl)-trimethoxysilane (GOTMS) as a coupling agent. Compatibility of the components can be readily achieved by the addition of coupling agent and the morphology of the hybrid films was strongly dependent on the molecular weight of polyamic acid, alkoxysilane solution composition, reaction time, and the type of coupling agent and catalyst. The tensile strength and ductility of hybrid materials was found to increase with the addition of low functionality alkoxysilane and the GOTMS coupling agent. Wang et al.[138] also studied the morphology, thermal stability, and mechanical properties of polyimide–silica composites. In their studies, an organically substituted alkoxysilane, (aminophenyl)-trimethoxysilane (APTMOS), was utilized to provide bonding sites between the polyimide and the silica-like phase. They found that small amounts of APTMOS can improve the modulus and strength of the resulting hybrid materials, and the transparency also increased with an increase of APTMOS.

6. Incorporation of Acrylate Polymers. Acrylate polymers, including poly(methyl methacrylate) (PMMA), poly(methyl acrylate) (PMA), and poly(butyl methacrylate) (PBMA), have been utilized to prepare organic–inorganic composite materials. However, in most of the polymeric component and the inorganic phase for this type of inorganic/organic composites although homogeneous and optically transparent products can be obtained due to the compatibility promoted by strong hydrogen-bonding interactions between the organic and inorganic species. Only a few studies have focused on developing covalent bonding between the two phases. As an example, Wei et al.[133] developed an approach that can covalently incorporate acrylate polymers into a silica network. In this approach, the acrylate polymers were first synthesized by group-transfer polymerization (GTP) of allyl methacrylate (AMA) and by copolymerization of AMA with methyl methacrylate (MMA). Then the allyl methacrylate polymers were functionalized by hydrosilylation of the allylic segments to convert allylic vinyl groups to triethoxysilyl groups. Finally, the triethoxysilyl groups in acrylate polymers and TEOS cohydrolyze and condense in the presence of acid catalyst via the sol–gel reaction. With this approach, transparent and monolithic hybrid materials can be obtained at room temperature by a slow evaporation of solvent and small molecule byproducts.

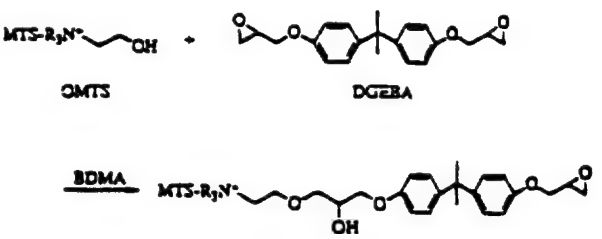

Figure 5. Based-catalyzed oxirane ring-opening reaction between hydroxyl groups of OMTS and DGEBA (reproduced with permission from ref 144).

7. Other Systems. Other examples of functionalized oligomers and polymers that have been covalently incorporated into an inorganic network are polystyrenes,[134] polyamide,[141] poly(ethyleneimine),[147,148] epoxy,[5,144,169] poly(ethylene oxide),[142] poly(oxypropylene),[116] poly(arylene ether phosphine oxide),[152] poly(arylene ether sulfone) (PSF),[153] cellulose acetate,[154] polyacrylics,[151] polyacrylonitrile,[155] and polybutadiene.[116,143] All these oligomers have been incorporated into the inorganic network utilizing terminal functional groups such as triethoxysilane.

While epoxy–inorganic composite can be obtained using epoxy-containing triethoxysilane as the precursor in the sol–gel process, epoxy–silicate nanocomposites consisting of individual mica-type silicate (MTS) layers embedded within a cross-linked epoxy matrix have also been prepared by dispersing an organically modified mica-type silicate (OMTS) in an epoxy and curing at 100–200 °C.[144] In this approach, OMTS is prepared by an ion-exchange reaction from Na–montmorillonite and bis(2-hydroxyethyl)methyl tallowalkylammonium chloride. Following the delamination of OMTS within an epoxy resin (diglycidyl ether of bisphenol-A, DGEBA), the curing is carried out in the presence of nadic methyl anhydride (NMA), benzyldimethylamine (BDMA), or boron trifluoride monoethylamine (BTFA). The hydroxyethyl groups of the alkylammonium ions located in the galleries of the OMTS participate in the cross-linking reaction and result in chemical bonding of the epoxy network to the OMTS as shown in Figure 5. The resulting composite exhibits molecular dispersion of the silicate layers with a layer spacing of 100 Å or more in

nanocomposite exhibits good optical clarity and dynamic modulus reinforcement greater than epoxies modified with comparable conventional filler amounts and may have applications as adhesives, coatings, electronic, or structural materials.

In summary, most of the research efforts in this area have focused on searching for hybrid materials with new properties. The study of structure–property relationships of these new materials has been less emphasized although its importance is obvious. A knowledge of the structure and its relationship to final properties is a powerful tool in designing the synthesis to obtain the desired properties. A typical example is the preparation of new organic/inorganic hybrid network materials with high refractive index.[152,153] Titanium tetraisopropoxide was chosen as the inorganic component due to its high refractive index. PSF, PEPO, or PEK were chosen as the organic components due to their high refractive index relative to most other organic polymers. The triethoxysilane-functionalized PEPO, PEK, and PSF were incorporated with titanium tetraisopropoxide through the sol–gel process. The refractive index of each of these materials exhibited a linear relationship with titanium oxide content. Also, they have a refractive index and an optical dispersion behavior between that of organic polymers and inorganic glasses. As we have alluded to, the morphology of organic/inorganic hybrid materials can be characterized by a variety of analytical techniques ranging from visual inspection, optical microscopy, SEM, TEM to DMS and small-angle scattering techniques such as SAXS and SANS.[7,38] The morphological details can be related to reaction mechanisms and ultimately to physical properties. As discussed earlier, for several of the organic/inorganic composites prepared from silane-functionalized polymeric/oligomeric species and metal alkoxide, detailed morphological studies have been carried out on the PTMO–TEOS systems and a general morphological model based on SAXS data has been proposed—recall Figure 3. However, it should be realized that with different chemical structures of the organic species and different reaction conditions will result in hybrid materials with variations to this general model. For example, the influence of reaction conditions on the morphology of hybrid materials was clearly demonstrated by a study of Rodrigues and Wilkes in which a fractal analysis was utilized to analyze the effect of cosolvent systems on the development of the structure of the inorganic phase in PTMO–TEOS hybrid networks. It was observed that PTMO–TEOS hybrid materials reacted in the cosolvent systems of DMF/IPA and THF/IPA displayed different SAXS profiles and the earlier proposed generalized morphological model did not provide sufficient information about the nature of the inorganic phase and the interaction of this phase with the organic component in the various hybrid systems. Therefore, an improved morphological model was proposed to account for the growth of the inorganic phase and its interaction with the organic component through fractal analysis. It was shown in this work that for the PTMO–TEOS hybrids reacted in DMF/IPA, the structure of inorganic components changed from mass fractal to surface fractal with the passage of reaction time. This feature could be attributed to the early attachment of the PTMO chains to the growing polymeric silicate species followed by the primary silicate species located at the chain ends. There was also greater mixing between TEOS and PTMO as the PTMO content was increased based on the broader scattering profiles. In the case of PTMO–TEOS hybrids reacted in THF/IPA, more mixing occurred between PTMO and silicate components. The silicate particles displayed mass fractal behavior and were more open and linear. Recently, Landry et al.[169] proposed two morphological models to describe small-angle X-ray scattering data of organic/inorganic composites based on a triethoxysilane-endcapped bisphenol A epoxide resin (EAS)–TEOS system reacted under slightly basic conditions, and a random trimethoxysilane-functionalized copolymer of poly(methyl methacrylate) (MMA–TMS) with added tetramethoxysilane (TMOS) reacted in an acidic medium. They concluded that for the EAS hybrid materials, the inorganic phase exhibits particle-like characteristics at length scales less than ca. 250 Å which can be described by a noninterpenetrating fractal cluster (NIFC) model, and the organic and inorganic components are bicontinuous at larger distances which can be interpreted by a bicontinuous two-phase (B2P) model. The MMA–TMS composite is better described by bicontinuous organic and inorganic phases with a periodic fluctuation of about 40 Å and the B2P model offers a more accurate picture of the MMA–TMS hybrid morphology.

Clearly, as more control develops for systematically varying the morphology of the hybrid systems, new properties will appear.

Incorporation of Small Organic Moieties

A direct way to introduce smaller organic moieties into a hybrid network through chemical bonding is to use bifunctional or/and trifunctional alkoxysilanes ($R'_nSi(OR)_{4-n}$, $n = 1-3$, R = alkyl, R′ = organic group) as one or more of the precursors for the sol–gel reaction. This approach has been extensively studied by Schmidt and co-workers since the late 1970s and the hybrid materials made in this way have been termed ORMOSILS or later as ORMOCERS.[2-5,53,65,77,108,170-173] The synthetic route in this approach is quite straightforward—instead of using metal alkoxide as the precursor for sol–gel reaction, alkoxysilanes are used as the only (or one of) the precursors and the organic groups X are introduced into the inorganic network through the ≡Si–C– bond in an alkoxysilane. Trifunctional alkoxysilanes, $R'Si(OR)_3$, are the most common precursors to introduce organic groups because a variety of such silanes are commercially available, while bifunctional alkoxysilanes have to be used in the presence of higher functionality precursors in order to form a three-dimensional network.

The organic/inorganic hybrid materials made by this approach can be viewed more as a molecular type of hybrid network because the organic groups have been chemically bonded with the inorganic component *before the reaction starts*. While these types of hybrid network materials still suffer the same drawbacks as classical sol–gel materials, e.g., generation of large amount of byproducts and shrinkage during the drying process, they have generated considerable interest. By tailoring the structure of the organic group R′, mechanical, optical, or electrical properties of the resulting composite materials can be greatly modified. Some example properties that can be introduced by organic molecules

are mechanical such as flexibility, toughness, optical such as NLO and UV adsorption, and electronic such as conduction and redox properties.[42,43,47,48,75,76] For example, when triethoxysilyl-functionalized NLO dyes are used as the only (or one of) the sol–gel reaction precursors, the resulting hybrid materials possess NLO response. Organic/inorganic composite materials made in this way combine the optical response of the organic structure with good optical quality, good mechanical property, and environmental stability of inorganic glasses. Depending on the type of organic materials used, second-order and third-order NLO materials, and other optical materials can be obtained. If the R′ group is a polymerizable organic group, an organic network can be formed within the inorganic network by either photochemical or thermal curing. For example, by using methacrylate monomers containing trialkoxysilane and TEOS as the precursors of the sol–gel reaction, Schmidt et al. introduced PMMA within the silica network through an in situ polymerization of methacrylate monomers following the hydrolysis and polycondensation of silane functional groups.[3] Recently, Schubert et al.[174] synthesized organically modified silica aerogels by base-catalyzed hydrolysis and condensation of alkoxysilanes ($RSi(OMe)_3$/TEOS mixtures, followed by supercritical drying of the alcogels with methanol or CO_2. By the proper choice of the organic groups, the ratio of $RSi(OMe)_3$/TEOS, and drying condition, aerogels with interesting new properties such as permanent hydrophobicity can be prepared by this approach.

Another area utilizing functionalized low molecular weight organics that has attracted interest from both the academic and industrial section is the preparation of inorganic/organic hard coatings for polymeric materials. Sol–gel coatings made from metal alkoxides already have commercial applications for glass and metal substrates. However, due to the thermal expansion coefficient difference and poor adhesion between sol–gel coating and polymeric materials, the applications of these pure metal alkoxide sol–gel coatings often encounter major difficulties for polymeric substrates. Using organic/inorganic composite as the coating materials can overcome many of these problems because the introduction of organic components into the inorganic network reduces the extent of shrinkage, brings flexibility to the brittle inorganic network, and increases the adhesion between the coating and polymer substrate. Schmidt has developed a series of scratch and abrasive-resistant coating materials which are based on Al_2O_3, ZrO_2, TiO_2, or SiO_2 as network formers and epoxy or methacrylate groups bound to Si via a ≡Si–C– bond.[66,108,170,175] More recently, organic/inorganic hybrid abrasion-resistant coating materials based on polyfunctional alkoxysilane and metal alkoxides as the precursors of composite networks have also been developed in our laboratory.[68–73,176] The polyfunctional alkoxysilane precursors are obtained by first functionalizing organic molecules with trialkoxysilane groups and then hydrolyzing and condensing the system with or without metal alkoxides to form an inorganic network with organic molecules inside the network. The organic molecules that have been incorporated into the hybrid network by this approach include diethylenetriamine (DETA),[71] 3,3′-iminopropytriamine (IMPA),[73] 4,4′-diaminodiphenyl sulfone (DDS),[70] melamine,[71] bis- and trismaleimides,[68] tris(*m*-aminophenyl)phosphine oxide compound,[69] resorcinol,[73] glycerol,[72,73] and a series of diols.[72,73] The metal alkoxides are tetraethoxysilane (TEOS), tetramethoxysilane (TMOS), titanium butoxide, zirconium propoxide, and aluminum tri-*sec*-butoxide. The adhesion between coating and substrate can be further improved by first treating the polymeric substrate surface with an oxygen plasma or a primer solution of isopropanol containing (3-aminopropyl)triethoxysilane. The resulting coating materials have been applied on several polymeric substrates such as PMMA, polycarbonate, and CR-39 lenses. Because reactive organic groups can be introduced into the inorganic networks, other functional coating materials such as fluorescent coatings and high refractive index optical coatings can also be obtained by this approach.[152]

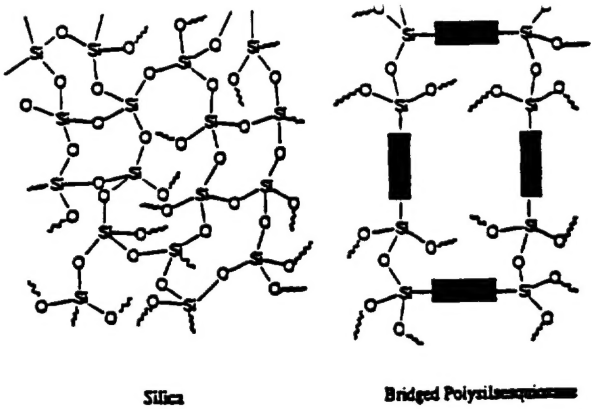

Figure 6. Representation of the chemical connectivities of a silica network and a bridged polysilsesquioxane network. The shaded rectangles correspond to the variable organic species (reproduced with permission from ref 178).

A final example of inorganic/organic hybrid network materials synthesized with lower molecular weight polyfunctional alkoxysilane and metal alkoxides as the precursors of the sol–gel reaction extend from the so-called "bridged polysilsesquioxanes" developed by Shea et al.[177,178] These bridged polysilsesquioxanes are three-dimensional network materials that are assembled by the sol–gel reaction of polyfunctional low molecular weight building blocks as shown in Figure 6. The trialkoxysilane terminated organic spacers can introduce a wide variety of organic functionality, such as arylene, alkylene, alkenylene, and alkynylene groups, into the final network materials. These materials have the potential for the fabrication of NLO materials and high surface area aerogels and xerogels.

Final Remarks

The area of organic/inorganic hybrid network materials prepared by the sol–gel approach has rapidly become a fascinating new field of research in materials science. The explosion of research in the past decade in this field has promoted considerable progress in both the fundamental understanding of the sol–gel process in general and its use in the development and applications of new organic/inorganic hybrid materials. As has been discussed within this review, a very wide range of material properties can be generated by combining the appropriate features of a given inorganic metal moiety with those of appropriately selected organic species. In some cases, these two different types of moieties can be directly bonded to each other to build a hybrid network, while in other cases just strong seconding bonding

components. It has also been demonstrated in this review that a more complete understanding of their structure–property behavior can be gained by employing many of the standard tools that are utilized for developing similar structure–property relationships of organic polymers. Specifically, use of mechanical, thermal analysis, X-ray scattering, and microscopy methods in conjunction with other standard tools such as NMR can be invaluable in leading to a truer understanding of how these materials function in light of their chemistry and morphological features. Although the number of commercial hybrid sol–gel products is still relatively small, the promise of their use in new technological applications remains high. It is expected that over the next decade, numerous such materials will enter into the marketplace and serve an important function in the ever growing field of materials science.

Acknowledgment. The authors greatly acknowledge the financial support of the Air Force Office of Scientific Research under Grant F49620-94-1-0149DEF.

References

(1) Wilkes, G. L.; Orler, B.; Huang, H. *Polym. Prepr.* **1985**, *26*, 300.
(2) Schmidt, H. *J. Non-Cryst. Solids* **1985**, *73*, 681.
(3) Schmidt, H; Philipp, G. *J. Non-Cryst. Solids* **1984**, *63*, 283.
(4) Schmidt, H; Scholze, H; Kaiser, H. *J. Non-Cryst. Solids* **1984**, *63*, 1.
(5) Schmidt, H. *Mater. Res. Soc. Symp. Proc.* **1984**, *32*, 327.
(6) Wilkes, G. L.; Brenann, A. B.; Huang, H.; Rodrigues, D.; Wang, B. *Mater. Res. Soc. Symp. Proc.* **1990**, *171*, 15.
(7) Wilkes, G. L.; Huang, H.; Glaser, R. H. *Silicon-Based Polymer Science: A Comprehensive Resource*; Advances in Chemistry Ser. 224; American Chemical Society: Washington, DC, 1990; p 207.
(8) Mark, J. E.; Pan, S. J. *Makromol. Chem. Rapid Commun.* **1982**, *3*, 681.
(9) Mark, J. E.; Jiang, C.; Tang, M. *Macromolecules* **1984**, *17*, 2613.
(10) Ning, Y. P.; Tang, M. Y.; Jiang, C. Y.; Mark, J. E.; Roth, W. C. *J. Appl. Polym. Sci.* **1984**, *29*, 3209.
(11) Mark, J. E. In *Frontiers of Macromolecular Science*; Saegusa, T., Higashimura, H., Abe, A., Eds.; Blackwell Scientific Publishers: Oxford, 1989.
(12) Mark, J. E. *Chemtech* **1989**, *19*, 230.
(13) Mark, J. E.; Wang, S.; Xu, P.; Wen, J. *Mater. Res. Soc. Symp. Proc.* **1992**, *274*, 77.
(14) Schaefer, D. W.; Jian, L.; Sun, C.-C.; McCarthy, D.; Jiang, C.-Y.; Ning, Y.-P.; Mark, J. E.; Spooner, S. In *Ultrastructure Processing of Advanced Materials*; Uhlmann, D. R., Ulrich, D. R., Eds.; Wiley & Sons: New York, 1992.
(15) Mark, J. E.; Calvert, P. D. *J. Mater. Sci., Part C* **1994**, *1*, 159.
(16) Wang, S. B.; Mark, J. E. *Polym. Bull.* **1987**, *17*, 231.
(17) Mark, J. E.; Wang, S. B. *Polym. Bull.* **1988**, *20*, 443.
(18) Wang, S. B.; Mark, J. E. *J. Macromol. Sci., Macromol. Rep.* **1991**, *A28*, 185.
(19) Clarson, S. J.; Mark, J. E. *Polym. Commun.* **1989**, *30*, 275.
(20) Landry, C. J. T.; Coltrain, B. K. *Polymer* **1992**, *33*, 1486.
(21) Landry, C. J. T.; Coltrain, B. K.; Wesson, J. A.; Zumbulyadis, N. *Polymer* **1992**, *33*, 1496.
(22) Sun, C.-C.; Mark, J. E. *J. Polym. Sci., Polym. Phys. Ed.* **1987**, *25*, 1561.
(23) Shelly, D. B.; Giannelis, E. P. *Chem. Mater.* **1995**, *7*, 1597.
(24) Krenceski, M. A.; Cantow, H. j.; Mulhaupt, R. *PMSE Prepr.* **1994**, *70*, 356.
(25) Shao, P. L.; Mauritz, K. A.; Moore, R. B. *Chem. Mater.* **1995**, *7*, 192.
(26) (a) Mauritz, K. A.; Stefanithis, I. D.; Davis, S. V.; Scheetz, R. W.; Pope, R. K.; Wilkes, G. L.; Huang, H. H. *J. Appl. Polym. Sci.* **1995**, *55*, 181. (c) Mauritz, K. A.; Warren, R. M. *Macromolecules* **1989**, *22*, 1730.
(27) Mauritz, K. A.; Jones, C. K. *J. Appl. Polym. Sci.* **1990**, *40*, 1401.
(28) Wen, J.; Mark, J. E. *Rubber Chem. Technol.* **1994**, *67*, 806.
(29) Wen, J.; Mark, J. E. *J. Appl. Polym. Sci.* **1995**, *58*, 1135.
(30) Mark, J. E.; Erman, B. *Rubberlike Elasticity: A Molecular Primer*; Wiley & Sons: New York, 1988.
(31) Pope, E. J. A.; Asami, M.; Mackenzie, J. D. *J. Mater. Res.* **1989**, *4*, 1017.
(32) Pope, E. J. A.; Mackenzie, J. D. *MRS. Bull.* **1987**, *12*, 29.
(33) Abramoff, B.; Klein, L. C. In *Sol-Gel Optics I*; Mackenzie, J. D., Ulrich, D. R., Eds.; Proc. SPIE 1328; Washington, DC, 1990; p 241.
(35) (a) Yoshida, M; Prasad, P. N. *Chem. Mtaer.* **1996**, *8*, 235. (b) Suzuki, F.; Onozato, K. *J. Appl. Polym. Sci.* **1990**, *39*, 371.
(36) Saegusa, T. *J. Macromol. Sci., Chem.* **1991**, *A28*, 817.
(37) Messermith, P. B.; Stupp, S. I. *Polym. Prepr.* **1991**, *32*, 536.
(38) (a) David, I. A.; Scherer, G. W. *Polym. Prepr.* **1991**, *32*, 530. (b) David, I. A.; Scherer, G. W. *Chem. Mater.* **1995**, *7*, 1957.
(39) Novak, B. M.; Ellsworth, N.; Wallow, T. I.; Davies, C. *Polym. Prepr.* **1990**, *31*, 698.
(40) Novak, B. M.; Davies, C. *Macromolecules* **1991**, *24*, 5481.
(41) Nakanishi, K.; Soga, N. *J. Non-Cryst. Solids* **1992**, *139*, 1.
(42) Prasad, P. N. *Polymer* **1991**, *32*, 1746.
(43) Avnir, D.; Levy, D.; Reisfeld, R. *J. Phys. Chem.* **1984**, *88*, 5956
(44) Levy, D.; Einhorn, S; Avnir, D. *J. Non-Cryst. Solids* **1989**, *113*, 137.
(45) Kobayashi, Y.; Kurokawa, Y.; Imai, Y.; Muto, S. *J. Non-Cryst. Solids* **1988**, *105*, 198.
(46) Avnir, D.; Kaufman, V. R.; Reisfeld, R. *J. Non-Cryst. Solids* **1985**, *74*, 395.
(47) Tanaka, H.; Takahashi, H.; Tsuchiya, J. *J. Non-Cryst. Solids* **1989**, *109*, 164.
(48) Pang, Y.; Samoc, M.; Prasad, P. N. *J. Chem. Phys.* **1991**, *94*, 5282.
(49) Avnir, D.; Braun, S.; Ovadia, L.; Ottolenghi, M. *Chem. Mater.* **1994**, *6*, 1605.
(50) Sanchez, C.; Alonso, B.; Chapusot, F.; Ribot, F. *J. Sol-Gel Sci. Technol.* **1994**, *1*, 161.
(51) Krug, H.; Schmidt, H. *New J. Chem.* **1994**, *18*, 1125.
(52) Nass, R.; Schmidt, H. *SPIE* **1990**, *1328*, 258.
(53) Schmidt, H.; Wolter, H. *J. Non-Cryst. Solids* **1990**, *121*, 428.
(54) Novak, B. M.; Grubbs, R. H. *J. Am. Chem. Soc.* **1988**, *110*, 7542.
(55) Brennan, A. B.; Miller, T. M.; Vinocur, R. B. In *Hybrid Organic-Inorganic Composites*; Mark, J. E., Ed.; ACS Series 585; American Chemical Society: Washington, DC, 1995; p 142.
(56) Ellsworth, M. W.; Novak, B. M. *J. Am. Chem. Soc.* **1991**, *113*, 2756.
(57) Ellsworth, M. W.; Novak, B. M. *Chem. Mater.* **1993**, *5*, 839.
(58) Giannelis, E. P. In *Synthesis and Processing of Ceramics: Scientific Issues*; Rhine, W. E., Ed.; MRS: Pittsburgh, PA, 1992.
(59) Giannelis, E. P. *JOM* **1992**, *44*, 28.
(60) Usuki, A.; Kujima, Y.; Kawasumi, M.; Okada, A.; Fukushima, Y.; Kurauchi, T.; Kamigaito, O. *J. Mater. Res.* **1993**, *8*, 1179.
(61) Kojima, Y.; Usuki, A.; Kawasumi, M.; Okada, A.; Kurauchi, T.; Kamigaito, O. *J. Polym. Sci., Polym. Chem.* **1993**, *31*, 983.
(62) Kojima, Y.; Usuki, A.; Kawasumi, M.; Okada, A.; Fukushima, Y.; Kurauchi, T.; Kamigaito, O. *J. Mater. Res.* **1993**, *8*, 1185.
(63) Heuer, A. H.; Fink, D. J.; Laraia, V. J.; Calvert, P. D.; Kendall, K.; Messing, G. L.; Blackwell, J.; Rieke, P. C.; Thompson, D. H.; Wheeler, A. P.; Veis, A.; Caplan, A. I. *Science* **1992**, *255*, 1098.
(64) Wen, J.; Wilkes, G. L. *J. Sol-Gel Sci. Technol.* **1995**, *5*, 115.
(65) Schmidt, H. *Mater. Res. Soc. Symp. Proc.* **1990**, *171*, 3.
(66) Kasemann, R.; Schmidt, H. *New J. Chem.* **1994**, *18*, 1117.
(67) Schmidt, H.; Kasemann, R.; Burkhart, T.; Wagner, G.; Arpac, E.; Geiter, E. In *Hybrid Organic-Inorganic Composites*; Mark, J. E., Ed.; ACS Series 585; American Chemical Society: Washington, DC, 1995; p 331.
(68) Tamami, B.; Betrabet, C.; Wilkes, G. L. *Polym. Bull.* **1993**, *30*, 393.
(69) Tamami, B.; Betrabet, C.; Wilkes, G. L. *Polym. Bull.* **1993**, *30*, 39.
(70) Wang, B.; Wilkes, G. L. *J. Macromol. Sci., Pure Appl. Chem.* **1994**, *A31*, 249.
(71) Betrabet, C.; Wilkes, G. l. *Polym. Prepr.* **1992**, *33(2)*, 286.
(72) Wen, J.; Wilkes, G. L. *J. Inorg. Organomet. Polym.* **1995**, *5*, 343.
(73) Wen, J.; Wilkes, G. L. *PMSE Prepr.* **1995**, *73*, 429.
(74) Lebeau, B.; Guermeur, Sanchez, C. *Mater. Res. Soc. Symp. Proc.* **1994**, *346*, 315.
(75) Wang, C. J.; Pang, Y.; Prasad, P. N. *Polymer* **1991**, *32*, 605.
(76) Prasad, P. N.; Bright, F. V.; Narang, U.; Wang, R.; Dunbar, R. A. *PMSE Prepr.* **1994**, *70*, 349.
(77) Schmidt, H.; Scholze, H.; Tunker, G. *J. Non-Cryst. Solids* **1986**, *80*, 557.
(78) Canva, M.; Georges, P.; Perelgritz, J.-F.; Brum, A.; Chapu., F.; Boilot, J.-P. *Appl. Opt.* **1995**, *34*, 428.
(79) Knobbe, E. T.; Dunn, B.; Fuqua, P. D.; Nishida, F. *Appl. Opt.* **1990**, *29*, 2729.
(80) Zusman, R.; Rottman, C.; Ottolenghi, M.; Avnir, D. *J. Non-Cryst. Solids* **1990**, *122*, 107.
(81) Dave, B. C.; Dunn, B.; Valentine, J. S.; Zink, J. I. *Anal. Chem.* **1994**, *66*, 1120A.
(82) (a) Sanchez, C.; Ribot, F. *New J. Chem.* **1994**, *18*, 1007. (b) Schubert, U.; Husing, N.; Lorenz, A. *Chem. Mater.* **1995**, *7*, 2010. (c) Mark, J. E. In *Diversity Into the Next Century*; Martinez, R. J., Arris, H., Emerson, J. A., Pike, G., Eds.; SAMPE Publications: Covina, CA, 1995; Vol. 27. (d) Mark, J. E. In *Heterogeneous Chemistry Reviews*, in press. (e) Mark, J. E.; Wang, S.; Ahmad, Z. *Macromol. Symp.* **1995**, *98*, 731.
(83) Novak, B. M. *Adv. Mater.* **1993**, *5*, 422.
(84) Komarneni, S. *J. Mater. Chem.* **1992**, *2*, 1219.
(85) Schmidt, H. *Top. Issues Glasses* **1993**, *1*, 13.
(86) Schmidt, H. *J. Sol-Gel Sci. Technol.* **1994**, *1*, 217.

(87) Brennan, A. B.; Miller, T. M. In *Kirk-Othmer Encyclopedia of Chemical Tech.*, 4th ed.; John Wiley & Sons, Inc.: New York, 1994; Vol. 12, p 644.
(88) Mascia, L. *Trends Polym. Sci.* **1995**, *3*, 61.
(89) Wen, J.; Wilkes, G. L. In *The Polymeric Materials Encyclopedia: Synthesis, Properties and Applications*; CRC Press: Boca Raton, FL, in press.
(90) Krug, H.; Schmidt, H. *New J. Chem.* **1994**, *18*, 1125.
(91) Prasad, P. N.; Bright, F. V.; Narang, U.; Wang, R.; Dunbar, R. A.; Jordan, J. D.; Gvishi, R. In *Hybrid Organic-Inorganic Composites*; Mark, J. E., Ed.; ACS Series 585; American Chemical Society: Washington, DC, 1995; p 317.
(92) Dislich, H. *Angew. Chem.* **1971**, *83*, 428.
(93) Sakka, S.; Kamiya, K. *J. Non-Cryst. Solids* **1980**, *42*, 403.
(94) Sakka, S. *J. Non-Cryst. Solids* **1985**, *73*, 651.
(95) Klein, L. C. *Sol-Gel Technology for Thin Films, Fibers, Preforms, Electronics, and Especially Shapes*; Noyes Publications: Park Ridge, NJ, 1988.
(96) Yoldas, B. E. *J. Non-Cryst. Solids* **1984**, *63*, 145.
(97) Ulrich, D. R. *Chemtech* **1988**, *18*, 242.
(98) Brinker, C. J.; Scherrer, G. W. *Sol-Gel Science, the Physics and Chemistry of Sol-Gel Processing*; Academic Press: San Diego, CA, 1990.
(99) *ltrastructure Processing of Advanced Ceramics*; Mackenzie, J. D., Ulrich, D. R., Eds.; Wiley-Interscience: New York, 1988.
(100) Yoldas, B. E. *J. Mater. Sci.* **1986**, *21*, 1086.
(101) Keefer, K. D. *Mater. Res. Soc. Symp. Proc.* **1984**, *32*, 15.
(102) Schaefer, D. W.; Wilcoxon, J. P.; Keefer, K. D.; Bunker, B. C.; Pearson, R. K.; Thomas, I. M.; Miller, D. E. *AIP Conf. Proc.* **1987**, *154*, 63.
(103) Bradley, D. C.; Mehrotra, R. C.; Gaur, D. P. *Metal alkoxides*; Academic: London, 1978.
(104) Ribot, F.; Toledano, P.; Sanchez, C. *Chem. Mater.* **1991**, *3*, 759.
(105) Mehrota, R. C.; Bohra, R.; Gaur, D. P. *Metal β-Diketonates and Allied Derivatives*; Academic: London, 1978.
(106) Guglielmi, M.; Carturan, G. *J. Non-Cryst. Solids* **1988**, *100*, 16.
(107) Schmidt, H. *J. Non-Cryst. Solids* **1988**, *100*, 51.
(108) Schmidt, H.; Seiferling, B. *Mater. Res. Soc. Symp. Proc.* **1986**, *73*, 739.
(109) Parkhurst, C. S.; Doyle, L. A.; Silverman, L. A.; Singh, S.; Anderson, M. P.; McClurg, D.; Wnek, G. E.; Uhlmann, D. R. *Mater. Res. Soc. Symp. Proc.* **1986**, *73*, 769.
(110) Huang, H.; Orler, B.; Wilkes, G. L. *Polym. Bull.* **1985**, *14*, 557.
(111) Glaser, R. H.; Wilkes, G. L. *Polym Bull.* **1988**, *19*, 51.
(112) Huang, H.; Orler, B.; Wilkes, G. L. *Macromolecules* **1987**, *20*, 1322.
(113) Brennan, A. B.; Wang, B.; Rodrigues, D. E.; Wilkes, G. L. *J. Inorg. Organomet. Polym.* **1991**, *1*, 167.
(114) Spinu, M.; McGrath, J. E. *J. Inorg. Organomet. Polym.* **1992**, *2*, 103.
(115) Wen, J.; Mark, J. E. *Polym. J.* **1995**, *27*, 492.
(116) Kohjiya, S.; Ochiai, K.; Yamashita, S. *J. Non-Cryst. Solids* **1990**, *119*, 132.
(117) Chung, Y. J.; Ting, S. J.; Mackenzie, J. D. *Mater. Res. Soc. Symp. Proc.* **1990**, *180*, 981.
(118) Morita, K.; Hu, Y.; Mackenzie, J. D. *Mater. Res. Soc. Symp. Proc.* **1992**, *271*, 693.
(119) Kramer, S. J.; Mackenzie, J. D. *Mater. Res. Soc. Symp. Proc.* **1994**, *346*, 709.
(120) Iwamoto, T.; Mackenzie, J. D. *Mater. Res. Soc. Symp. Proc.* **1994**, *346*, 397.
(121) Babonneau, F. *Polyhedron* **1994**, *13*, 1123.
(122) Joardar, S. S. Ph.D. Thesis, Virginia Tech., 1992.
(123) Huang, H.; Wilkes, G. L. *Polym. Bull.* **1987**, *18*, 455.
(124) Huang, H.; Wilkes, G. L. *Polymers* **1989**, *30*, 2001.
(125) Huang, H.; Glaser, R. H.; Wilkes, G. L. In *Inorganic & Organometallic Polymers*; Zeldin, M., Wynne, K. J., Allcock, H. R., Eds.; ACS Symp. Ser. 360; American Chemical Society: Washington, DC, 1987; p 354.
(126) Brennan, A. B.; Wang, B.; Rodrigues, D. E.; Wilkes, G. L. *J. Inorg. Organomet. Polym.* **1991**, *1*, 167.
(127) Rodrigues, D. E.; Wilkes, G. L. *J. Inorg. Organomet. Polym.* **1993**, *3*, 197.
(128) (a) Rodrigues, D. E.; Brennan, A. B.; Betrabet, C.; Wang, B.; Wilkes, G. L. *Chem. Mater.* **1992**, *4*, 1437. (b) Betrabet, C. S. Ph.D. Thesis, Virginia Tech., 1993.
(129) Betrabet, C. S.; Wilkes, G. L. *J. Inorg. Organomet. Polym.* **1994**, *4*, 343.
(130) Brennan, A. B. Ph.D. Thesis, Virginia Tech., 1990.
(131) Rodrigues, D. Ph.D. Thesis, Virginia Tech., 1991.
(132) Brennan, A. B.; Wilkes, G. L. U.S. Patent 5,316,695.
(133) (a) Wei, Y.; Bakthavatchalam, R.; Whitecar, C. K. *Chem. Mater.* **1990**, *2*, 337. (b) Sunkara, H. B.; Jethmalani, J. M.; Ford, W. T. *Chem. Mater.* **1994**, *6*, 362.
(134) Mourey, T. H.; Miller, S. M.; Wesson, J. A.; Long, T. E.; Reis, L. W. *Macromolecules* **1992**, *25*, 45.
(135) Chujo, Y.; Ihara, E.; Kure, S.; Suzuki, K.; Saegusa, T. *Makromol. Chem. Macromol. Symp.* **1991**, *42/43*, 303.
(136) Morikawa, A.; Iyoku, Y.; Kakimoto, M.; Imai, Y. *J. Mater. Chem.* **1992**, *2*, 679.
(137) Nandi, M.; Conklin, J. A.; Salvati, L., Jr.; Sen, A. *Chem. Mater.* **1991**, *3*, 201.
(138) Wang, S.; Ahmad, Z.; Mark, J. E. *Chem. Mater.* **1994**, *6*, 943.
(139) Kioul, A.; Mascia, L. *J. Non-Cryst. Solids* **1994**, *175*, 169.
(140) (a) Iyoku, Y.; Kakimoto, M.; Imai, Yoshio. *High Perform. Polym.* **1994**, *6*, 95. (b) Jeng, R. J.; Chen, Y. M.; Jain, A. K.; Kumar, J.; Tripathy, S. K. *Chem. Mater.* **1992**, *4*, 1141. (c) Morikawa, A.; Iyoku, Y.; Kakimoto, M.; Imai, Y. *Polym. J.* **1992**, *24*, 107. (d) Morikawa, A.; Yamaguchi, H.; Kakimoto, M.; Imai, Y. *Chem. Mater.* **1994**, *6*, 913.
(141) Ahmad, Z.; Wang, S.; Mark, J. E. In *Hybrid Organic-Inorganic Composites*; Mark, J. E., Ed.; ACS Series 585; American Chemical Society: Washington, DC, 1995; p 291.
(142) Surivet, F.; Lam, T. M.; Pascault, J. P.; Pham, Q. T. *Macromolecules* **1992**, *25*, 4309.
(143) Surivet, F.; Lam, T. M.; Pascault, J. P.; Pham, Q. T. *Macromolecules* **1992**, *25*, 5742.
(144) Messersmith, P. B.; Giannelis, E. P. *Chem. Mater.* **1994**, *6*, 1719.
(145) Landry, C. J. T.; Coltrain, B. K. *J. M. S.—Pure Appl. Chem.* **1994**, *A31*, 1965.
(146) Yano, S.: Nakamura, K.; Kodomari, M.; Yamauchi, N. *J. Appl. Polym. Sci.* **1994**, *54*, 163.
(147) Wen, J.; Vasudevan, V. J.; Wilkes, G. L. *J. Sol-Gel Sci. Technol.* **1995**, *5*, 115.
(148) Boulton, J. M.; Thompson, J.; Fox, H. H.; Gorodisher, I.; Teowee, G.; Calvert, P. D.; Uhlmann, D. R. *Mater. Res. Soc. Symp. Proc.* **1990**, *180*, 987.
(149) Saegusa, T. *PMSE Polym. Prepr.* **1994**, *70*, 371.
(150) Saegusa, T. *Polym. Prepr.* **1993**, *34*, 804.
(151) Wei, Y.; Wang, W.; Yang, D.; Tang, L. *Chem. Mater.* **1994**, *6*, 1737.
(152) Wang, B.; Wilkes, G. L.; Smith, C. D.; McCrath, J. E. *Polym. Commun.* **1991**, *32*, 400.
(153) Wang, B.; Wilkes, G. L.; Hedrick, J. C.; Liptak, S. C.; McCrath, J. E. *Macromolecules* **1991**, *24*, 3449.
(154) Shojaie, S. S.; Rials, T. G.; Kelley, S. S. *J. Appl. Polym. Sci.* **1995**, *58*, 1263.
(155) Wei, Y.; Yang, D. C.; Tang, L. G. *Makromol. Chem., Rapid Commun.* **1993**, *14*, 273.
(156) Brinker, C. J.; Scherer, G. W. *J. Non-Cryst. Solids* **1985**, *70*, 301.
(157) Wang, B.; Huang, H.; Brennan, A. B.; Wilkes, G. L. *Polym. Prepr.* **1989**, *30*, 227.
(158) Noell, J. L. W.; Wilkes, G. L.; Mohanty, D. K.; McCrath, J. E. *J. Appl. Polym. Sci.* **1990**, *40*, 1177.
(159) (a) Betrabet, C. S.; Wilkes, G. L. *J. Inorg. Organomet. Polym.* **1995**, *7*, 535. (b) Brennan, A. B.; Miller, T. M. *Chem. Mater.* **1994**, *6*, 262.
(160) Gillham, J. K. In *Developments in Polymer Characterization*; Dawkins, J. V., Ed.; Applied Science: London, 1982; Vol. 3, Chapter 5.
(161) Brennan, A. B.; Wilkes, G. L. *Polymer* **1991**, *32*, 733.
(162) Wang, B.; Brennan, A. B.; Huang, H.; Wilkes, G. L. *J. Macromol. Sci., Chem.* **1990**, *A27*, 1447.
(163) Wang, B.; Huang, H.; Brennan, A. B.; Wilkes, G. L. *Polym. Prepr.* **1989**, *30*, 146.
(164) Wang, B.; Wilkes, G. L. *J. Polym. Sci., Part A* **1991**, *29*, 905.
(165) Rodrigues, D. E.; Wilkes, G. L. *Polym. Prepr.* **1989**, *30*, 227.
(166) (a) Saegusa, T. *PMSE Prepr.* **1994**, *70*, 371. (b) Saegusa, T.; Chujo, Y. *J. Macromol. Sci., Chem.* **1990**, *A27*, 1603.
(167) Wen, J.; Wilkes, G. L., unpublished results.
(168) Saegusa, T. *Macromol. Sci., Chem.* **1991**, *A28*, 817.
(169) Landry, M. J.; Coltrain, B. K.; Landry, C. J. T.; O'Reilly, J. M. *J. Polym. Sci., Part B: Polym. Phys.* **1995**, *33*, 637.
(170) Schmidt, H. *J. Non-Cryst. Solids* **1989**, *112*, 419.
(171) Schmidt, H. *Mater. Res. Soc. Symp. Proc.* **1990**, *180*, 961.
(172) Luneau, I. G.; Mosset, A.; Galy, J.; Schmidt, H. *J. Mater. Sci.* **1990**, *89*, 3739.
(173) Nab, R.; Schmidt, H. *SPIE* **1990**, *1328*, 258.
(174) Schubert, U.; Schwertfeger, F.; Husing, N.; Seyfried, E. *Mater. Res. Soc. Symp. Proc.* **1994**, *346*, 151.
(175) Schmidt, H.; Seiferling, B.; Philipp, G.; Deichmann, K. In *Ultrastructure of Processing of Advanced Ceramics*; Mackenzie, J. D., Ulrich, D. R., Eds.; New York, 1988; p 651.
(176) Wang, B; Wilkes, G. L. U.S. Patent 5,316,855.
(177) Shea, K. J.; Loy, D. A. *Chem. Mater.* **1989**, *1*, 572.
(178) Loy, D. A.; Shea, K. J. *Chem. Rev.* **1995**, *95*, 1431.

CM9601143